AFRL-RI-RS-TR-2008-4
Final Technical Report
January 2008

SIGNAL AND IMAGE PROCESSING IN DIFFERENT REPRESENTATIONS

Hunter College of The City University of New York

APPROVED FOR PUBLIC RELEASE; DISTRIBUTION UNLIMITED.

STINFO COPY

AIR FORCE RESEARCH LABORATORY
INFORMATION DIRECTORATE
ROME RESEARCH SITE
ROME, NEW YORK

NOTICE AND SIGNATURE PAGE

AFRL-RI-RS-TR-2008-4 HAS BEEN REVIEWED AND IS APPROVED FOR PUBLICATION IN ACCORDANCE WITH ASSIGNED DISTRIBUTION STATEMENT.

FOR THE DIRECTOR:

/s/ /s/

DAVID HENCH
Work Unit Manager

WARREN H. DEBANY, Jr.
Technical Advisor, Information Grid Division
Information Directorate

REPORT DOCUMENTATION PAGE

Form Approved
OMB No. 0704-0188

1. REPORT DATE *(DD-MM-YYYY)*	2. REPORT TYPE	3. DATES COVERED *(From - To)*
JAN 2008	Final	Sep 01 – May 07

4. TITLE AND SUBTITLE

SIGNAL AND IMAGE PROCESSING IN DIFFERENT REPRESENTATIONS

5a. CONTRACT NUMBER

5b. GRANT NUMBER
F30602-01-1-0590

5c. PROGRAM ELEMENT NUMBER
62702F

6. AUTHOR(S)

Leon Cohen

5d. PROJECT NUMBER
558B

5e. TASK NUMBER
11

5f. WORK UNIT NUMBER
05

7. PERFORMING ORGANIZATION NAME(S) AND ADDRESS(ES)
Hunter College of The City University of New York
Dept of Physics
695 Park Avenue
New York NY 10021

8. PERFORMING ORGANIZATION REPORT NUMBER

9. SPONSORING/MONITORING AGENCY NAME(S) AND ADDRESS(ES)

AFRL/RIGC
525 Brooks Rd
Rome NY 13441-4505

10. SPONSOR/MONITOR'S ACRONYM(S)

11. SPONSORING/MONITORING AGENCY REPORT NUMBER
AFRL-RI-RS-TR-2008-4

12. DISTRIBUTION AVAILABILITY STATEMENT
APPROVED FOR PUBLIC RELEASE; DISTRIBUTION UNLIMITED. PA# WPAFB 08-0035

13. SUPPLEMENTARY NOTES

14. ABSTRACT
One of the fundamental and powerful ideas of signal processing is that of a system function and input-output relations. Traditionally input-output relations are formulated in the time domain or, equivalently, in the spectral domain. However, over the last sixty years it has been found that many natural and man made signals are nonstationary, and the standard formulation does not fully describe what is happening, and therefore is not effective. We have shown that an immense simplification occurs, both conceptually and technically, when input-output relations are formulated in the combined time-frequency plane. We have developed an approach for formulating time-frequency/input-output systems for both the deterministic and random case. Using our approach we have solved a number of hitherto unsolved problems. In particular, we have been able to obtain the exact time-dependent solution of the Wiener process, the exact solution to the gliding tone problem, and the full exact solution to the RC circuit driven by white noise, among other problems. In addition, using our formulation we have clarified the issues with the ABC algorithm proposed by A. Noga, and we have also been able to formulate nonstationary noise so that it produces images that are similar to real clouds.

15. SUBJECT TERMS
Nonstationary signals, input-output relations, nonstationary random systems, gliding tone problem, adjustable bandwidth concept

16. SECURITY CLASSIFICATION OF:			17. LIMITATION OF ABSTRACT	18. NUMBER OF PAGES	19a. NAME OF RESPONSIBLE PERSON
a. REPORT	b. ABSTRACT	c. THIS PAGE			David Hench
U	U	U	UL	98	19b. TELEPHONE NUMBER (*Include area code*) N/A

Contents

1 Introduction

One of the fundamental and powerful ideas of signal processing is that of a system function and input-output relations. This is commonly symbolized in the following way. If we have an input time function, $f(t)$ which passes through a system characterized by a system function $h(t)$, then the output is given by $x(t)$. This is symbolized in Fig. 1.

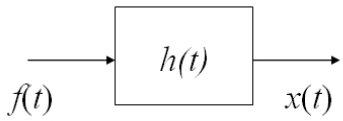

Figure 1: Input-output representation of a system in the time domain.

Equivalently in the Fourier domain, if the input, system and output transforms of the time functions are given by $F(\omega)$, $H(\omega)$ and $X(\omega)$ respectively, then the input-output relations are symbolized as in Fig. 2.

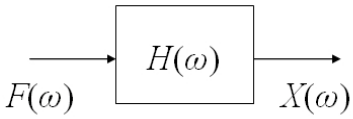

Figure 2: Input-output representation of a system in the frequency domain.

However, over the last fifty years it has been found that many natural and man made signals are nonstationary, and the above formulation does not fully describe what is happening. Our fundamental point to be developed in this report is that if the signals are nonstationary an immense simplification and advantage occurs if we have input-output relations in the time-frequency plane. We symbolize this in Fig. 3. where $C_f(t,\omega)$ and $C_x(t,\omega)$ (e.g. spectrogram, Wigner, etc. distribution) are the input and output time-frequency distributions and the box with the question mark is meant to symbolize the time-frequency system function. It is one of the aims of this report to explain how the time-frequency system function can be obtained and to show the advantages of such a formulation.

To illustrate and motivate our method we start with a simple example. Consider the differential equation

$$\frac{d^2x(t)}{dt^2} + 2\mu\frac{dx(t)}{dt} + \omega_0^2 x(t) = f(t) \tag{1}$$

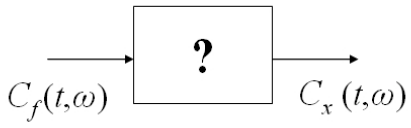

Figure 3: Input-output representation of a system in the time-frequency domain.

where $f(t)$ is a given driving force. Perhaps there is no more studied equation than this one. In principle this equation can be solved "exactly" by many methods. For both practical reasons and to gain insight, one often transforms this equation into the Fourier domain. Defining

$$X(\omega) = \frac{1}{\sqrt{2\pi}} \int x(t)\, e^{-it\omega}\, dt \tag{2}$$

$$F(\omega) = \frac{1}{\sqrt{2\pi}} \int f(t)\, e^{-it\omega}\, dt \tag{3}$$

the differential equation transforms into

$$[-\omega^2 + 2i\mu\omega + \omega_0^2]X(\omega) = F(\omega) \tag{4}$$

whose exact solution is

$$X(\omega) = \frac{F(\omega)}{[-\omega^2 + 2i\mu\omega + \omega_0^2]} \tag{5}$$

The reasons for going into the Fourier domain are many. First, it offers a practical way of solution since now one can find the time solution by way of

$$x(t) = \frac{1}{\sqrt{2\pi}} \int \frac{F(\omega)}{[-\omega^2 + 2i\mu\omega + \omega_0^2]}\, e^{it\omega}\, dt \tag{6}$$

Perhaps more importantly the reason for going into the Fourier domain is that one can gain insight into the nature of the solution and both reasons have become part of standard analysis in both engineering and physics, as exemplified by input-output relations.

Now consider a specific example. Take

$$\frac{d^2x(t)}{dt^2} + 2\mu\frac{dx(t)}{dt} + \omega_0^2 x = \; e^{-\alpha t^2/2 + i\beta t^2/2 + i\omega_1 t} \tag{7}$$

The solution obtained numerically is shown in Fig. 4. The Fourier transform of the driving force is

$$F(\omega) = \frac{1}{\sqrt{\alpha - i\beta}} \;\; \exp\left[-\frac{\alpha(\omega-\omega_1)^2}{2(\alpha^2+\beta^2)} - i\frac{\beta(\omega-\omega_1)^2}{2(\alpha^2+\beta^2)} \right] \tag{8}$$

which gives

$$X(\omega) = \frac{\exp\left[-\frac{\alpha(\omega-\omega_1)^2}{2(\alpha^2+\beta^2)} - i\frac{\beta(\omega-\omega_1)^2}{2(\alpha^2+\beta^2)} \right]}{\sqrt{\alpha - i\beta}\, [-\omega^2 + 2i\mu\omega + \omega_0^2]} \tag{9}$$

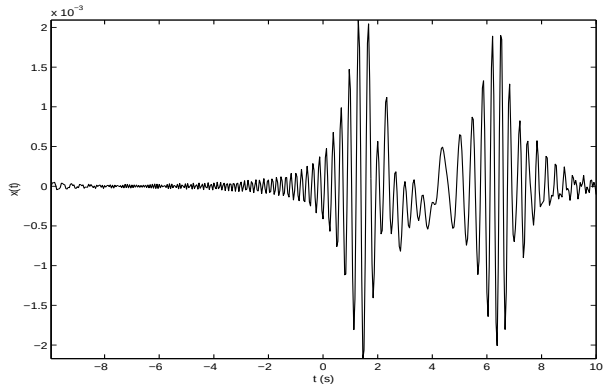

Figure 4: Solution of Eq. (351), $x(t)$. The parameters are $\mu = 1$, $\omega_0 = 6\pi$ rad/as, $\alpha = .001$, $\beta = 6/5\pi$, $\omega_1 = -8\pi$ rad/as.

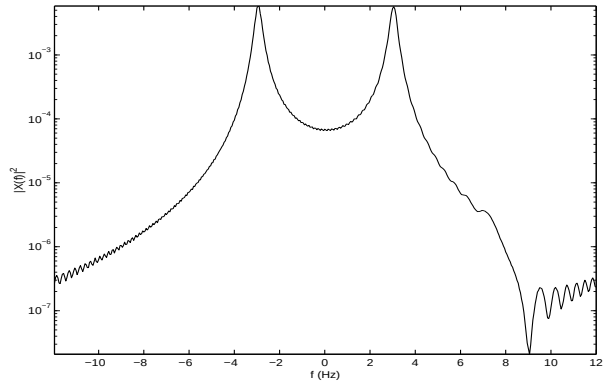

Figure 5: Frequency spectrum of $x(t)$ shown in Fig. 4. The two peaks are due to the resonances of the oscillator located at $f = \pm 3$ Hz.

and the squared magnitude of this is shown in Fig. 5.

In Figs. 4-5 we plot the signal and spectrum for the values indicated in the caption. Much can be learned from a study of $x(t)$ and $X(\omega)$. However, even more can be learned than is commonly discussed in textbooks as we now show if we plot the time-frequency distribution. In Fig. 6 we plot a possible $C(t, \omega)$ for the signal $x(t)$. We see that something remarkable happens: one gets a simple, clear picture of what is going on and of the regions which are important [**?**]. Such distributions have been studied for over seventy years in the field of time-frequency analysis in engineering [**?**, **?**, **?**], but the system function approach has not been developed

In this report we consider systems that are described by differential equations. For the sake of clarity we will developed the ideas for ordinary differential equations with constant coefficients and then give the other cases in the Appendix. However in the next Section we first give a brief review of

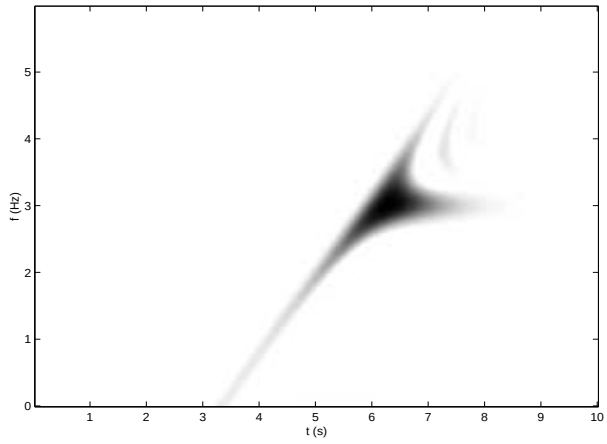

Figure 6: Time-frequency distribution of $x(t)$ represented in Fig. 4. The main energy response occurs when the forcing function hits the resonant frequency of the oscillator, which is located at $f = 3$ Hz. Note that the picture shows only positive time and frequencies.

time-frequency distributions.

2 Brief Review of Time-frequency distributions

Starting in the early 1940s it was realized that for many natural and man made signals their spectra change over time. The development of the physical and mathematical ideas needed to explain and understand time-varying spectra has evolved into the field now called "time-frequency analysis" or time-varying spectral analysis. The purpose of time-frequency analysis is to understand the nature of signals so that we may understand the physical phenomena generating them, the medium of propagation, their structure, classification, detection, etc. The basic idea is to find a joint density of time and frequency that indicates what frequencies are present in the signal and how they are changing in time. The main initial impetus occurred at Bell Laboratories, with the development of the "sound spectrograph" for studying speech. Sometime later it was realized that the principle methods used in engineering for time-frequency analysis are mathematically analogous to the development that occurred in quantum mechanics starting with Wigner, and now called the phase space formulation of quantum mechanics independently of their use in quantum mechanics, these distributions have been developed in signal analysis as a means of understanding how the spectral content of a signal changes in time for classical variables. This development has a long history and originated with the work of Koenig, Dunn, and L. Lacy XciteKoenig, Gabor XciteGabor, and Ville XciteVille, and since that time there have been many quasi-distributions or representations that have been used and developed. A general formulation of quasi-distributions was given by Cohen Xciteleon3, and many methods have been devised

for obtaining distributions with desirable properties Xcitechoi,Zhao,Jeong,Sala1,Sala2,Amin2,pat3.

Of particular relevance to our considerations is the wide range of applications of these distributions to classical systems, that includes acoustics XciteGaun2,pat4, speech processing XcitePitton, musical instruments XcitePielemeier, machine monitoring XciteRizzoni,Atlas, stochastic processes XciteAmin3,pitton2, biomedical signals XciteWilliams,Wood, sonar and radar XciteGaun1, nonlinear dynamic al systems XciteLorenzo, among many others Xcitepat. The fundamental idea of this approach is to study the time-frequency properties of a classical variable such as a pressure wave, current, etc. The distributions are typically calculated from experimental data or by first generating the numerical solution from the governing differential equation.

2.1 Mathematical Development

The development of quasi-distributions or time-frequency representations occurred more or less simultaneously in both quantum mechanics and signal analysis although from very different perspectives [**?**, **?**]. The basic objective is to devise a joint density in time and frequency. One can set up the issue as follows. If we have a signal $s(t)$ and its Fourier transform $S(\omega)$, then the instantaneous power is

$$|\, s(t)\,|^2 \;=\; \text{intensity per unit time at } t$$

and the density in frequency, the energy density spectrum, is

$$|\, S(\omega)\,|^2 \;=\; \text{intensity per unit frequency at } \omega$$

What one seeks is a joint density, $P(t,\omega)$, so that

$$P(t,\omega) \quad = \text{ the density (or intensity) at time } \;\; t \;\; \text{ and frequency } \;\; \omega.$$

Ideally the joint density should satisfy

$$\int P(t,\omega)\, d\omega \;=\; |\, s(t)\,|^2 \tag{10}$$

$$\int P(t,\omega)\, dt \;=\; |\, S(\omega)\,|^2 \tag{11}$$

which are called the time and frequency marginal conditions. Wigner, and later Ville, gave such a function, which is now called the Wigner-Ville distribution [**?**, **?**],

$$W(t,\omega) = \frac{1}{2\pi} \int s^*(t-\tau/2)\, s(t+\tau/2)\, e^{-i\tau\omega}\, d\tau \tag{12}$$

It satisfies the time-frequency marginal, Eqs. (10) and (11), but in addition it has the property that the first conditional moment of time at a given frequency is given by the instantaneous frequency of

the signal. An important associated concept is the instantaneous frequency requirement. If we write a signal in terms of amplitude and phase as

$$s(t) \;=\; A(t)\, e^{j\varphi(t)} \tag{13}$$

one takes the instantaneous frequency to be

$$\omega_i(t) = \frac{d\varphi(t)}{dt} \tag{14}$$

Now, the conditional frequency for a given time is given by

$$\langle\, \omega \,\rangle_t = \frac{1}{|\, s(t)\,|^2} \int \omega\, P(t,\omega)\, d\omega \tag{15}$$

For many distributions, such as the Wigner distribution

$$\langle\, \omega \,\rangle_t = \omega_i(t) = \frac{d\varphi(t)}{dt} \tag{16}$$

From this point of view the instantaneous frequency can be thought of as the average frequency at a particular time. We point out that for certain distributions, Eq. (16) is exactly satisfied and also, often, the peak of the distribution is approximately given by $\frac{d\varphi(t)}{dt}$. It is important to mention though that writing a real signal in a complex form as given by Eq. (13) has a long history. The basic issue is that there are an infinite number of ways to generate a complex signal from a real signal. Currently the most widely accepted method is the one devised by Gabor and called the analytic signal. We do not address these issues here. This is not true for all distributions, but is so for the Wigner and others.

Among other quasi-distributions subsequently proposed in signal analysis and quantum mechanics were the Rihaczek, Page, and Margenau-Hill, among others. In 1966 a method was devised that could generate in a simple manner an infinite number of new ones [**?**]. This general class is given by

$$C(t,\omega) \;=\; \frac{1}{4\pi^2} \iiint s^*(u-\tau/2)\, s(u+\tau/2)\, \phi(\theta,\tau)\, e^{-i\theta t - i\tau\omega + i\theta u}\, du\, d\tau\, d\theta \tag{17}$$

where $\phi(\theta,\tau)$ is a two dimensional function called the kernel. The properties of a distribution are reflected as simple constraints on the kernel, and by examining the kernel one readily can ascertain the properties of the distribution. This allows one to pick and choose those kernels that produce distributions with prescribed, desirable properties. Williams and co-workers devised and crystallized the idea of kernel design. They developed a methodology for the construction of densities with desirable properties. At about the same time, Zhao, Atlas and Marks similarly produced a density that resolved many of the difficulties with the Wigner distribution. These works and others led to major developments in trying to understand the nature of these time-frequency densities and also to practical applications to the fields mentioned above [**?**, **?**, **?**, **?**].

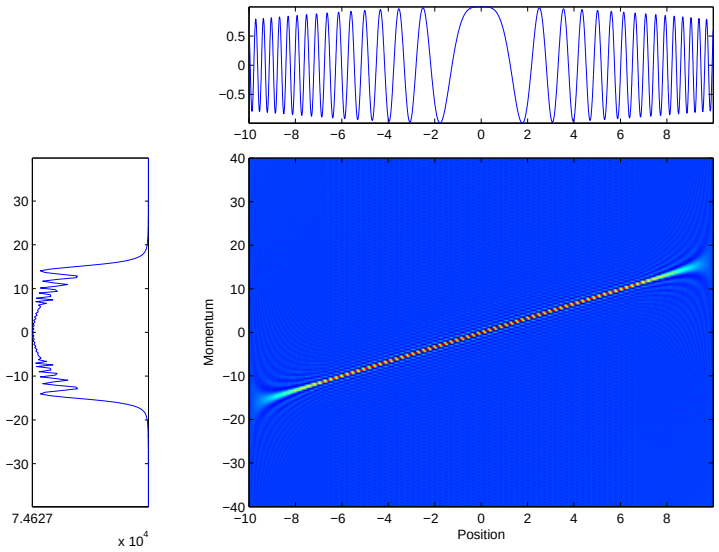

Figure 7: The Wigner distribution of $s(t) = e^{-\alpha t^2/2 + i\beta t^2/2 + i\omega_0 t}$ is shown in the central part. The top figure is the real part of the signal and the left figure is the absolute of the spectrum.

One can think of a time-frequency distribution as a two dimensional transform of a one dimensional function. In the mathematical sense the distribution contains the same information as the signal since it is constructed from it and for many distributions the signal can be obtained from it uniquely. However a dramatic thing happens when one plots or studies the time-frequency distribution instead of the signal or spectrum, namely the physical nature of the signal becomes much clearer. The best way to understand the concept of a time-frequency representation is to consider a number of examples.

2.2 Example 1

Consider the signal,

$$s(t) \;=\; e^{-\alpha t^2/2 + i\beta t^2/2 + i\omega_0 t} \tag{18}$$

In Fig. 7 we plot the distribution. In the top panel is the real part of the signal, the left panel is the absolute value of the spectrum and in the main figure we have the time-frequency distribution, and in this we show the Wigner distribution. Notice that it is totally concentrated along the curve

$$\omega = \omega_0 + \beta t \tag{19}$$

which is exactly the instantaneous frequency.

2.3 Example: Multipart signals

One of the interesting aspects of time-frequency analysis is that it reveals when a signal consists of parts. We use the word parts instead of components since sometime "components" is often associated

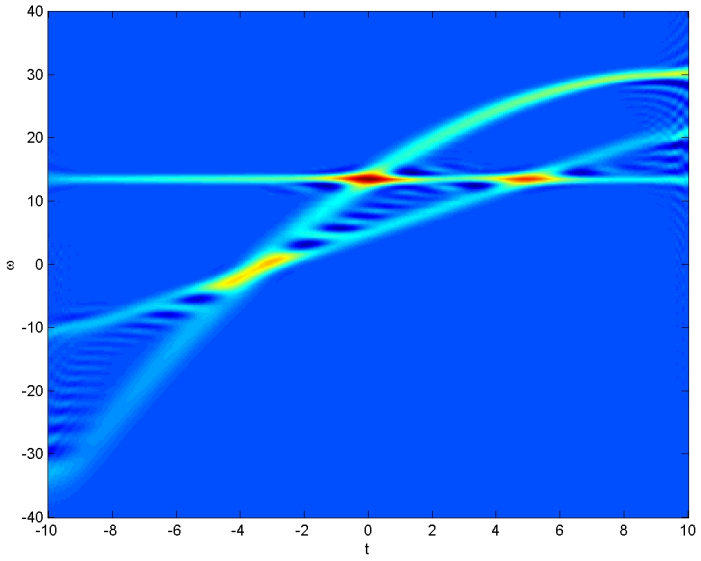

Figure 8: The Wigner distribution of Eq. (20).

with orthogonal components which is not necessarily the case here. Consider the signal

$$s(t) = e^{-\alpha_1 t^2/2 + i\omega_2 t} + e^{-\alpha_1 t^2/2 + i\beta_1 t^2/2 + i\omega_1 t} + e^{-\alpha t^2/2 + i\gamma t^3/3 + i\beta t^2/2 + i\omega_0 t} \tag{20}$$

In Fig. 8 we show the Wigner distribution of $s(t)$. Note how clearly the time-frequency distribution reveals that it consists of three parts and moreover note that each part is in some sense approximately concentrated along its instantaneous frequency, respectively $\omega_1(t)$, $\omega_2(t)$ and $\omega_3(t)$

$$\omega_1(t) = \omega_2 \tag{21}$$

$$\omega_2(t) = \omega_1 + \beta_1 t \tag{22}$$

$$\omega_3(t) = \gamma t^2 + \beta t + \omega_0 \tag{23}$$

Example: whale sound

For a first example we take a whale sound. In Fig. 9, running across the page, above the main figure is the sound, that is the air pressure as a function time. To the left of the main figure is the energy density spectrum, that is, the absolute square of the Fourier transform of the signal. The energy density spectrum indicates what frequencies existed and what their relative strengths were for the duration of the signal but it does not indicate when these frequencies occurred. For this sound it tells us that the frequencies ranged from about 175 to about 375 cycles per second. The main figure is a time-frequency plot and now we can determine not only what frequencies occurred by when they occurred and what were their relative intensities were as time evolves. At the start the starting

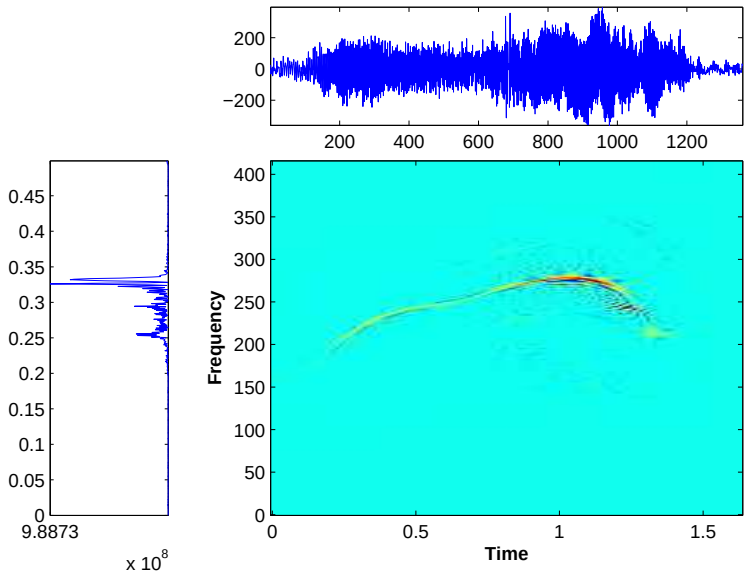

Figure 9: A whale sound.

frequency was about 175 Hz and increased more or less linearly to about 375 Hz in about half a second, stayed there for about a tenth of a second, and then decreased approximately linearly to about 200 Hz.

Now consider Fig. 10 where the signal is made up of four sine waves with varying duration. If one were to look at the spectrum the only conclusions one could arrive at is that four constant frequency signals existed, but with no information about when they existed. The time-frequency plot does that so clearly and also shows the amplitude variations.

Now consider the signal

$$s(t) = e^{-\alpha_1 t^2/2 + i\omega_1 t} + e^{-\alpha_2 t^2/2 + i\beta t^2/2 + i\omega_2 t} \tag{24}$$

The distribution is plotted in Fig. 11. It is concentrated along the instantaneous frequency of each part

$$\omega = \omega_0 + \beta t \quad ; \quad \omega = \omega_0 \tag{25}$$

We call such signals Multipart because they consists of parts, in this case two. One of the advantages of time-frequency analysis is that it effectively shows that a signal consists of parts, something that can not be seen directly in the signal or spectrum.

As a last example consider

$$s(t) = (\alpha/\pi)^{1/4} e^{-\alpha t^2/2 + i\eta t^4/4 + i\gamma t^3/3 + i\beta t^2/2 + i\omega_0 t} \tag{26}$$

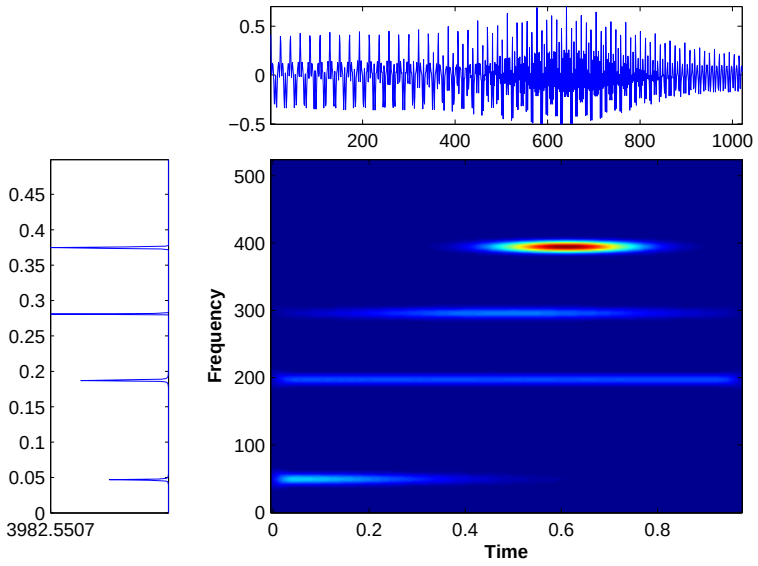

Figure 10: Four constant frequency sine waves of different duration.

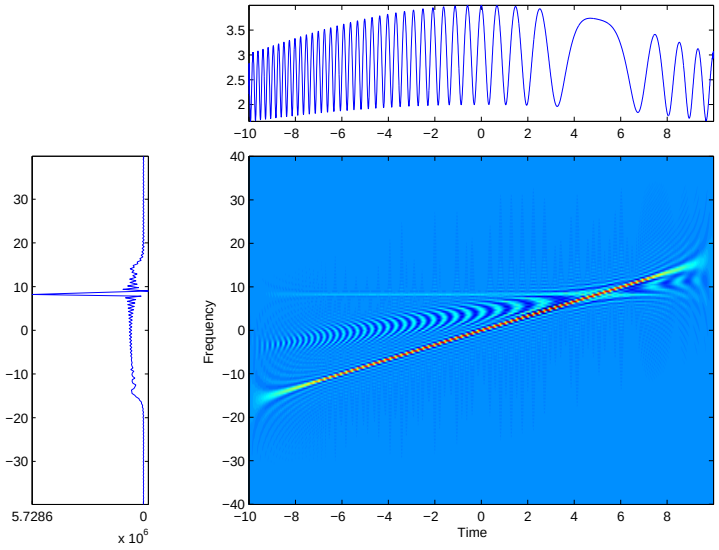

Figure 11: The Wigner distribution of Eq. (24).

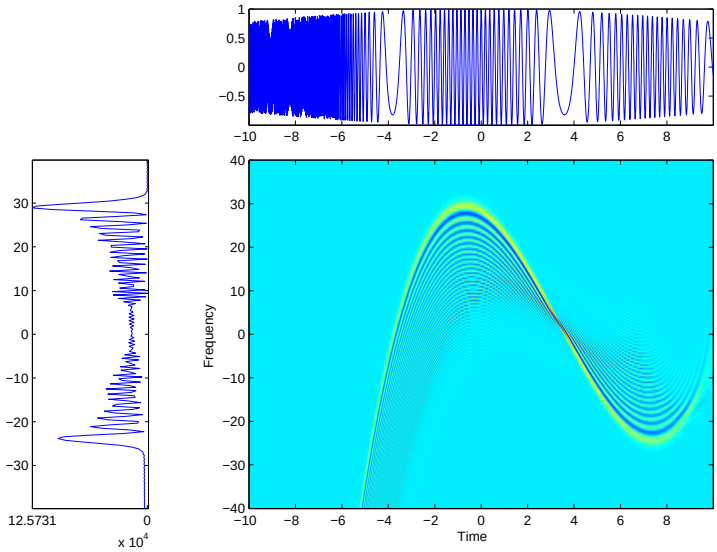

Figure 12: The Wigner distribution of Eq. (26).

whose distribution is illustrated in Fig. 12. Again the concentration is along the instantaneous frequency

$$\omega = \eta t^3 + \gamma t^2 + \beta t + \omega_0 \tag{27}$$

3 Outline of the Approach

Our aim is to develop input-output relations for nonstationary situations and when the governing equations relating input and output is a differential equation. Although the details will change when dealing with ordinary and partial differential equations, the general approach is conceptually the same, and hence we outline the method in broad terms. Details can be found in the published papers. Suppose the governing equation is

$$L[u] = f \tag{28}$$

where L is a linear operator and f is a known driving force. This situation covers both the ordinary and partial differential equation possibility. In the former case u is $x(t)$, and in the case of a field u would be a function of x and t, that is $u(x,t)$.

We will now show the approach in the case of ordinary differential equations. The aim is to obtain a differential equation for the Wigner distribution of $x(t)$ which will involve the Wigner distribution of $f(t)$, and therefore the starting equation is

$$L[x(t)] = f(t) \tag{29}$$

Step 1: Take the Wigner distribution of both sides to obtain

$$W_{L[x],L[x]}(t,\omega) = W_{f,f}(t,\omega) \tag{30}$$

We now have to express $W_{L[x],L[x]}(t,\omega)$ in terms of $W_{x,x}(t,\omega)$.

Step 2: As is often the case L itself is the sum of operators,

$$L = \sum_n L_n \tag{31}$$

giving

$$\sum_{n,m} W_{L_n[x],L_m[x]}(t,\omega) = W_{f,f}(t,\omega) \tag{32}$$

Step 3: Express

$$W_{L_n[x],L_m[x]}(t,\omega) \qquad \text{in terms of} \qquad W_{x,x}(t,\omega) \tag{33}$$

This will be discussed in detail for a variety of operators.

Other Equations. It is also of some interest to consider equations of motion for the cross Wigner distributions. Starting with Eq. 29 write

$$L[x(t+\tfrac{1}{2}\tau)] = f(t+\tfrac{1}{2}\tau) \tag{34}$$

and multiply both sides by $x^*(t-\frac{1}{2}\tau)e^{-i\tau\omega}$ and integrate with respect to τ. We have therefore

$$\int x^*(t-\tfrac{1}{2}\tau)\, L[x(t+\tfrac{1}{2}\tau)]\, e^{-i\tau\omega} d\tau = \int x^*(t-\tfrac{1}{2}\tau)\, f(t+\tfrac{1}{2}\tau)\, e^{-i\tau\omega} d\tau \tag{35}$$

which gives

$$W_{x,L[x]}(t,\omega) = W_{x,f}(t,\omega) \tag{36}$$

Similarly,

$$W_{L[x],x}(t,\omega) = W_{f,x}(t,\omega) \tag{37}$$

These equations can be used to manipulate intermediate results in the derivation of the equation for $W_{x,x}$.

4 Transformation of Ordinary Differential Equations with constant coefficients into phase space

Many input-output linear systems are characterized by ordinary differential equations and the study of such systems is fundamental in a number of branches in signal processing [**?**]. The differential equation may or may not have time-dependent coefficients. It is often the case that these systems exhibit time-varying frequencies, but generally speaking time-frequency methods have not been applied directly to

these types of systems. It has been done only in a circuitous way, namely by first numerically solving the differential equation and then substituting the solution into a time-frequency distribution [**?**]. For the input signal we use $f(t)$ and for the output $x(t)$, while for the governing equation we take

$$a_n \frac{d^n x}{dt^n} + a_{n-1} \frac{d^{n-1} x}{dt^{n-1}} \ \cdots + a_1 \frac{dx}{dt} + a_0 x = f(t) \tag{38}$$

or, in polynomial notation

$$P(D)x(t) = f(t) \tag{39}$$

where

$$P(D) = a_n D^n + a_{n-1} D^{n-1} ... + a_1 D + a_0 \tag{40}$$

The Wigner distribution is defined by XciteWigner

$$W_{x,x}(t,\omega) = \frac{1}{2\pi} \int x^*(t - \tfrac{1}{2}\tau)\, x(t + \tfrac{1}{2}\tau)\, e^{-i\tau\omega}\, d\tau \tag{41}$$

Now, take the Wigner distribution of both sides of Eq. (39) to obtain

$$W_{P(D)x,P(D)x}(t,\omega) = W_{f,f}(t,\omega) \tag{42}$$

We now state our main result: the input-output governing equation for the Wigner distribution associated with Eq. (38) is given by

$$P^*(A)P(B)W_{x,x}(t,\omega) = W_{f,f}(t,\omega) \tag{43}$$

where

$$A = \frac{1}{2}\frac{\partial}{\partial t} - j\omega \qquad\qquad B = \frac{1}{2}\frac{\partial}{\partial t} + j\omega \tag{44}$$

and the star sign stands for complex conjugation of the constants $a_0, \ldots, a_n$. The distribution $W_{f,f}(t,\omega)$ is the Wigner of is the Wigner distribution of the input

$$W_{f,f}(t,\omega) = \frac{1}{2\pi} \int f^*(t - \tfrac{1}{2}\tau)\, f(t + \tfrac{1}{2}\tau)\, e^{-i\tau\omega}\, d\tau \tag{45}$$

This equation can be seen to be in the variables t, ω, and is in general a partial differential equation of twice the order of the original differential equation, that is order $2n$.

4.1 Zero Driving Force situation

If the driving force is zero then

$$P^*(A)P(B)W_{x,x} = 0 \tag{46}$$

In this case the equation of evolution can be simplified to two equations

$$P^*(A)W_{x,x} = P(B)W_{x,x} = 0 \tag{47}$$

These equations can be derived in two equivalent ways. First, directly from Eq. (38) with $f = 0$, or one can start from the definition of the Wigner distribution and show it straightforwardly. We note that while Eq. (43) is a differential equation of order $2n$, Eqs. (47) are of order n.

5 Ordinary Differential Equations with time dependent coefficients into phase space

Consider the case of an ordinary differential equation with time-varying coefficients,

$$a_n(t)\frac{d^n x(t)}{dt^n} + a_{n-1}(t)\frac{d^{n-1}x(t)}{dt^{n-1}} \cdots + a_1(t)\frac{dx(t)}{dt} + a_0(t)x(t) = f(t) \tag{48}$$

As before we rewrite this in polynomial notation

$$P(D,t)x(t) = f(t) \tag{49}$$

where

$$P(D,t) = a_n(t)D^n + a_{n-1}(t)D^{n-1} \ldots + a_1(t)D + a_0(t) \tag{50}$$

A similar derivation that led to Eq. (43) leads now to

$$P^*(A,\mathcal{E})P(B,\mathcal{F})W_{x,x}(t,\omega) = W_{f,f}(t,\omega) \tag{51}$$

where

$$\mathcal{E} = \frac{1}{2i}\frac{\partial}{\partial\omega} + t \qquad\qquad \mathcal{F} = -\frac{1}{2i}\frac{\partial}{\partial\omega} + t \tag{52}$$

and the operators A and B are given in Eq. (44).

For the zero driving force case one obtains

$$P^*(A,\mathcal{E})W_{x,x}(t,\omega) = P(B,\mathcal{F})W_{x,x}(t,\omega) = 0 \tag{53}$$

In Eq. (51) $P(B,\mathcal{F})$ means that in the polynomial $P(D,t)$ one substitutes B for D,and $\mathcal{F}$ for t, and $P^*(A,\mathcal{E})$ is obtained similarly. Also, the complex conjugation in $P^*(A,\mathcal{E})$ means that the original polynomial is conjugated and not the arguments A, $\mathcal{E}$. Note that Eq. (51) is a partial differential equation, and that makes sense since we are dealing with two variables jointly, namely time and frequency. The derivation of Eq. (51) is given in the Appendix.

6 Analysis of differential Equations in Time-Frequency Phase Space for the Bilinear Distributions

We consider a linear system defined by an ordinary differential equation of the type

$$a_n(t)\frac{d^n x(t)}{dt^n} + a_{n-1}(t)\frac{d^{n-1}x(t)}{dt^{n-1}} \cdots + a_1(t)\frac{dx(t)}{dt} + a_0(t)x(t) = f(t) \tag{54}$$

where $f(t)$ is the input or forcing term, $x(t)$ is the output of the system and $a_n(t), \ldots, a_0(t)$ are the time-varying coefficients, generally complex. As mentioned we have been able to obtain the governing equation for the Wigner distribution for the solution of this equation. We consider here the possibility of transforming such equations into the time-frequency domain for a general bilinear class of distributions. We will show that this is possible for a bilinear distribution associated to the solution of Eq. (54). We will do so in the kernel notation and the general K formalism

6.1 Equation of motion in the kernel notation

The general class of bilinear distributions is

$$C(t,\omega) = \frac{1}{4\pi^2}\iiint x^*(u-\tau/2)x(u+\tau/2)\phi_c(\theta,\tau)e^{-i\theta t - i\tau\omega + i\theta u}dud\theta d\tau \tag{55}$$

where $\phi_c(\theta,\tau)$ is the kernel. To obtain an equation for $C(t,\omega)$ associated to Eq. (54) we first put it into polynomial notation

$$P(D,t)x(t) = f(t) \tag{56}$$

where, as usual

$$P(D,t) = a_n(t)D^n + a_{n-1}(t)D^{n-1} + \cdots + a_1(t)D + a_0(t) \tag{57}$$

and

$$D = \frac{d}{dt} \tag{58}$$

Then the equation for an arbitrary bilinear time-frequency distribution $C(t,\omega)$ is

$$P^*(A_c,\mathcal{E}_c)P(B_c,\mathcal{F}_c)C_x(t,\omega) = C_f(t,\omega) \tag{59}$$

where

$$A_c = \phi_c\left(\frac{1}{i}\frac{\partial}{\partial t},\frac{1}{i}\frac{\partial}{\partial\omega}\right)\left(\frac{1}{2}\frac{\partial}{\partial t} - i\omega\right)\phi_c^{-1}\left(\frac{1}{i}\frac{\partial}{\partial t},\frac{1}{i}\frac{\partial}{\partial\omega}\right) \tag{60}$$

$$B_c = \phi_c\left(\frac{1}{i}\frac{\partial}{\partial t},\frac{1}{i}\frac{\partial}{\partial\omega}\right)\left(\frac{1}{2}\frac{\partial}{\partial t} + i\omega\right)\phi_c^{-1}\left(\frac{1}{i}\frac{\partial}{\partial t},\frac{1}{i}\frac{\partial}{\partial\omega}\right) \tag{61}$$

$$\mathcal{E}_c = \phi_c\left(\frac{1}{i}\frac{\partial}{\partial t},\frac{1}{i}\frac{\partial}{\partial\omega}\right)\left(t + \frac{1}{2i}\frac{\partial}{\partial\omega}\right)\phi_c^{-1}\left(\frac{1}{i}\frac{\partial}{\partial t},\frac{1}{i}\frac{\partial}{\partial\omega}\right) \tag{62}$$

$$\mathcal{F}_c = \phi_c\left(\frac{1}{i}\frac{\partial}{\partial t},\frac{1}{i}\frac{\partial}{\partial\omega}\right)\left(t - \frac{1}{2i}\frac{\partial}{\partial\omega}\right)\phi_c^{-1}\left(\frac{1}{i}\frac{\partial}{\partial t},\frac{1}{i}\frac{\partial}{\partial\omega}\right) \tag{63}$$

We have already derived the operators A_c and B_c in [**?**, **?**]. Here we present the derivation of the operators $\mathcal{E}_c$ and $\mathcal{F}_c$. We use the following relation

$$C_{f,g}(t,\omega) = \phi_c\left(\frac{1}{i}\frac{\partial}{\partial t}, \frac{1}{i}\frac{\partial}{\partial \omega}\right) W_{f,g}(t,\omega) \tag{64}$$

Now we evaluate

$$C_{tf,g} = \phi_c\left(\frac{1}{i}\frac{\partial}{\partial t}, \frac{1}{i}\frac{\partial}{\partial \omega}\right) W_{tf,g} \tag{65}$$

$$= \phi_c\left(\frac{1}{i}\frac{\partial}{\partial t}, \frac{1}{i}\frac{\partial}{\partial \omega}\right) \mathcal{E} W_{f,g} \tag{66}$$

$$= \phi_c\left(\frac{1}{i}\frac{\partial}{\partial t}, \frac{1}{i}\frac{\partial}{\partial \omega}\right) \mathcal{E}\phi_c^{-1}\left(\frac{1}{i}\frac{\partial}{\partial t}, \frac{1}{i}\frac{\partial}{\partial \omega}\right) C_{f,g} \tag{67}$$

$$= \mathcal{E}_c C_{f,g} \tag{68}$$

Where we have used that

$$W_{tf,g} = \mathcal{E} W_{f,g} \tag{69}$$

$$= \left(t + \frac{1}{2i}\frac{\partial}{\partial \omega}\right) W_{f,g} \tag{70}$$

Following the same approach one has

$$C_{f,tg} = \mathcal{F}_c C_{f,g} \tag{71}$$

We can now evaluate

$$C_{a(t)f,g} = C_{\sum \alpha_n t^n f,g} \tag{72}$$

$$= \sum \alpha_n^* C_{t^n f,g} \tag{73}$$

$$= \sum \alpha_n^* \mathcal{E}_c^n C_{f,g} \tag{74}$$

$$= a^*(\mathcal{E}_c) C_{f,g} \tag{75}$$

With the identical procedure one also obtains

$$C_{f,b(t)g} = b(\mathcal{F}_c) C_{f,g} \tag{76}$$

6.2 Equation of motion in the K notation

All the bilinear distributions can also be written in the following way

$$C(t,\omega) = \iint K_c(t,\omega,t',t'') x^*(t')\, x(t'')\, dt' dt'' \tag{77}$$

where now $K_c(t,\omega,t',t'')$ is the new kernel associated to every distribution $C(t,\omega)$. In particular $K_c(t,\omega,t',t'')$ is given by

$$K_c(t,\omega,x',x) = \frac{1}{4\pi^2} e^{-i\omega(x'-x)} \int \phi_c(\theta, x'-x) e^{-i(t-(x+x')/2)\theta} d\theta \tag{78}$$

We now claim that the equation for the K notation associated to Eq. (54) is

$$P^*(\overline{A}_c, \overline{\mathcal{E}}_c) P(\overline{B}_c, \overline{\mathcal{F}}_c) C_x(t,\omega) = C_f(t,\omega) \tag{79}$$

where the operators have the same form given in Eqs. (60)-(63), where one has to make the substitution

$$\phi_c\left(\frac{1}{i}\frac{\partial}{\partial t}, \frac{1}{i}\frac{\partial}{\partial \omega}\right) = 2\pi e^{\omega \frac{\partial}{\partial \omega}} \int K_c\left(t, \omega, t - t' + \frac{1}{2i}\frac{\partial}{\partial \omega}, t - t' - \frac{1}{2i}\frac{\partial}{\partial \omega}\right) e^{t' \frac{\partial}{\partial t}} dt' \tag{80}$$

To prove Eq. (80) one considers that Eq. (78) is basically a Fourier transform for every fixed x, x'. Hence we make the following change of variables

$$\tau = x' - x \tag{81}$$

$$t' = t - (x + x')/2 \tag{82}$$

which gives

$$x' = t - t' + \tau/2 \tag{83}$$

$$x = t - t' - \tau/2 \tag{84}$$

We substitute in Eq. (78) and we obtain

$$\int \phi_c(\theta, \tau) e^{-it'\theta} d\theta = 4\pi^2 e^{i\omega\tau} K_c(t, \omega, t - t' + \tau/2, t - t' - \tau/2) \tag{85}$$

Then we obtain

$$\phi_c(\theta, \tau) = 2\pi e^{i\omega\tau} \int K_c(t, \omega, t - t' + \tau/2, t - t' - \tau/2) e^{it'\theta} dt' \tag{86}$$

By substituting

$$\theta \to \frac{1}{i}\frac{\partial}{\partial t} \tag{87}$$

$$\tau \to \frac{1}{i}\frac{\partial}{\partial \omega} \tag{88}$$

we finally obtain Eq. (80).

7 Differential equations for the Short-Time Fourier Transform domain

We define the Short-Time Fourier transform, $S_x(t,\omega)$, of a signal, $x(t)$, by

$$S_x(t,\omega) = \frac{1}{\sqrt{2\pi}} \int h(\tau - t) x(\tau) e^{-i\tau\omega} d\tau \tag{89}$$

where $h(t)$ is the window function. The equation for the Short-Time Fourier Transform associated to Eq. (54) is

$$P(A_s, \mathcal{E}_s) S_x(t,\omega) = S_f(t,\omega) \tag{90}$$

where

$$A_s = \left(\frac{\partial}{\partial t} + i\omega \right) \tag{91}$$

$$\mathcal{E}_s = i\frac{\partial}{\partial \omega} \tag{92}$$

To prove Eq. (90) we first evaluate

$$S_{\frac{dx}{dt}}(t,\omega) = \frac{1}{\sqrt{2\pi}} \int h(\tau - t) \frac{dx(\tau)}{d\tau} e^{-i\tau\omega} d\tau \tag{93}$$

$$= \frac{1}{\sqrt{2\pi}} \left(h(\tau - t)x(\tau)e^{-i\tau\omega} \right)_{-\infty}^{+\infty} + \tag{94}$$

$$- \frac{1}{\sqrt{2\pi}} \int \left(\frac{dh(\tau - t)}{d\tau} x(\tau)e^{-i\tau\omega} - i\omega h(\tau - t)x(\tau)e^{-i\tau\omega} \right) d\tau \tag{95}$$

$$= \frac{1}{\sqrt{2\pi}} \frac{\partial}{\partial t} \int h(\tau - t)x(\tau)e^{-i\tau\omega} d\tau + i\omega \frac{1}{\sqrt{2\pi}} \int h(\tau - t)x(\tau)e^{-i\tau\omega} d\tau \tag{96}$$

$$= \left(\frac{\partial}{\partial t} + i\omega \right) S_x(t,\omega) \tag{97}$$

$$= A_s S_x(t,\omega) \tag{98}$$

where we have used

$$h(-\infty) = h(+\infty) = 0 \tag{99}$$

$$\frac{dh(\tau - t)}{d\tau} = -\frac{\partial h(\tau - t)}{\partial t} \tag{100}$$

Then we consider

$$S_{a(t)x}(t,\omega) = \frac{1}{\sqrt{2\pi}} \int h(\tau - t)a(\tau)x(\tau)e^{-i\tau\omega} d\tau \tag{101}$$

$$= a\left(i\frac{\partial}{\partial \omega} \right) \frac{1}{\sqrt{2\pi}} \int h(\tau - t)x(\tau)e^{-i\tau\omega} d\tau \tag{102}$$

$$= a(\mathcal{E}_s) S_x(t,\omega) \tag{103}$$

which gives Eq. (90).

8 Transformation to the Wavelet domain

We now consider the problem of writing an equation for the Continuous Wavelet Transform (CWT) whose solution corresponds to the time domain function $x(t)$ as given by Eq. (54). Here we present a restricted version of the problem, addressing linear differential equations with constant coefficients

$$a_n \frac{d^n x(t)}{dt^n} + a_{n-1} \frac{d^{n-1} x(t)}{dt^{n-1}} \cdots + a_1 \frac{dx(t)}{dt} + a_0 x(t) = f(t) \tag{104}$$

The CWT of a signal $x(t)$ is defined as

$$C_x(a,b) = \frac{1}{\sqrt{a}} \int \psi^* \left(\frac{t-b}{a} \right) x(t) dt \tag{105}$$

where $a > 0$, $-\infty < b < +\infty$. We rewrite Eq. (104) in the simplified polynomial notation

$$P(D)x(t) = f(t) \tag{106}$$

The equation for the CWT is

$$P(A_w)C_x(a,b) = C_f(a,b) \tag{107}$$

where

$$A_w = \frac{\partial}{\partial b} \tag{108}$$

To prove Eq. (107) we evaluate

$$C_{\frac{dx}{dt}}(a,b) = \frac{1}{\sqrt{a}} \int \psi^* \left(\frac{t-b}{a} \right) \frac{dx(t)}{dt} dt \tag{109}$$

$$= \frac{1}{\sqrt{a}} \left(\psi^* \left(\frac{t-b}{a} \right) x(t) \right)_{-\infty}^{+\infty} - \frac{1}{\sqrt{a}} \int x(t) \frac{d}{dt} \psi^* \left(\frac{t-b}{a} \right) dt \tag{110}$$

$$= \frac{1}{\sqrt{a}} \frac{\partial}{\partial b} \int \psi^* \left(\frac{t-b}{a} \right) \frac{dx(t)}{dt} dt \tag{111}$$

$$= A_w C_x(a,b) \tag{112}$$

where we have used

$$\psi(-\infty) = \psi(+\infty) = 0 \tag{113}$$

$$\frac{d}{dt} \psi^* \left(\frac{t-b}{a} \right) = -\frac{\partial}{\partial b} \psi^* \left(\frac{t-b}{a} \right) \tag{114}$$

Also, we note that since $C_x(a,b)$ is a linear operation, then, for any given complex constant, k, we have that $C_{kx}(a,b) = kC_x(a,b)$. This fact was used in the above derivation

9 Transformation to the Ambiguity function domain

We have considered a number of topics that involve two fundamental problems in signal analysis, systems governed by differential equations and whose solutions generally give a nonstationary spectrum. We also point out that while in this paper we have just considered ordinary differential equations these methods can be readily extended to situations governed by partial differential equations, and to systems of ordinary differential equations. In conclusion we also mention that we have worked out differential equations for the ambiguity function and the autocorrelation function. The ambiguity function is defined by

$$\mathcal{A}_x(t,\omega) = \frac{1}{2\pi} \int x^*(t-\tau/2) x(t+\tau/2) e^{i\theta t} dt \tag{115}$$

and the differential equations that is satisfied is

$$P^*(A_a, \mathcal{E}_a)P(B_a, \mathcal{F}_a)\mathcal{A}_x(t,\omega) = \mathcal{A}_f(t,\omega) \tag{116}$$

where

$$A_a = -\frac{1}{2}i\theta - \frac{\partial}{\partial\tau}, \qquad B_a = -\frac{1}{2}i\theta + \frac{\partial}{\partial\tau} \tag{117}$$

$$\mathcal{E}_a = \frac{1}{i}\frac{\partial}{\partial\theta} - \frac{1}{2}\tau, \qquad \mathcal{F}_a = \frac{1}{i}\frac{\partial}{\partial\theta} + \frac{1}{2}\tau \tag{118}$$

For the autocorrelation function, defined by

$$R_X(t_1,t_2) = E[X(t_1)X^*(t_2)] \tag{119}$$

the differential equation is given by

$$P\left(\frac{\partial}{\partial t_1}, t_1\right) P^*\left(\frac{\partial}{\partial t_2}, t_2\right) R_X(t_1,t_2) = R_F(t_1,t_2) \tag{120}$$

10 Partial Differential Equations

For partial differential equations of the form

$$\sum_{k=1}^{N} a_k(x,t)\frac{\partial^k}{\partial x^k}u(x,t) + \sum_{l=1}^{M} b_l(x,t)\frac{\partial^l}{\partial t^l}u(x,t) = f(x,t) \tag{121}$$

it is possible to obtain an equation in the Wigner distribution domain similar to the ordinary differential equation case, provided that we use the four dimensional Wigner distribution, Z, defined as

$$Z_{u,u}(x,p,t,\omega) = \frac{1}{(2\pi)^2}\int u^*(x-\tfrac{1}{2}\tau_x, t-\tfrac{1}{2}\tau)u(x+\tfrac{1}{2}\tau_x, t+\tfrac{1}{2}\tau)e^{-i\tau\omega - i\tau_x p}d\tau d\tau_x \tag{122}$$

This distribution is discussed in the Appendix, here we have reported its definition again for clarity. We shall need to use the following operators,

$$A_x = \frac{1}{2}\frac{\partial}{\partial x} - ip \qquad A_t = \frac{1}{2}\frac{\partial}{\partial t} - i\omega \tag{123}$$

$$B_x = \frac{1}{2}\frac{\partial}{\partial x} + ip \qquad B_t = \frac{1}{2}\frac{\partial}{\partial t} + i\omega \tag{124}$$

and

$$\mathcal{E}_x = \frac{1}{2j}\frac{\partial}{\partial p} + x \qquad \mathcal{F}_x = -\frac{1}{2j}\frac{\partial}{\partial p} + x \tag{125}$$

$$\mathcal{E}_t = \frac{1}{2j}\frac{\partial}{\partial \omega} + t \qquad \mathcal{F}_t = -\frac{1}{2j}\frac{\partial}{\partial \omega} + t \tag{126}$$

The same approach of the previous sections for ordinary differential equations gives

$$\left[\sum_{k=1}^{N} a_k^*(\mathcal{E}_x, \mathcal{E}_t)A_x^k + \sum_{l=1}^{M} b_l^*(\mathcal{E}_x, \mathcal{E}_t)A_t^l\right]\left[\sum_{m=1}^{N} a_m(\mathcal{F}_x, \mathcal{F}_t)B_x^m + \sum_{n=1}^{M} b_n(\mathcal{F}_x, \mathcal{F}_t)B_t^n\right] Z_{u,u} = Z_{f,f} \tag{127}$$

If the driving force $f(x,t)$ is zero one has that

$$\sum_{k=1}^{N}\left[a_k^*(\mathcal{E}_x,\mathcal{E}_t)A_x^k\right]Z_{u,u} = -\sum_{l=1}^{M}\left[b_l^*(\mathcal{E}_x,\mathcal{E}_t)A_t^l\right]Z_{u,u} \tag{128}$$

$$\sum_{k=1}^{N}\left[a_k(\mathcal{F}_x,\mathcal{F}_t)B_x^k\right]Z_{u,u} = -\sum_{l=1}^{M}\left[b_l(\mathcal{F}_x,\mathcal{F}_t)B_t^l\right]Z_{u,u} \tag{129}$$

We have found it convenient to combine these two equations by adding and subtracting them

$$\sum_{k=1}^{N}\left[a_k^*(\mathcal{E}_x,\mathcal{E}_t)A_x^k \pm a_k(\mathcal{F}_x,\mathcal{F}_t)B_x^k\right]Z_{u,u} = \sum_{l=1}^{M}\left[b_l^*(\mathcal{E}_x,\mathcal{E}_t)A_t^l \pm b_l(\mathcal{F}_x,\mathcal{F}_t)B_t^l\right] \tag{130}$$

10.1 Notation and Definitions

All the integrals without limits mean integration from $-\infty$ to ∞.

Ordinary differentiation of functions with respect to time will be indicated by

$$\dot{g}(t) = \frac{d}{dt}g(t) \qquad\qquad g^{(n)} = \frac{d^n}{dt^n}g(t) \tag{131}$$

We define the Wigner distribution for a signal $x(t)$ by

$$W_{x,x}(t,\omega) = \frac{1}{2\pi}\int x^*(t-\tfrac{1}{2}\tau)\,x(t+\tfrac{1}{2}\tau)\,e^{-i\tau\omega}\,d\tau \tag{132}$$

and the cross-Wigner distribution between two signals, $x(t)$ and $y(t)$ by

$$W_{x_1,x_2}(t,\omega) = \frac{1}{2\pi}\int x_1^*(t-\tfrac{1}{2}\tau)\,x_2(t+\tfrac{1}{2}\tau)\,e^{-i\tau\omega}\,d\tau \tag{133}$$

When we deal with partial differential equations, we need to consider multidimensional signals (fields), $u(x,t)$. For a field the Wigner distribution is

$$W_{u,u}(x,p,t) = \frac{1}{2\pi}\int u^*(x-\tfrac{1}{2}\tau_x,t)\,u(x+\tfrac{1}{2}\tau_x,t)e^{-i\tau_x p}\,d\tau_x \tag{134}$$

and analogously the cross-Wigner distribution between two fields, $u_1(x,t)$ and $u_2(x,t)$ is

$$W_{u_1,u_2}(x,p,t) = \frac{1}{2\pi}\int u_1^*(x-\tfrac{1}{2}\tau_x,t)\,u_2(x+\tfrac{1}{2}\tau_x,t)e^{-i\tau_x p}\,d\tau_x \tag{135}$$

For partial differential equations it is generally not possible to write an equation for the Wigner distribution, $W_{u,u}(x,p,t)$, corresponding to an arbitrary equation governing the field. It is nevertheless possible to always derive such an equation for the more general Wigner distribution which we define by

$$Z_{u,u}(x,p,t,\omega) = \frac{1}{(2\pi)^2}\int u^*(x-\tfrac{1}{2}\tau_x, t-\tfrac{1}{2}\tau)u(x+\tfrac{1}{2}\tau_x, t+\tfrac{1}{2}\tau)e^{-i\tau\omega - i\tau_x p}\,d\tau\,d\tau_x \tag{136}$$

We note that the ordinary Wigner distribution, $W(x,p,t)$, may be obtained from $Z(x,p,t,\omega)$ by way of

$$W_{u,u}(x,p,t) = \int Z_{u,u}(x,p,t,\omega)\,d\omega \tag{137}$$

A significant simplification in notation is achieved by defining the following operators

$$A_t = \frac{1}{2}\frac{\partial}{\partial t} - i\omega \qquad\qquad B_t = \frac{1}{2}\frac{\partial}{\partial t} + i\omega \tag{138}$$

$$\mathcal{E}_t = t + \frac{1}{2i}\frac{\partial}{\partial \omega} \qquad\qquad \mathcal{F}_t = t - \frac{1}{2i}\frac{\partial}{\partial \omega} \tag{139}$$

Operators of this kind were defined by Moyal. When dealing with a field $u(x,t)$ one has to introduce the additional operators

$$A_x = \frac{1}{2}\frac{\partial}{\partial x} - ip \qquad\qquad B_x = \frac{1}{2}\frac{\partial}{\partial x} + ip \tag{140}$$

$$\mathcal{E}_x = x + \frac{1}{2i}\frac{\partial}{\partial p} \qquad\qquad \mathcal{F}_x = x - \frac{1}{2i}\frac{\partial}{\partial p} \tag{141}$$

Also, we will indicate ordinary differentiation in the following alternative ways

$$\dot{g}(t) = \frac{d}{dt}g(t) \qquad\qquad g^{(n)} = \frac{d^n}{dt^n}g(t) \tag{142}$$

and we will use the differential operator,

$$D = \frac{d}{dt} \tag{143}$$

As mentioned above, we will see that it is not always possible to obtain an equation of motion for the Wigner distribution $W_{u,u}(x,p,t)$, but it is always possible to obtain an equation of motion for a Wigner type distribution of the four variables, namely position, momentum time and frequency. We define such a function by

$$Z_{u,u}(x,p,t,\omega) = \frac{1}{(2\pi)^2}\int u^*(x-\tfrac{1}{2}\tau_x, t-\tfrac{1}{2}\tau)u(x+\tfrac{1}{2}\tau_x, t+\tfrac{1}{2}\tau)e^{-i\tau\omega - i\tau_x p}\,d\tau\,d\tau_x \tag{144}$$

The relation between W and Z is that W is the marginal of Z

$$\int Z_{u,u}(x,p,t,\omega)\,d\omega = W_{u,u}(x,p,t) \tag{145}$$

It is convenient to define the following operators[1]

$$A_t = \frac{1}{2}\frac{\partial}{\partial t} - i\omega \qquad\qquad B_t = \frac{1}{2}\frac{\partial}{\partial t} + i\omega \tag{146}$$

$$\mathcal{E}_t = t + \frac{1}{2i}\frac{\partial}{\partial \omega} \qquad\qquad \mathcal{F}_t = t - \frac{1}{2i}\frac{\partial}{\partial \omega} \tag{147}$$

Also, the operators A_x, B_x, E_x, F_x for fields are similarly defined as per Eq. (146) and Eq. (147), where t is replaced by x and ω by the momentum, p.

11 Example: $\dot{x} = f(t)$

We consider an example that to some extent is analytically doable. For the differential equation we take

$$\dot{x} = f(t) \tag{148}$$

with

$$f(t) = ct\, e^{-\alpha t^2/2 + i\beta t^2/2} \tag{149}$$

which with the boundary condition that $x(-\infty) = 0$ gives

$$x(t) = -\frac{c}{\alpha - i\beta} e^{-\alpha t^2/2 + j\beta t^2/2} \tag{150}$$

The Wigner distribution of both x and f can be done exactly

$$W_{f,f}(t,\omega) \;=\; \frac{2c^2}{\pi}\sqrt{\frac{\pi}{4\alpha^3}}\,\left[\,\alpha t^2 + (\omega-\beta t)^2/\alpha - \tfrac{1}{2}\,\right]\;\; e^{-\alpha t^2 - (\omega-\beta t)^2/\alpha}$$

$$W_{x,x}(t,\omega) \;=\; \frac{1}{\pi}\sqrt{\frac{\pi}{\alpha}}\frac{c^2}{\alpha^2+\beta^2}\, e^{-\alpha t^2 - (\omega-\beta t)^2/\alpha} \tag{151}$$

We now show how our procedure can be used to obtain the Wigner distribution directly. Using Eq. (39) the equation of motion for the Wigner distribution is

$$ABW_{x,x}(t,\omega) = W_{f,f}(t,\omega) \tag{152}$$

that is

$$\frac{1}{4}\frac{\partial}{\partial t}W_{x,x}(t,\omega) + \omega^2 W_{x,x}(t,\omega) = W_{f,f}(t,\omega) \tag{153}$$

[1] Operators of this kind were defined by Moyal.

This equation is a partial differential equation but since there are no derivatives with respect to ω we can solve it as an ordinary differential equation keeping ω fixed. By repeating the process for a range of ω we hence get a numerical solution for $W_{x,x}(t,\omega)$. We have done so and compared to the exact answer, Eq. (151), with the result that the answers are identical to within a fraction of a percent.

12 Example: RC circuit with deterministic chirp driving force

As an example consider an RC circuit that is being driven by a driving force whose instantaneous frequency varies linearly with time. The governing equation is

$$\frac{dx(t)}{dt} + kx = e^{i\omega_0 t + i\beta t^2/2} \tag{154}$$

where k is a positive constant. Using Eq. (43) we have that the associated equation for the Wigner distribution is

$$[A+k][B+k]W_{x,x}(t,\omega) = \delta(\omega - \omega_0 - \beta t) \tag{155}$$

This equation can be solved exactly, giving

$$W_{x,x}(t,\omega) = \frac{4}{|\beta|} u(\tau) e^{-2k\tau} \frac{\sin 2\omega\tau}{2\omega} \tag{156}$$

where $u(\tau)$ is the step function and

$$\tau = t - \frac{\omega - \omega_0}{\beta} \tag{157}$$

As initial conditions we have taken

$$W_{x,x}(-\infty,\omega) = 0 \tag{158}$$

$$\frac{\partial}{\partial t} W_{x,x}(-\infty,\omega) = 0 \tag{159}$$

that can be proved to correspond to the case

$$x(-\infty) = 0$$

In Fig. 13 we give a specific case where $k = 20,\ \omega_0 = 0$, and $\beta = 113$. The dashed line represents the instantaneous frequency of the input chirp $f(t)$,

$$\omega_i = \omega_0 + \beta t = \beta t \tag{160}$$

while the gray image is the Wigner distribution obtained from Eq. (156) with the given parameters. The figure clearly reveals the bandpass behavior of the system, that gradually filters out the forcing term $f(t)$.

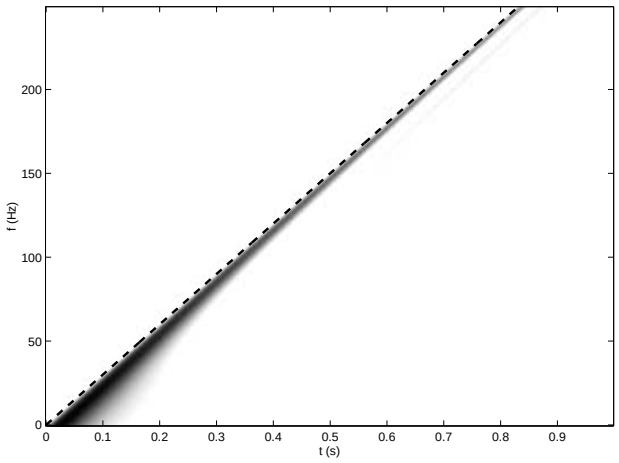

Figure 13: The dashed line indicates the instantaneous frequency of the input chirp. The gray image is the Wigner distribution $W_{x,x}(t,\omega)$ given in Eq. (156) and corresponding to the solution $x(t)$ to Eq. (154). The Wigner distribution highlights the lowpass behavior of the system, that filters out the input signal as $t \to \infty$.

13 Example: RLC circuit with generic deterministic input

Consider the harmonic oscillator with a deterministic driving force,

$$\frac{d^2x(t)}{dt^2} + 2\mu\frac{dx(t)}{dt} + \omega_0^2 x = f(t) \tag{161}$$

where $x(t)$ is the state variable (e.g. current, position) and $f(t)$ is the driving term. If we want to study the time-frequency properties we could solve this equation and substitute the answer into the Wigner distribution,

$$W_{x,x}(t,\omega) = \frac{1}{2\pi}\int x^*(t-\tfrac{1}{2}\tau)\, x(t+\tfrac{1}{2}\tau)\, e^{-i\tau\omega}\, d\tau \tag{162}$$

We want to write the equation of motion for the Wigner distribution and solve that directly. We first rewrite the equation in polynomial notation

$$\left[\ D^2 + 2\mu D + \omega_0^2\ \right]\ x(t) = f(t) \tag{163}$$

Using our method for ordinary differential equations with constant coefficients, Eq. (43), we obtain the equation of motion for the Wigner distribution

$$\left[\ A^2 + 2\mu A + \omega_0^2\ \right]\left[\ B^2 + 2\mu B + \omega_0^2\ \right] W_{x,x} = W_{f,f} \tag{164}$$

Explicitly,

$$\left[a_4\frac{\partial^4}{\partial t^4} + a_3\frac{\partial^3}{\partial t^3} + a_2\frac{\partial^2}{\partial t^2} + a_1\frac{\partial}{\partial t} + a_0\right] W_{x,x}(t,\omega) = W_{f,f}(t,\omega) \tag{165}$$

where,

$$a_0 = (\omega_0^2 - \omega^2)^2 + 4\mu^2\omega^2 \tag{166}$$

$$a_1 = 2\mu(\omega_0^2 + \omega^2) \tag{167}$$

$$a_2 = \frac{1}{2}(\omega_0^2 + \omega^2 + 2\mu^2) \tag{168}$$

$$a_3 = \frac{1}{2}\mu \tag{169}$$

$$a_4 = 1/16 \tag{170}$$

14 Example: The Exact Solution to the Gliding Tone Problem

In 1948 Barber and Ursell [1] and independently Hok [3] considered the problem of the response of a harmonic oscillator to a "gliding tone".[2] Specifically the issue is the behavior of the solution to a resonant circuit [1,3,4]

$$\frac{d^2x(t)}{dt^2} + 2\mu\frac{dx(t)}{dt} + \omega_0^2 x(t) = e^{i\omega_1 t + i\beta t^2/2} \tag{171}$$

with

$$f(t) = e^{i\beta t^2/2} \tag{172}$$

Subsequent to Barber and Ursell, and Hok, many investigators have considered this problem in a variety of contexts and have tried to qualitatively understand the solution and also obtain approximate solutions. An exact solution to this problem has not been achieved. We, also, have not been able to obtain an exact explicit solution; but we have been able to obtain the exact solution to the Wigner distribution of $x(t)$! We have been able to obtain the exact solution by using our method, that is by transforming the original equation in time to the domain of the Wigner distribution, and by solving it.

We give here the explicit solution to the gliding tone problem and subsequently we give a few numerical examples. The reason this is called the gliding tone problem is because the instantaneous frequency of the driving force increases linearly,

$$\omega_i(t) = \omega_1 + \beta t \tag{173}$$

In the gliding tone problem one wants to ascertain the instantaneous frequency of the response. There have been a number of studies made by examining *approximate* solutions of Eq. (171), because indeed an exact solution to Eq. (161) with $f(t)$ given by Eq. (171) has not been achieved. However, we have been able to solve the equation for the Wigner distribution of the gliding tone problem exactly. That

[2]The phrase "gliding tone" was used by Barber and Ursell.

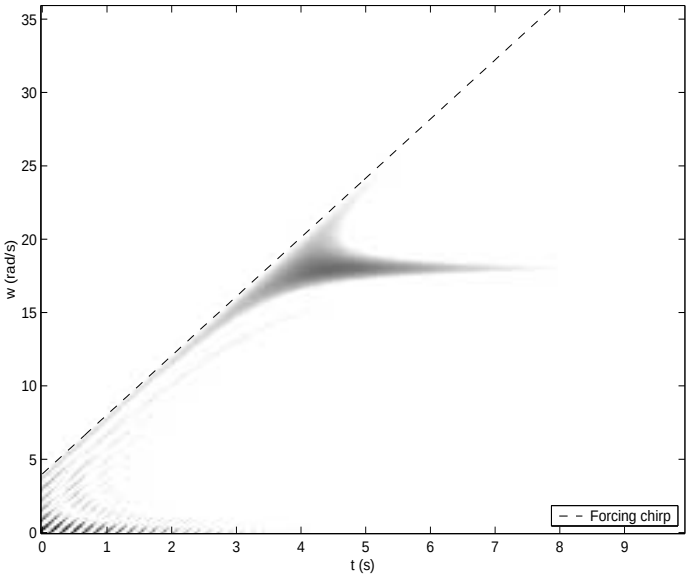

Figure 14: Wigner distribution of the solution to the gliding tone problem. Underdamped case with $\mu = 0.5$.

is, we have been able to solve Eq. (165) when the input term is the Wigner distribution of the gliding tone, Eq. (172). The detailed answer is given in Sect. 14.1.

We now give some graphical examples to illustrate the results. We first consider the underdamped case, that is, when $\mu < \omega_0$. In Figs. 14-16 we plot the Wigner $W_{x,x}(t, \omega)$ for the three cases $\mu = 0.5, \mu = 1$, and $\mu = 1.5$, respectively . In both of the three cases we chose $\omega_0 = 18$ and $\omega_1 = \beta = 4$. The gray scale image in every picture is the exact Wigner distribution of $x(t)$; the dashed line represents the instantaneous frequency of the forcing chirp, that is $\omega_i(t) = \omega_1 + \beta t$. The input chirp $f(t)$ is concentrated only along this line, because its representation in the Wigner distribution domain is $\delta(\omega - \omega_1 - \beta t)$. We see that the response of the system is mainly concentrated around the critical frequency ω_c (it is $\omega_c \approx \omega_0$), while it is weaker at all the other frequencies. Also, observing the limit at $\omega = \omega_c$, one can see that the Wigner distribution has an exponential damping factor, where the damping coefficient is 2μ, which is twice the damping of the free oscillation factor μ of the system. Comparing the three pictures we see how changing the damping factor μ influences the system response. Smaller values of μ imply less damping and hence longer tails in the response along ω_c. Increasing μ forces the system to have a stronger damping and that is reflected in the shorter tail of the main response located around the resonant frequency ω_c.

In Fig. 17 we give an example of an overdamped case where $\mu > \omega_0$, and in particular we take $\mu = 30$. Here the system response is Inharmonic, and we do not have any special resonant frequency. Notice that the output is greater for small times t, while when $t \to \infty$ the response goes to zero. This

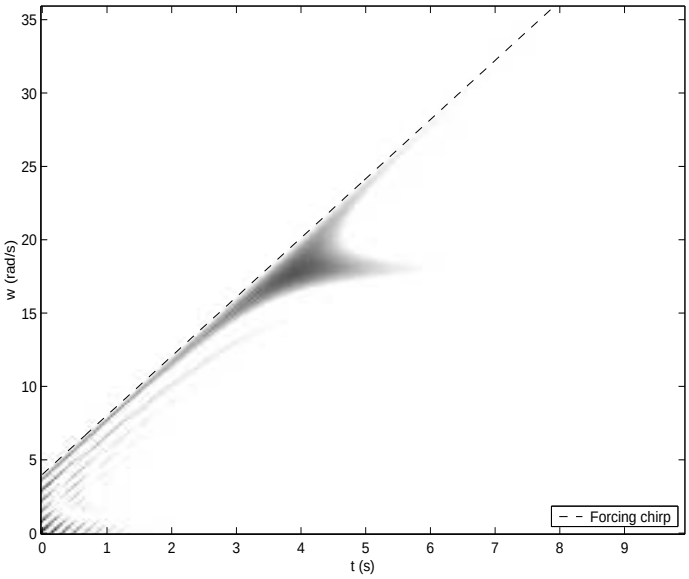

Figure 15: Wigner distribution of the solution to the gliding tone problem. Underdamped case with $\mu = 1$

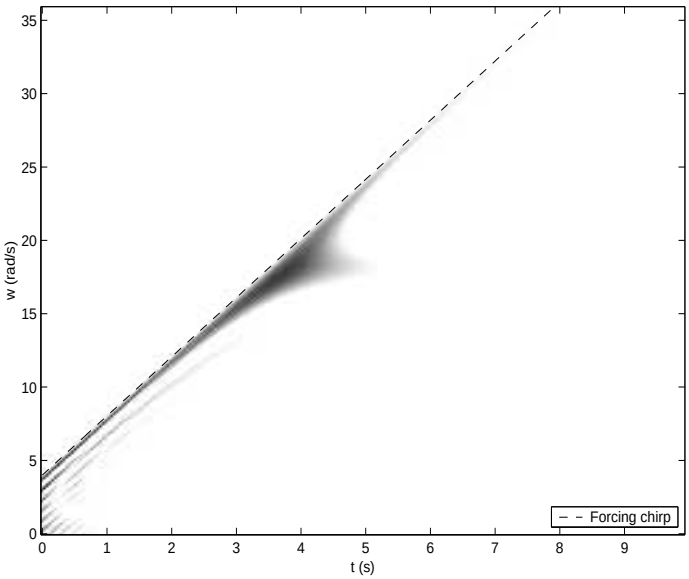

Figure 16: Wigner distribution of the solution to the gliding tone problem. Underdamped case with $\mu = 1.5$

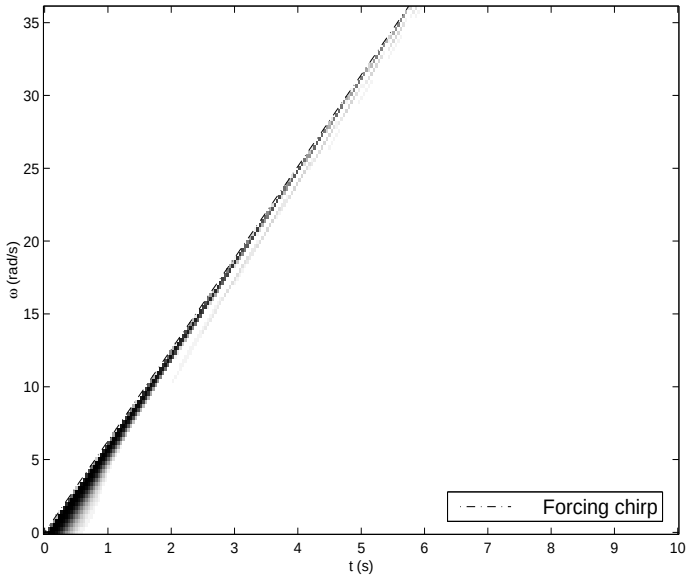

Figure 17: Wigner distribution of the solution to the gliding tone problem for a overdamped case, $\mu > \omega_0$.

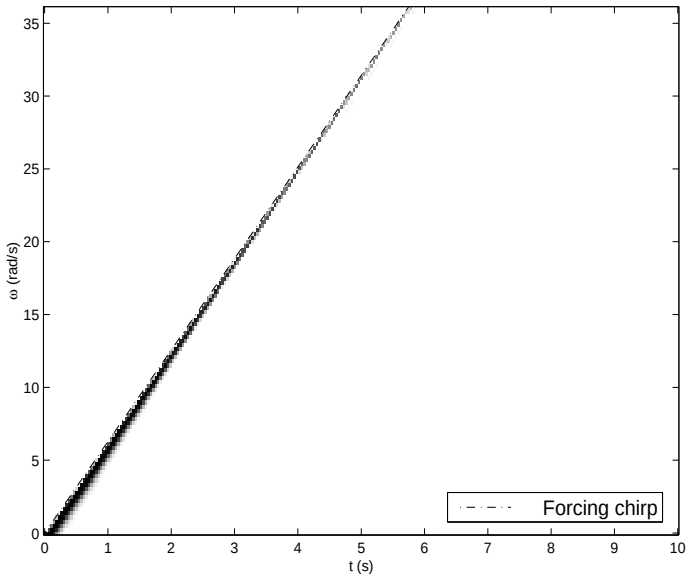

Figure 18: Wigner distribution of the solution to the gliding tone problem for a critically damped case, $\mu = \omega_0$.

is in complete agreement with the result obtained considering the system transfer function.

Finally in Fig. 18 we show a critically damped case, with $\mu = \omega_c = 18$. Considerations on this case are similar to those for the overdamped case.

We point out that we have obtained the Wigner distribution from Eq. (165) by choosing the following initial conditions:

$$W_{x,x}(-\infty,\omega) = \frac{\partial W_{x,x}(-\infty,\omega)}{\partial t} = \frac{\partial^2 W_{x,x}(-\infty,\omega)}{\partial t^2} = \frac{\partial^3 W_{x,x}(-\infty,\omega)}{\partial t^3} = 0 \tag{174}$$

We have proven XciteRepresent ability that this choice corresponds to finding the Wigner distribution of the solution $x(t)$ that has zero initial conditions at $t = -\infty$.

14.1 The exact solution to the Gliding Tone Problem

We now give the exact solution of the Wigner distribution of $x(t)$ which satisfies Eq. (165)

$$W(t,\omega) = \frac{2}{|\beta|}\frac{u(\tau)}{z_2 - z_1}\times \left[\frac{1}{\bar{z}_1 - z_1}\left(\frac{e^{-2z_1\tau} - e^{-2\bar{z}_2\tau}}{\bar{z}_2 - z_1} - \frac{e^{-2\bar{z}_1\tau} - e^{-2\bar{z}_2\tau}}{\bar{z}_2 - \bar{z}_1}\right) + -\frac{1}{\bar{z}_1 - z_2}\left(\frac{e^{-2z_2\tau} - e^{-2\bar{z}_2\tau}}{\bar{z}_2 - z_2} - \frac{e^{-2\bar{z}_1\tau} - e^{-2\bar{z}_2\tau}}{\bar{z}_2 - \bar{z}_1}\right)\right] \tag{175}$$

with

$$\tau = t - \omega/\beta \tag{176}$$

and

$$z_1 = -j\omega + \mu - \sqrt{\mu^2 - \omega_0^2} \tag{177}$$

$$\bar{z}_1 = j\omega + \mu - \sqrt{\mu^2 - \omega_0^2} \tag{178}$$

$$z_2 = -j\omega + \mu + \sqrt{\mu^2 - \omega_0^2} \tag{179}$$

$$\bar{z}_2 = j\omega + \mu + \sqrt{\mu^2 - \omega_0^2} \tag{180}$$

and where $u(t)$ is the Heaviside step function given by

$$u(t) = \begin{cases} 1, & t \geq 0 \\ 0, & t < 0 \end{cases} \tag{181}$$

14.1.1 Underdamped, Overdamped, and Critically Damped Cases

We now explicitly specialize to the underdamped, overdamped and critically damped cases. As is standard we define the critical frequency, ω_c, for these three cases

$\omega_c = \sqrt{\omega_0^2 - \mu^2}$	$\mu < \omega_0$	Underdamped
$\omega_c = \sqrt{\mu^2 - \omega_0^2}$	$\mu > \omega_0$	Overdamped
$\omega_c = 0$	$\mu = \omega_0$	Critically damped

The explicit Wigner distributions are

Underdamped:

$$W(t,\omega) = \frac{1}{2|\beta|\omega_c} u(\tau) e^{-2\mu\tau} \times \left[\frac{\sin(2(\omega\ -\omega_c)\tau)}{\omega(\omega-\omega_c)} - \frac{\sin(2(\omega\ +\omega_c)\tau)}{\omega(\omega+\omega_c)} \right]$$

Overdamped:

$$W(t,\omega) = \frac{1}{|\beta|} u(\tau) e^{-2\mu\tau} \times \left[\frac{\sin(2\omega\tau)\cosh(2\omega_c\tau)}{\omega(\omega^2+\omega_c^2)} - \frac{\cos(2\omega\tau)\sinh(2\omega_c\tau)}{\omega_c(\omega^2+\omega_c^2)} \right]$$

Critically Damped:

$$W(t,\omega) = \frac{1}{|\beta|} u(\tau) e^{-2\mu\tau} \frac{\sin(2\omega\tau) - 2\omega\tau\cos(2\omega\tau)}{\omega^3} \tag{182}$$

In the above solutions there are singularities at some values of ω. We give the limits at those singular values for the three cases:

Underdamped:

$$\lim_{\omega\to\pm\omega_c} W(t,\omega) = \frac{1}{2|\beta|\omega_c} u(\tau) e^{-2\mu\tau} \ \left[\frac{4\omega_c\tau - \sin(4\omega_c\tau)}{2\omega_c^2} \right] \tag{183}$$

$$\lim_{\omega\to 0} W(t,\omega) = \frac{1}{|\beta|} u(t) e^{-2\mu t} \left[\frac{\sin(2\omega_c t) - 2\omega_c t\cos(2w_c t)}{\omega_c^3} \right] \tag{184}$$

Overdamped :

$$\lim_{\omega\to 0} W(t,\omega) = \frac{1}{|\beta|} u(t) e^{-2\mu t} \times \left[\frac{2\omega_c t\cosh(2\omega_c t) - \sinh(2\omega_c t)}{\omega_c^3} \right]$$

Critically Damped:

$$\lim_{\omega\to 0} W(t,\omega) = \frac{8}{3}\frac{1}{|\beta|} u(t) t^3 e^{-2\mu t} \tag{185}$$

15 Example: $a\frac{\partial^2 u}{\partial q^2} + V(x,t)u(x,t) = b\frac{\partial u}{\partial t}$

To bring forth some of the ideas discussed above, let us consider the following type of equation

$$a\frac{\partial^2 u}{\partial q^2} + V(x,t)u(x,t) = b\frac{\partial u}{\partial t} \tag{186}$$

where for the moment we do not make any assumptions about a or b, except that they are complex constants. This leads to the following equations for the Wigner distribution for fields (see the Appendix)

$$a^* A_x^2 Z_{u,u} + V^*(\mathcal{E}_x, \mathcal{E}_t) Z_{u,u} = b^* A_t Z_{u,u} \tag{187}$$

$$a B_x^2 Z_{u,u} + V(\mathcal{F}_x, \mathcal{F}_t) Z_{u,u} = b B_t Z_{u,u} \tag{188}$$

Adding and subtracting the above two equations we have

$$\left[a^* A_x^2 \pm a B_x^2\right] Z_{u,u} + \left[V^*(\mathcal{E}_x, \mathcal{E}_t) \pm V(\mathcal{F}_x, \mathcal{F}_t)\right] Z_{u,u} = \left[b^* A_t \pm b B_t\right] Z_{u,u} \tag{189}$$

The case where b is pure imaginary and a real

We consider the special case where a is real and b pure imaginary and write

$$b = i|b| \tag{190}$$

Taking the negative sign in Eq. (189), we have

$$a\left[A_x^2 - B_x^2\right] Z_{u,u} + \left[V^*(\mathcal{E}_x, \mathcal{E}_t) - V(\mathcal{F}_x, \mathcal{F}_t)\right] Z_{u,u} = -i|b|\left[A_t + B_t\right] Z_{u,u} \tag{191}$$

But

$$A_x^2 - B_x^2 = -2ip\frac{\partial}{\partial x} \tag{192}$$

$$A_t + B_t = \frac{\partial}{\partial t} \tag{193}$$

and therefore

$$-i|b|\frac{\partial Z_{u,u}}{\partial t} = -i2ap\frac{\partial}{\partial x} Z_{u,u} + \left[V^*(\mathcal{E}_x, \mathcal{E}_t) - V(\mathcal{F}_x, \mathcal{F}_t)\right] Z_{u,u} \tag{194}$$

or

$$|b|\frac{\partial Z_{u,u}}{\partial t} = 2ap\frac{\partial}{\partial x} Z_{u,u} + i\left[V^*(\mathcal{E}_x, \mathcal{E}_t) - V(\mathcal{F}_x, \mathcal{F}_t)\right] Z_{u,u} \tag{195}$$

This is the equation of motion in its most general terms. It can be written in a more explicit way. First we mention that for any four dimensional function $K(x, p, t, \omega)$

$$V(\mathcal{F}_x, \mathcal{F}_t) K(x, p, t, \omega) = \left(\frac{1}{2\pi}\right)^2 \int V(x + x'/2, t + t' {}^{i(p'-p)x' + i(\omega' - \omega)t'} K(x, p', t, \omega') dx' dp' dt' d\omega' \tag{196}$$

and

$$V^*(\mathcal{E}_x, \mathcal{E}_t) K(x, p, t, \omega) = \left(\frac{1}{2\pi}\right)^2 \int V^*(x + x'/2, t + t' {}^{-i(p'-p)x' - i(\omega' - \omega)t'} K(x, p', t, \omega') dx' dp' dt' d\omega' \tag{197}$$

Now consider real potentials, then

$$[V(\mathcal{E}_x,\mathcal{E}_t)-V(\mathcal{F}_x,\mathcal{F}_t)]\,Z_{u,u}(x,p,t,\omega)=\frac{2i}{(2\pi)^2}\int V(x+x'/2,t+t'/2)\times \sin[(p'-p)x'+(\omega'-\omega)t']Z_{u,u}(x,p',t,\omega')dx'dp'dt'd\omega'$$

and hence we have for the equation of motion

$$|b|\frac{\partial Z_{u,u}}{\partial t}=2ap\frac{\partial}{\partial x}Z_{u,u}+\frac{2}{(2\pi)^2}\int \sin[(p'-p)x'+(\omega'-\omega)t']\times V(x+x'/2,t+t'/2)Z_{u,u}(x,p',t,\omega')dx'dp'dt'd\omega' \quad (198)$$

which can also be written as

$$|b|\frac{\partial Z_{u,u}}{\partial t}=2ap\frac{\partial}{\partial x}Z_{u,u}+\frac{8}{(2\pi)^2}\int \sin[2(p'-p)(x'-x)+2(\omega'-\omega)(t'-t)]\times V(x',t')Z_{u,u}(x,p',t,\omega')dx'dp'dt'd\omega' \quad (199)$$

15.1 The Schroeder Equation

Let us now specialize explicitly to the Schroeder equation.

$$|b|=1 \qquad a=-\frac{1}{2m} \quad (200)$$

By using the results above we have

$$\frac{\partial Z_{\psi,\psi}}{\partial t}=-\frac{p}{m}\frac{\partial}{\partial q}Z_{\psi,\psi}+i\,[V^*(\mathcal{E}_q,\mathcal{E}_t)-V(\mathcal{F}_q,\mathcal{F}_t)]\,Z_{\psi,\psi} \quad (201)$$

and

$$\frac{\partial Z_{\psi,\psi}}{\partial t}=-\frac{p}{m}\frac{\partial}{\partial q}Z_{\psi,\psi}+\frac{8}{(2\pi)^2}\times \int \sin[2(p'-p)(q'-q)+2(\omega'-\omega)(t'-t)]V(q',t')Z_{\psi,\psi}(q,p',t,\omega')dq'dp'dt'd\omega' \quad (202)$$

These are the equations of motion for the Wigner distribution for time dependent potentials. Notice that one cannot integrate out ω and get a differential equation for the ordinary Wigner distribution. However, if we have time-independent potentials then one can integrate out ω to obtain such an equation. We take

$$V(q,t)=V(q) \quad (203)$$

and use

$$\int \sin[(p'-p)q'+(\omega'-\omega)t']dt'=2\pi\delta(\omega-\omega')\sin[(p'-p)q'] \quad (204)$$

then Eq. (202) reduces to

$$\frac{\partial W_{\psi,\psi}}{\partial t} = -\frac{p}{m}\frac{\partial}{\partial q}W_{\psi,\psi} + \frac{1}{\pi}\int V(q+q'/2)\sin[(p'-p)q']W_{\psi,\psi}(q,p',t)dq'dp' \tag{205}$$

or

$$\frac{\partial W_{\psi,\psi}}{\partial t} = -\frac{p}{m}\frac{\partial}{\partial q}W_{\psi,\psi} + \frac{2}{\pi}\int V(q')\sin[2(p'-p)(q'-q)]W_{\psi,\psi}(q,p',t)dq'dp' \tag{206}$$

which is the equation originally obtained by Wigner and Moyal.

Liouville sine operator form of the equation of motion. Moyal derived the equation of motion for the Wigner distribution in a Liouville type operator form. This was done for time-independent potentials. We now ask whether the same type of equation can be obtained for the time-dependent case. First we recollect the Liouville type expression Moyal XciteMoyal obtained for Eq. (206). We shall present the result in a somewhat different way then Moyal. The main formula to be used is that for any function of $q, K(q)$, and any function of q, p , $M(q,p)$ one has that [3]

$$\sin\frac{1}{2}\left[\frac{\partial}{\partial p_K}\frac{\partial}{\partial q_M} - \frac{\partial}{\partial p_M}\frac{\partial}{\partial q_K}\right]K(q)M(q,p) = \\ -\frac{1}{\pi}\int \sin[2(p'-p)(q'-q)]K(q')M(q,p')dp'dq' \tag{207}$$

Therefore Eq. (206) can be put in the form

$$\frac{\partial W_{\psi,\psi}}{\partial t} = -\frac{p}{m}\frac{\partial}{\partial q}W_{\psi,\psi} + 2\sin\frac{1}{2}\left[\frac{\partial}{\partial p_W}\frac{\partial}{\partial q_V} - \frac{\partial}{\partial p_V}\frac{\partial}{\partial q_W}\right]V(q)W_{\psi,\psi}(q,p,t) \tag{208}$$

But we also have (trivially) that

$$-\frac{p}{m}\frac{\partial}{\partial q}W_{\psi,\psi} = 2\sin\frac{1}{2}\left[\frac{\partial}{\partial p_W}\frac{\partial}{\partial q_A} - \frac{\partial}{\partial p_A}\frac{\partial}{\partial q_W}\right]A(p)W_{\psi,\psi}(q,p,t) \tag{209}$$

$$A(p) = \frac{p^2}{2m} \tag{210}$$

and therefore if one defines

$$H(q,p) = \frac{p^2}{2m} + V(q) \tag{211}$$

then we have the Moyal form of the equation of motion,

$$\frac{\partial W_{\psi,\psi}}{\partial t} = 2\sin\frac{1}{2}\left[\frac{\partial}{\partial p_W}\frac{\partial}{\partial q_H} - \frac{\partial}{\partial p_H}\frac{\partial}{\partial q_W}\right]H(q,p)W_{\psi,\psi}(q,p,t) \tag{212}$$

[3]To change the sign of the right member to a plus, just switch the order of the differentials in the sine bracket.

16 Example $\frac{\partial u}{\partial t} = D\frac{\partial^2 u}{\partial x^2}$

As with the case of ordinary differential equations we will illustrate our method with specific examples. The examples we use are the Schroeder free particle equation and the diffusion equation

$$\frac{\partial \psi}{\partial t} = ia\frac{\partial^2 \psi}{\partial x^2} \qquad \text{Schroedinger free particle; } a = \hbar/(2m) \tag{213}$$

$$\frac{\partial u}{\partial t} = D\frac{\partial^2 u}{\partial x^2} \qquad \text{Diffusion equation; } D = \text{diffusion coefficient} \tag{214}$$

We have chosen these equations because they are fundamental. In addition they are superficially similar. We want to illustrate how these equations compare in the Wigner representation, that is, in phase space. The Wigner distribution for the Schroeder equation has been studied for over 70 years but we believe it has not been applied to the diffusion equation and equations of that type. The respective momentum functions defined by

$$\phi(p,t) = \frac{1}{\sqrt{2\pi}}\int \psi(x,t)e^{-ixp}dx \tag{215}$$

$$U(p,t) = \frac{1}{\sqrt{2\pi}}\int u(x,t)e^{-ixp}dx \tag{216}$$

satisfy the following equations of motion

$$\frac{\partial \phi}{\partial t} = -iap^2\phi \tag{217}$$

$$\frac{\partial U}{\partial t} = -Dp^2 U \tag{218}$$

The Wigner distribution combines both representations, that is, it is a joint representation of position and momentum. However, we point out a fundamental difference between the interpretation of the solution of the Schroeder and diffusion equation. In the case of the Schroeder equation, $|\psi(x,t)|^2$ and $|\phi(p,t)|^2$ are the densities of position and momentum. However, in the case of diffusion, $u(x,t)$ and $U(p,t)$ are the densities. Thus, in the case of the Schroeder equation the Wigner distribution satisfies the so called marginal conditions, but that is not the case for the diffusion equation. None the less the Wigner distribution gives an indication on how momentum and position are jointly related. More precisely one should think of the representation as a joint representation in position and spatial frequency.

We recall the Wigner distribution for a field, $u(x,t)$

$$W_u(x,p,t) = \frac{1}{2\pi}\int u^*(x-\frac{1}{2}\tau,t)\,u(x+\frac{1}{2}\tau,t)e^{-i\tau p}d\tau \tag{219}$$

$$= \frac{1}{2\pi}\int U^*(p+\frac{1}{2}\theta,t)\,U(p-\frac{1}{2}\theta,t)e^{-i\theta x}d\,\theta \tag{220}$$

We will use ψ and u to signify the solution of Schroeder and diffusion equations respectively and use $W_\psi(x,p,t)$ and $W_u(x,p,t)$ for their respective Wigner distributions. When we apply our method to the above equations we obtain

$$\frac{\partial W_\psi}{\partial t} = -2pa\frac{\partial W_\psi}{\partial x} \tag{221}$$

$$\frac{\partial W_u}{\partial t} = \frac{D}{2}\frac{\partial^2 W_u}{\partial x^2} - 2Dp^2 W_u \tag{222}$$

Eq. (221) was first obtained by Wigner and Moyal and its properties have been studied for many years.

It is quite interesting that, while the only difference between the two original equations, Eq. (213) and Eq. (214), is an i, the difference in the Wigner distribution equation of motion is quite dramatic. More importantly we will see that in the Wigner domain both the mathematics and insight become clearer. We point out that the results we present for the Schroeder equation are classic in the work of Wigner, Moyal, and many others, but the results we present for the diffusion equation we believe to be new. We mention that these equations may be related to the respective Fokker-Planck equations but that will not be pursued here.

We point out that the equation for diffusion with drift is

$$\frac{\partial u}{\partial t} + c\frac{\partial u}{\partial x} = D\frac{\partial^2 u}{\partial x^2} \tag{223}$$

and the respective Wigner equation of motion is

$$\frac{\partial W_u}{\partial t} + c\frac{\partial W_u}{\partial x} = \frac{D}{2}\frac{\partial^2 W_u}{\partial x^2} - 2Dp^2 W_u \tag{224}$$

However, no generality is lost by taking the drift term equal to zero because if $u(x,t)$ solves the no drift equation, Eq. (214), then $u(x-ct,t)$ will solve the equation with drift. Similarly, if $W_u(x,p,t)$ satisfies Eq. (222) then $W_u(x-ct,p,t)$ satisfies Eq. (224).

16.1 Green's function

Schroeder equation. Suppose we want to solve the initial value problem for the Schroeder equation. That is, given $\psi(x,0)$ we want $\psi(x,t)$, where $t>0$. The solution is

$$\psi(x,t) = \int G_\psi(x,x',0)\psi(x',0)dx' \tag{225}$$

where $G_\psi(x,x',t)$ is the Green's function,

$$G_\psi(x,x',t) = \frac{1}{\sqrt{4\pi iat}}\exp\left[-\frac{(x-x')^2}{4iat}\right] \tag{226}$$

In momentum space the initial value problem becomes particularly easy. From Eq. (217) we have

$$\phi(p,t) = e^{-iap^2 t}\phi(p,0) \tag{227}$$

Now consider the same problem for the Wigner distribution, that is, given $W(x,p,0)$ we want $W(x,p,t)$. From Eq. (?????) it follows that

$$W_\psi(x,p,t) = W_\psi(x - 2apt, p, 0) \tag{228}$$

a result first obtained by Wigner and Moyal. Thus a remarkable simplification is achieved in phase space. But furthermore in phase space we understand what is going on. It shows that as time progresses the phase space point moves with a constant velocity in the x direction but does not move at all in the p direction. The velocity in the x direction being $2ap$.

Diffusion equation. Now consider the diffusion equation. Using the Green's function approach one has

$$u(x,t) = \int G_u(x,x',t)u(x',0)dx' \tag{229}$$

where

$$G_u(x,x',t) = \frac{1}{\sqrt{4\pi Dt}} \exp\left[-\frac{(x-x')^2}{4Dt}\right] \tag{230}$$

and in momentum space

$$U(p,t) = e^{-Dp^2t}U(p,0) \tag{231}$$

Now consider the Wigner distribution. One can show that

$$W_u(x,p,t) = \frac{1}{\sqrt{2\pi Dt}} e^{-Dp^2t} \int \exp\left[-\frac{(x-x')^2}{2Dt}\right] W_u(x',p,0)dx' \tag{232}$$

In Figs. 19-22 we show the Wigner distribution computed at times $t = 0.01, 0.1, 1, 10$ respectively, and with $D = 100$.

16.2 Wigner distribution of the Green's function

It is of interest to calculate the Wigner distribution of the Green's function for each case. For the Schroeder case

$$G_\psi(x,x',t,t') = \frac{1}{\sqrt{4\pi iat}} \exp\left[-\frac{(x-x')^2}{4iat}\right] \tag{233}$$

the Wigner distribution is (time is assumed to be positive)

$$W_{G_\psi}(x,p,t) = \frac{1}{2\pi}\delta\left(x' - x - 2apt\right) \tag{234}$$

For the diffusion equation where

$$G_u(x,x',t) = \frac{1}{\sqrt{4\pi Dt}} \exp\left[-\frac{(x-x')^2}{4Dt}\right] \tag{235}$$

the Wigner distribution is

$$W_{G_u}(x,p,t) = \frac{1}{\sqrt{8\pi^3 Dt}} \exp\left[-\frac{(x-x')^2}{2Dt} - 2Dtp^2\right] \tag{236}$$

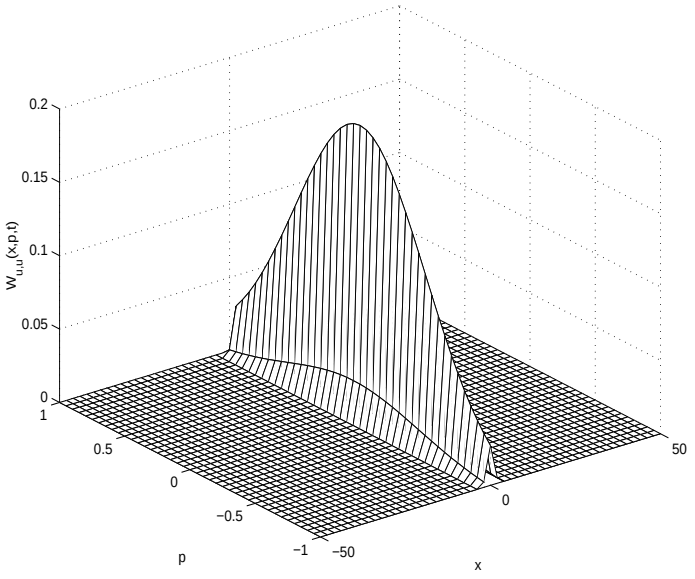

Figure 19: Wigner distribution of the Green's function for the diffusion equation, for $t = 0.01$.

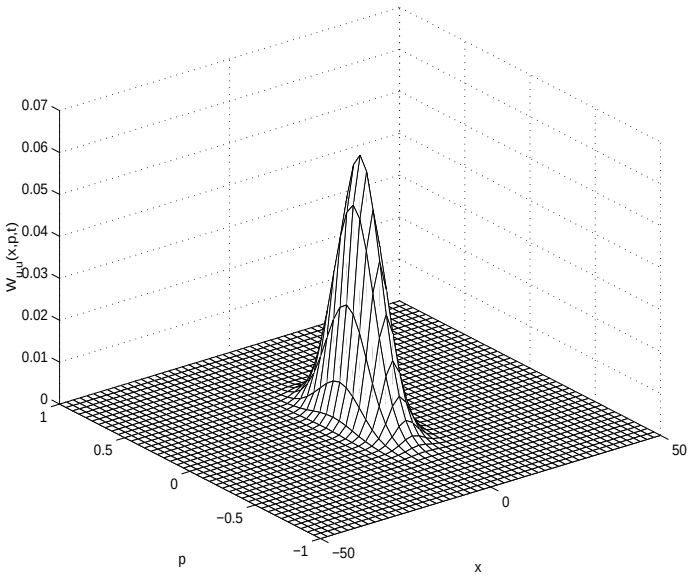

Figure 20: Wigner distribution of the Green's function for the diffusion equation, for $t = 0.1$.

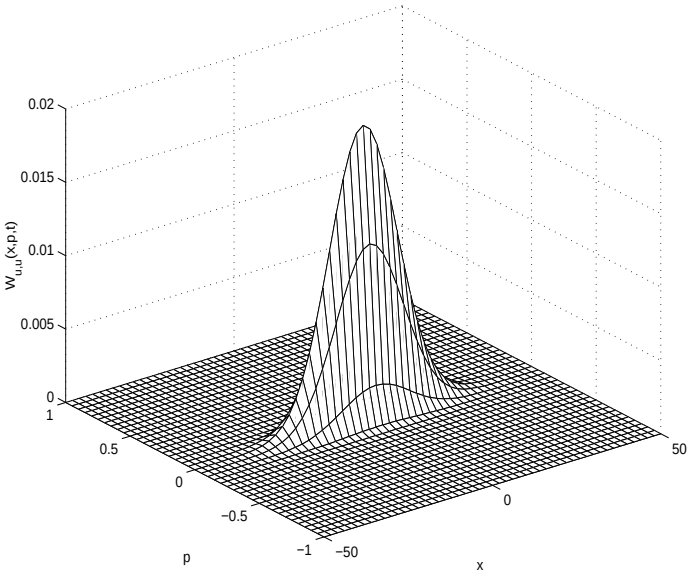

Figure 21: Wigner distribution of the Green's function for the diffusion equation, for $t = 1$.

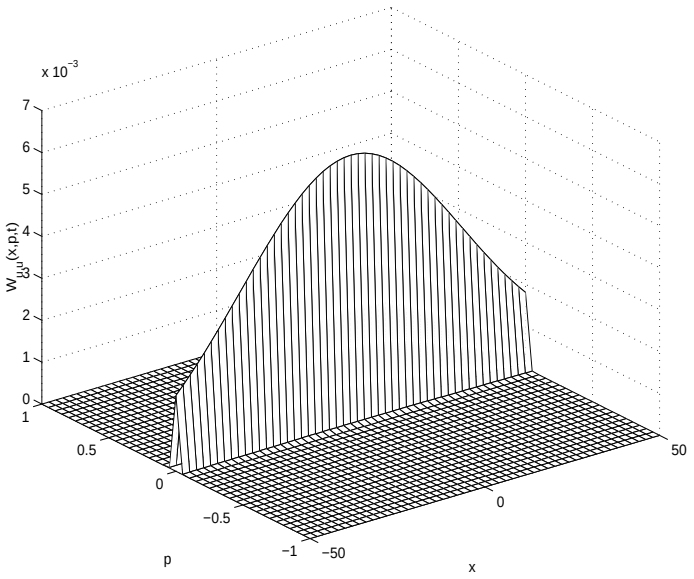

Figure 22: Wigner distribution of the Green's function for the diffusion equation, for $t = 10$.

Thus we see the Wigner distribution shows a significant physical difference between the two Green's functions though superficially the original wave equations and Green's functions are very similar. In the case of $W_{G_\psi}(x,p,t)$, Eq. (234) shows that each spatial point gets transformed by a translation phase space, the translation being $x' \to x + 2apt$. But for the case $G_u(x,x',t)$ we see that each point gets spread/contracted. The position spreads but the momentum contracts!

Example. We take a specific example and we work out the two cases side by side. Take

$$\psi(x,0) = \frac{1}{(2\pi\sigma^2)^{1/4}} \exp\left[-\frac{(x-x_0)^2}{4\sigma^2} + ip_0 x\right] \tag{237}$$

$$u(x,0) = \frac{1}{\sqrt{2\pi\sigma^2}} \exp\left[-\frac{(x-x_0)^2}{2\sigma^2}\right] \tag{238}$$

and we note that the densities in both cases are the same. The respective initial Wigner distributions are calculated to be

$$W_\psi(x,p,0) = \frac{1}{\pi} \exp\left[-\frac{(x-x_0)^2}{2\sigma^2} - 2\sigma^2(p-p_0)^2\right] \tag{239}$$

$$W_u(x,p,0) = \frac{1}{2\pi\sqrt{\pi}\sigma} \exp\left[-\frac{(x-x_0)^2}{\sigma^2} - \sigma^2 p^2\right] \tag{240}$$

Thus, initially, as expected both Wigner distributions are essentially the same. However as time evolves

$$W_\psi(x,p,t) = \frac{1}{2\pi^2} \exp\left[-\frac{(x-2apt-x_0)^2}{2\sigma^2} - 2\sigma^2(p-p_0)^2\right] \tag{241}$$

$$W_u(x,p,t) = \frac{e^{-(2Dt+\sigma^2)p^2}}{4\pi^3\sigma\sqrt{2Dt}} \int \exp\left[-\frac{(x'-x)^2}{2Dt}\right] \exp\left[-\frac{(x'-x_0)^2}{\sigma^2}\right] dx' \tag{242}$$

$$= \frac{1}{4\pi^{5/2}} \frac{1}{\sqrt{2Dt+\sigma^2}} \exp\left[-\frac{(x-x_0)^2}{2Dt+\sigma^2} - (2Dt+\sigma^2)p^2\right] \tag{243}$$

where for the last step we have used

$$\int e^{-\alpha(x-x_1)^2-\beta(x-x_2)^2} dx = \sqrt{\frac{\pi}{\alpha+\beta}} \exp\left[-\frac{\alpha\beta}{\alpha+\beta}(x_1-x_2)^2\right] \tag{244}$$

We now discuss the physical meaning. In the case of the Schroeder equations the Wigner distributions is just rotating. However, for the diffusion case it is spreading in the x direction and contracting in the p direction.

17 Example: diffusion: $\frac{\partial u}{\partial t} + c\frac{\partial u}{\partial x} = D\frac{\partial^2 u}{\partial x^2}$

We show the derivation of the equation of motion for the Wigner distribution for the diffusion equation. We work out the case of diffusion with drift,

$$\frac{\partial u}{\partial t} + c\frac{\partial u}{\partial x} = D\frac{\partial^2 u}{\partial x^2} \tag{245}$$

where $u = u(x,t)$ is the field, c the drift coefficient, and D the diffusion coefficient. To apply our method we first rewrite the equation as

$$\left[\frac{\partial}{\partial t} + c\frac{\partial}{\partial x} - D\frac{\partial^2}{\partial x^2}\right] u(x,t) = 0 \tag{246}$$

We now apply our method and obtain two equations for $Z(x,p,t,\omega)$

$$\left[A_t + cA_x - DA_x^2\right] Z(x,p,t,\omega) = 0 \tag{247}$$

$$\left[B_t + cB_x - DB_x^2\right] Z(x,p,t,\omega) = 0 \tag{248}$$

Expanding the operators we have

$$\left[\frac{1}{2}\frac{\partial}{\partial t} - i\omega + \frac{c}{2}\frac{\partial}{\partial x} - icp - \frac{D}{4}\frac{\partial^2}{\partial x^2} + Dp^2 + iDp\frac{\partial}{\partial x}\right] Z(x,p,t,\omega) = 0 \tag{249}$$

$$\left[\frac{1}{2}\frac{\partial}{\partial t} + i\omega + \frac{c}{2}\frac{\partial}{\partial x} + icp - \frac{D}{4}\frac{\partial^2}{\partial x^2} + Dp^2 - iDp\frac{\partial}{\partial x}\right] Z(x,p,t,\omega) = 0 \tag{250}$$

We add the two equations in order to have a real equation for the Wigner $Z(x,p,t,\omega)$

$$\left[\frac{\partial}{\partial t} + c\frac{\partial}{\partial x} - \frac{D}{2}\frac{\partial^2}{\partial x^2} + 2Dp^2\right] Z(x,p,t,\omega) = 0 \tag{251}$$

This is the equation of motion for $Z(x,p,t,\omega)$. However, since ω does not appear in the equation, we can integrate it out to obtain an equation for the standard Wigner distribution, $W(x,p,t)$,

$$\frac{\partial W}{\partial t} + c\frac{\partial W}{\partial x} = \frac{D}{2}\frac{\partial^2 W}{\partial x^2} - 2Dp^2 W \tag{252}$$

18 Example: Heat Equation

We consider the heat equation

$$a\frac{\partial^2 u(x,t)}{\partial x^2} = \frac{\partial u(x,t)}{\partial t} \tag{253}$$

where a is a real constant. We have hence

$$aA_x^2 Z_{u,u} = A_t Z_{u,u} \tag{254}$$

$$aB_x^2 Z_{u,u} = B_t Z_{u,u} \tag{255}$$

Adding and subtracting these equations we have

$$a\left[A_x^2 \pm B_x^2\right] Z_{u,u} = \left[A_t \pm B_t\right] Z_{u,u} \tag{256}$$

We choose the plus sign to obtain

$$a\left[A_x^2 + B_x^2\right] Z_{u,u} = \frac{\partial Z_{u,u}}{\partial t} \tag{257}$$

But

$$A_x^2 + B_x^2 = \frac{1}{2}\frac{\partial^2}{\partial x^2} + 2p^2 \tag{258}$$

and hence we have that

$$\frac{a}{2}\frac{\partial^2 Z_{u,u}}{\partial x^2} + 2ap^2 Z_{u,u} = \frac{\partial Z_{u,u}}{\partial t} \tag{259}$$

Since ω does not appear in the coefficients we can integrate it out, and we obtain

$$\frac{a}{2}\frac{\partial^2 W_{u,u}}{\partial x^2} + 2ap^2 W_{u,u} = \frac{\partial W_{u,u}}{\partial t} \tag{260}$$

An interesting issue is whether such an equation can be put into a form that is close to the Liouville sin equation as was done with Schroedinger's equation. This is currently being investigated.

19 Example: Burger's Equation

For the Equation

$$a\frac{\partial^2 u(x,t)}{\partial x^2} + \frac{\partial u(x,t)}{\partial t} + c\frac{\partial u(x,t)}{\partial x} = 0 \tag{261}$$

The same derivation as above leads to

$$-\frac{a}{2}\frac{\partial^2 Z_{u,u}}{\partial x^2} + 2ap^2 Z_{u,u} - c\frac{\partial Z_{u,u}}{\partial x} = \frac{\partial Z_{u,u}}{\partial t} \tag{262}$$

20 Example: Wave Equation

We now consider the ordinary wave equation

$$\left[\frac{\partial^2}{\partial x^2} - \frac{1}{c^2}\frac{\partial^2}{\partial t^2}\right] u(x,t) = f(x,t) \tag{263}$$

Applying the methods developed we have that

$$\left[A_x^2 - \frac{1}{c^2}A_t^2\right]\left[B_x^2 - \frac{1}{c^2}B_t^2\right] Z_{u,u}(x,p,t,\omega) = Z_{f,f}(x,p,t,\omega) \tag{264}$$

Substituting the operators, expanding and collecting one has

$$LZ_{u,u}(x,p,t,\omega) = Z_{f,f}(x,p,t,\omega) \tag{265}$$

where

$$L = \frac{1}{16}\left[\frac{\partial^4}{\partial x^4} - \frac{1}{c^2}\left(\frac{\partial^4}{\partial x^2 \partial t^2} + \frac{\partial^4}{\partial t^2 \partial x^2}\right) + \frac{1}{c^4}\frac{\partial^4}{\partial t^4}\right]$$
$$+ \frac{i}{4c^2}\left[\omega\frac{\partial^3}{\partial x^2 \partial t} - p\frac{\partial^3}{\partial x \partial t^2} + p\frac{\partial^3}{\partial t^2 \partial x} - \omega\frac{\partial^3}{\partial t \partial x^2}\right]$$
$$+ \frac{1}{2}p^2\frac{\partial^2}{\partial x^2} - \frac{1}{c^2}\left[-\frac{\omega^2}{2}\frac{\partial^2}{\partial x^2} - \frac{p^2}{2}\frac{\partial^2}{\partial t^2} + p\omega\frac{\partial^2}{\partial x \partial t} + p\omega\frac{\partial^2}{\partial t \partial x}\right]$$
$$+ \frac{1}{2c^4}\omega^2\frac{\partial^2}{\partial t^2} + p^4 - \frac{2}{c^2}p^2\omega^2 + \frac{1}{c^4}\omega^4$$

21 Classical Wave Equation

We want to apply the same method developed for the case of ordinary differential equations to the classic wave equation

$$\left[\frac{\partial^2}{\partial x^2} - \frac{1}{c^2}\frac{\partial^2}{\partial t^2}\right] u(x,t) = f(x,t) \tag{266}$$

One can prove with the same considerations used for ordinary differential equations that the equation for the four dimensional Wigner distribution is

$$\left[A_x^2 - \frac{1}{c^2}A_t^2\right]\left[B_x^2 - \frac{1}{c^2}B_t^2\right] K_{\psi,\psi}(x,p,t,\omega) = K_{f,f}(x,p,t,\omega) \tag{267}$$

However we believe that it is impossible to obtain a differential equation for the three dimensional Wigner distribution in this case. One can convince oneself of this by attempting to do so directly by the same methods that have been applied to the Schroeder equation. Alternatively one attempt to get it is by integrating out ω from Eq. (267). But it is not possible to integrate out ω to obtain an equation for $W(x,p,t)$. This is due to the fact that the operators A_t and B_t contain ω.

22 Random systems

Historically, stochastic processes methods have been developed for the time-invariant stationary case. However, typically in nature stochastic processes are nonstationary, but very little work has been done on this case because of the difficulties involved. Nonstationary processes come about in two general ways. First, is that the physical parameters of the process can vary in time and secondly even for a process that is generally thought to be stationary there is a nonstationary part, the transient, which is usually neglected, but which is very important and interesting. We believe that it is usually neglected because proper methods have not been developed to study it. In what follows we present a new approach that can handle nonstationary stochastic systems. We now motivate the need for this development by examples. Many systems are described by differential equations that have a

driving function that is random and in particular the driving function is often white noise. The output of such systems is also "noise", but it is generally colored noise and may be time-varying. Such differential equations are stochastic differential equations and of course the most venerable is the original equation of Langevin to describe Brownian motion, and also the standard Wiener process is such a system. When the output of such differential equations is stationary, then the description is given by the power spectrum. However, since it is generally the case that the output is nonstationary at least for a certain interval of time, a generalization of the power spectrum is needed. We present a method that allows one to study situations where indeed the output is nonstationary and also colored. Using the methods presented we will study some important cases and in particular we will derive new time-varying spectral properties of nonstationary random processes.

Suppose we have a differential equation that governs the process $\boldsymbol{x}(t)$[4]

$$a_n \frac{d^n \boldsymbol{x}(t)}{dt^n} + a_{n-1} \frac{d^{n-1} \boldsymbol{x}(t)}{dt^{n-1}} \cdots + a_1 \frac{d\boldsymbol{x}(t)}{dt} + a_0 \boldsymbol{x}(t) = \boldsymbol{f}(t) \tag{268}$$

and where $\boldsymbol{f}(t)$ is white Gaussian noise with

$$E[\boldsymbol{f}(t)] = 0 \tag{269}$$

$$R_{\boldsymbol{f}}(t_1, t_2) = E[\boldsymbol{f}(t_1)\boldsymbol{f}(t_2)] = N_0 \delta(t_1 - t_2) \tag{270}$$

and where $E[\ ]$ is the ensemble averaging operator. We consider systems defined by Eq. (268) where we take the coefficients to be constants. Our aim is to understand the spectrum of the output, $\boldsymbol{x}(t)$. As mentioned, the spectrum will in general be colored and nonstationary. We use the Wigner-Ville approach for describing such time-varying spectra. The Wigner distribution of a deterministic signal $x(t)$ is [**?**, **?**]

$$W_x(t, \omega) = \frac{1}{2\pi} \int x^*(t - \tau/2) x(t + \tau/2) e^{-i\tau\omega} d\tau \tag{271}$$

The Wigner-Ville spectrum of a random process $\boldsymbol{x}(t)$ is defined as the ensemble average of the Wigner distribution of $\boldsymbol{x}(t)$ [5] [**?**, **?**]

$$\overline{W}_{\boldsymbol{x}}(t, \omega) = \frac{1}{2\pi} \int E[\boldsymbol{x}^*(t - \tau/2) \boldsymbol{x}(t + \tau/2)] e^{-i\tau\omega} d\tau \tag{272}$$

23 Nonstationary stochastic system

Our aim is to obtain the equation of motion for the Wigner spectrum for a stochastic process that is the solution of an ordinary stochastic differential equation

$$a_n \frac{d^n \boldsymbol{x}(t)}{dt^n} + a_{n-1} \frac{d^{n-1} \boldsymbol{x}(t)}{dt^{n-1}} \cdots + a_1 \frac{d\boldsymbol{x}(t)}{dt} + a_0 \boldsymbol{x}(t) = \boldsymbol{f}(t) \tag{273}$$

[4] We use bold symbols for stochastic quantities.

[5] We use the following simplified notation $\int \equiv \int_{-\infty}^{+\infty}$

where $\boldsymbol{f}(t)$ is a given stochastic process. One could solve this equation for $\boldsymbol{x}(t)$ and then find the ensemble average as needed to calculate the Wigner spectrum in Eq. (272), and then do the integration as required. This is generally a difficult procedure. We have developed a method that is more direct: we obtain the equation of evolution for the Wigner spectrum and solve it [**?**, **?**, **?**, **?**]. To accomplish that we write the differential equation in polynomial form

$$P(D)\boldsymbol{x}(t) = \boldsymbol{f}(t) \tag{274}$$

where, as usual, D and $P(D)$ are respectively

$$D = \frac{d}{dt} \tag{275}$$

$$P(D) = a_n D^n + a_{n-1} D^{n-1} ... + a_1 D + a_0 \tag{276}$$

The differential equation for the Wigner spectrum $\overline{W}_{\boldsymbol{x}}(t,\omega)$, of $\boldsymbol{x}(t)$, is then given by

$$P^*(A)P(B)\overline{W}_{\boldsymbol{x}}(t,\omega) = \overline{W}_{\boldsymbol{f}}(t,\omega) \tag{277}$$

where

$$A = \frac{1}{2}\frac{\partial}{\partial t} - i\omega \quad ; \quad B = \frac{1}{2}\frac{\partial}{\partial t} + i\omega \tag{278}$$

For the case of time dependent coefficients

$$a_n(t)\frac{d^n\boldsymbol{x}(t)}{dt^n} + a_{n-1}(t)\frac{d^{n-1}\boldsymbol{x}(t)}{dt^{n-1}} + \ldots + a_1(t)\frac{d\boldsymbol{x}(t)}{dt} + a_0(t)\boldsymbol{x}(t) = \boldsymbol{f}(t) \tag{279}$$

where $a_0(t), \ldots, a_n(t)$ are time-varying deterministic coefficients. We rewrite Eq. (279) in polynomial notation

$$P(D,t)\boldsymbol{x}(t) = \boldsymbol{x}(t) \tag{280}$$

where now

$$P(D,t) = a_n(t)D^n + a_{n-1}(t)D^{n-1} + \ldots + a_1(t)D + a_0(t) \tag{281}$$

The equation for the Wigner spectrum is

$$P^*(A,\mathcal{E})P(B,\mathcal{F})\overline{W}_{\boldsymbol{x}}(t,\omega) = \overline{W}_{\boldsymbol{f}}(t,\omega) \tag{282}$$

Eq. (282) is a partial differential equation in time and frequency.

24 Example: The Nonstationary Wiener Process

We now apply our method to the Wiener process [**?**]

$$\frac{d\boldsymbol{x}(t)}{dt} = \boldsymbol{f}(t) \tag{283}$$

with initial conditions $\boldsymbol{x}(0) = \boldsymbol{x}_0$, where $\boldsymbol{x}_0$ is a stochastic variable. We will turn the system on at a finite time and hence we will obtain the complete solution of the problem. That is we will get the total solution, including the transient behavior. First we point out that for Eq. (283) the power spectrum is given by

$$P_{\boldsymbol{x}}(\omega) = \frac{N_0}{\sqrt{2\pi}} \frac{1}{\omega^2} \tag{284}$$

It is important to appreciate that the $1/\omega^2$ spectrum for the Wiener process is reached in either of two different ways:

1. The initial condition is set to zero at $t = 0$ and by taking $t = \infty$ in the general solution of Eq. (283);

2. Alternatively by setting the initial condition to zero at $t = -\infty$ and this has the effect of the passage of an infinite amount of time.

For both types of initial conditions the stationary spectrum is reached because an infinite amount of time has passed. Using our method we will obtain the full solution, that is the full evolution of the instantaneous spectrum. Rewriting Eq. (283) in the polynomial form of Eq. (274)

$$D\boldsymbol{x}(t) = \boldsymbol{f}(t) \tag{285}$$

and using Eq. (277) we obtain

$$AB\overline{W}_{\boldsymbol{x}}(t,\omega) = \overline{W}_{\boldsymbol{f}}(t,\omega) \tag{286}$$

Using the definitions of the operators we have that

$$AB = \frac{1}{4}\frac{\partial^2}{\partial t^2} + \omega^2 \tag{287}$$

and hence

$$\frac{1}{4}\frac{\partial^2 \overline{W}_{\boldsymbol{x}}(t,\omega)}{\partial t^2} + \omega^2 \overline{W}_{\boldsymbol{x}}(t,\omega) = \overline{W}_{\boldsymbol{f}}(t,\omega) \tag{288}$$

where $\overline{W}_{\boldsymbol{f}}(t,\omega)$ is the Wigner spectrum of $\boldsymbol{f}(t)$. If $\boldsymbol{f}(t)$ is white Gaussian noise with autocorrelation

$$R_{\boldsymbol{f}}(\tau) = N_0\delta(\tau) \tag{289}$$

then one can readily show that

$$\overline{W}_{\boldsymbol{f}}(t,\omega) = \frac{N_0}{2\pi} \tag{290}$$

and hence

$$\frac{1}{4}\frac{\partial^2 \overline{W}_{\boldsymbol{x}}(t,\omega)}{\partial t^2} + \omega^2 \overline{W}_{\boldsymbol{x}}(t,\omega) = \frac{N_0}{2\pi} \tag{291}$$

The exact solution to Eq. (291) is

$$\overline{W}_{\boldsymbol{x}}(t,\omega) = \frac{N_0}{2\pi\omega^2}\left[1 - \cos 2\omega t\right] + \frac{E[\boldsymbol{x}_0^2]}{\pi\omega}\sin 2\omega t, \qquad t \geq 0 \tag{292}$$

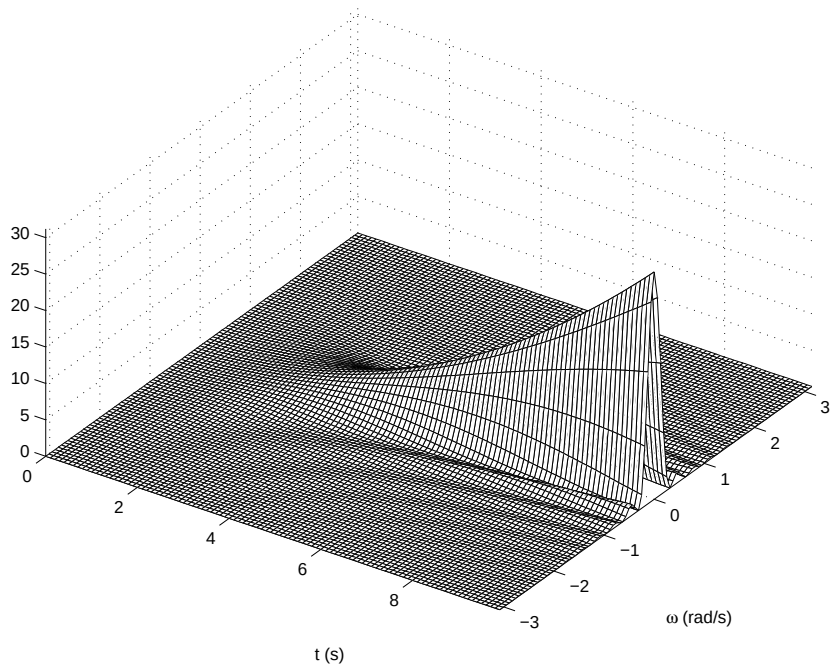

Figure 23: The instantaneous spectrum of the Wiener process defined in Eq. (283). The spectrum grows to infinity at $\omega = 0$ and reaches the singularity in the classical frequency spectrum that has a $1/\omega^2$ distribution. Notice that the Wigner spectrum, given in Eq. (293), is nonnegative.

and $\overline{W}_{\boldsymbol{x}}(t,\omega) \equiv 0$ when $t < 0$. For $E[\boldsymbol{x}_0^2] = 0$ one has

$$\overline{W}_{\boldsymbol{x}}(t,\omega) = \frac{N_0}{2\pi\omega^2}\left[1 - \cos 2\omega t\right] = \frac{N_0}{\pi}\frac{\sin^2 \omega t}{\omega^2} \tag{293}$$

In Fig. 23 we show the transient of the Wiener process.

It is interesting to note that for $\omega \to 0$

$$\lim_{\omega\to 0} \overline{W}_{\boldsymbol{x}}(t,\omega) = \lim_{\omega\to 0} \frac{N_0}{2\pi\omega^2}\left[1 - \cos 2\omega t\right] = \frac{N_0}{\pi} t^2 \tag{294}$$

and hence at $\omega = 0$ the instantaneous spectrum grows to infinity and approaches the singularity in the classical power spectrum of Eq. (284) with a second order in time.

24.1 Direct Solution

We now show how to obtain the same solution by the direct method which is essentially a brute force method. The Wiener equation is first rewritten as

$$\frac{d\boldsymbol{x}(t)}{dt} = u(t)\boldsymbol{f}(t) \tag{295}$$

where $u(t)$ is the Heaviside step function, defined as

$$u(t) = \begin{array}{ll} 0, & t < 0 \\ 1 & t \geq 0 \end{array} \tag{296}$$

The use of the step function makes the calculation much easier. Now, we write the solution to Eq. (295) as

$$\boldsymbol{x}(t) = u(t) \left[\boldsymbol{x}_0 + \int_0^t u(t') \boldsymbol{f}(t') dt' \right] \tag{297}$$

To obtain the Wigner spectrum we will make use of the following relation of the Wigner spectrum with the autocorrelation function, $R_{\boldsymbol{x}}(t_1, t_2)$,

$$\overline{W}_{\boldsymbol{x}}(t, \omega) = \int R_{\boldsymbol{x}}(t + \tau/2, t - \tau/2) e^{-i\tau\omega} d\tau \tag{298}$$

Hence, we need to evaluate the autocorrelation directly

$$R_{\boldsymbol{x}}(t_1, t_2) = E[\boldsymbol{x}(t_1) \boldsymbol{x}^*(t_2)] \tag{299}$$

$$= u(t_1) u(t_2) \left[E[\boldsymbol{x}_0^2] + \int_0^{t_1} \int_0^{t_2} R_{\boldsymbol{f}}(t_1', t_2') dt_1' dt_2' \right] \tag{300}$$

where the cross-terms have disappeared because $E[\boldsymbol{f}(t)] = 0$. By substituting $R_{\boldsymbol{f}}(t_1', t_2')$ from Eq. (270) one obtains

$$R_{\boldsymbol{x}}(t_1, t_2) = u(t_1) u(t_2) \min(t_1, t_2) \tag{301}$$

Now, one applies Eq. (298) to obtain

$$\overline{W}_{\boldsymbol{x}}(t, \omega) = \int u(t + \tau/2) u(t - \tau/2) \left(\min(t + \tau/2, t - \tau/2) + E[\boldsymbol{x}_0^2] \right) e^{-i\tau\omega} d\tau \tag{302}$$

and after some manipulation and simplification (shown in the next Section) one has

$$\overline{W}_{\boldsymbol{x}}(t, \omega) = \frac{N_0}{2\pi\omega^2} \left[1 - \cos 2\omega t \right] + \frac{E[\boldsymbol{x}_0^2]}{\pi\omega} \sin 2\omega t, \qquad t \geq 0 \tag{303}$$

which is precisely Eq. (292). We note that $\overline{W}_{\boldsymbol{x}}(t, \omega) \equiv 0$ for negative times.

24.2 Direct derivation of the Wiener process

We now give the details of the derivation of the direct approach leading to Eq. (272). We start from Eq. (299). By substituting Eq. (270) into Eq. (300) we have

$$R_{\boldsymbol{x}}(t_1, t_2) = u(t_1) u(t_2) \left[E[\boldsymbol{x}_0^2] + \int_0^{t_1} \int_0^{t_2} N_0 \delta(t_1' - t_2') dt_1' dt_2' \right] \tag{304}$$

Now, if $t_1 < t_2$ we have that

$$R_{\boldsymbol{x}}(t_1, t_2) = u(t_1) u(t_2) \left[E[\boldsymbol{x}_0^2] + N_0 t_1 \right] \tag{305}$$

while if $t_2 < t_1$

$$R_{\boldsymbol{x}}(t_1, t_2) = u(t_1)u(t_2)\left[E[\boldsymbol{x}_0^2] + N_0 t_2\right] \tag{306}$$

which can be combined into one expression,

$$R_{\boldsymbol{x}}(t_1, t_2) = u(t_1)u(t_2)\left[E[\boldsymbol{x}_0^2] + N_0 \min(t_1, t_2)\right] \tag{307}$$

Also, it is convenient to write,

$$R_{\boldsymbol{x}}(t_1, t_2) = u(t_1)u(t_2)\left[E[\boldsymbol{x}_0^2] + N_0 \left(u(t_1 - t_2)t_2 + u(t_2 - t_1)t_1\right)\right] \tag{308}$$

Now we apply Eq. (298) that links the autocorrelation to the Wigner spectrum

$$\overline{W}_{\boldsymbol{x}}(t, \omega) = \underbrace{\frac{E[\boldsymbol{x}_0^2]}{2\pi}\int u(t + \tau/2)u(t - \tau/2)e^{-i\tau\omega}d\tau}_{I_1} + \tag{309}$$

$$\underbrace{\frac{N_0}{2\pi}\int u(t + \tau/2)u(t - \tau/2)u(\tau)(t - \tau/2)e^{-i\tau\omega}d\tau}_{I_2} + \tag{310}$$

$$\underbrace{\frac{N_0}{2\pi}\int u(t + \tau/2)u(t - \tau/2)u(\tau)(t + \tau/2)e^{-i\tau\omega}d\tau}_{I_3} \tag{311}$$

We solve the three integrals separately. Starting with the first, we have that

$$I_1 = u(t)\frac{E[\boldsymbol{x}_0^2]}{2\pi}\int_{-2t}^{2t} e^{-i\tau\omega}d\tau \tag{312}$$

$$= u(t)E[\boldsymbol{x}_0^2]\frac{\sin 2t\omega}{\pi\omega} \tag{313}$$

For the second

$$I_2 = u(t)\frac{N_0}{2\pi}\int_0^{2t}(t - \tau/2)e^{-i\tau\omega}d\tau \tag{314}$$

which after a few calculations becomes

$$I_2 = u(t)\frac{N_0}{2\pi}\left[t\frac{1 - e^{-i2t\omega}}{i\omega} - \frac{1}{2}\left[e^{-i2t\omega}\left(\frac{1}{\omega^2} - \frac{2t}{i\omega}\right) - \frac{1}{\omega^2}\right]\right] \tag{315}$$

With a similar procedure one has that

$$I_3 = u(t)\frac{N_0}{2\pi}\int_{-2t}^{0}(t + \tau/2)e^{-i\tau\omega}d\tau \tag{316}$$

$$= u(t)\frac{N_0}{2\pi}\int_0^{2t}(t - \tau/2)e^{i\tau\omega}d\tau \tag{317}$$

which evaluates to

$$I_3 = u(t)\frac{N_0}{2\pi}\left[t\frac{1 - e^{-i2t\omega}}{i\omega} - \frac{1}{2}\left[e^{i2t\omega}\left(\frac{1}{\omega^2} + \frac{2t}{i\omega}\right) - \frac{1}{\omega^2}\right]\right] \tag{318}$$

Note that

$$I_2 + I_3 = u(t)\frac{N_0}{2\pi\omega^2}[1 - \cos 2t\omega] \tag{319}$$

and now adding to I_1 we obtain

$$\overline{W}_{\boldsymbol{x}}(t,\omega) = u(t)\left[\frac{N_0}{2\pi\omega^2}\left[1 - \cos 2\omega t\right] + \frac{E[\boldsymbol{x}_0^2]}{\pi\omega}\sin 2\omega t\right] \tag{320}$$

which is Eq. (303) of the text. We note that the phase space method used before is much easier.

25 Example: The full exact solution to the Langevin Equation

Our aim is to show how to find the transient spectrum of the Langevin equation

$$\frac{d\boldsymbol{v}(t)}{dt} + \beta\boldsymbol{v}(t) = \boldsymbol{f}(t) \tag{321}$$

where $\boldsymbol{f}(t)$ is white Gaussian noise. We apply our method by first rewriting the Langevin equation in polynomial form

$$[D + \beta]\boldsymbol{v}(t) = \boldsymbol{f}(t) \tag{322}$$

Using our method the equation for the Wigner spectrum is now

$$[A + \beta][B + \beta]\overline{W}_{\boldsymbol{x}}(t,\omega) = \overline{W}_{\boldsymbol{f}}(t,\omega) \tag{323}$$

We substitute for the operators A and B from Eq. (278) to obtain

$$\frac{1}{4}\frac{\partial^2}{\partial t^2}\overline{W}_{\boldsymbol{x}}(t,\omega) + \beta\frac{\partial}{\partial t}\overline{W}_{\boldsymbol{x}}(t,\omega) + (\beta^2 + \omega^2)\overline{W}_{\boldsymbol{x}}(t,\omega) = \overline{W}_{\boldsymbol{f}}(t,\omega) \tag{324}$$

where $\overline{W}_{\boldsymbol{f}}(t,\omega)$ is the Wigner spectrum of the input random process $\boldsymbol{f}(t)$.

The solution to Eq. (324) can be found with the standard methods for differential equations. It is

$$\overline{W}_{\boldsymbol{v}}(t,\omega) = \frac{1}{\pi}\left(E[\boldsymbol{v}_0^2] - \frac{N_0}{2\beta}\right)e^{-2\beta t}\frac{\sin 2\omega t}{\omega} + \frac{N_0}{2\pi}\frac{1}{\beta^2+\omega^2} - \frac{N_0}{2\pi}\frac{e^{-2\beta t}}{\beta^2+\omega^2}\left(\cos 2\omega t - \omega/\beta \sin 2\omega t\right) \qquad ; t \geq 0 \tag{325}$$

and where $\overline{W}_{\boldsymbol{v}}(t,\omega) \equiv 0$ for negative times. In the solution we are considering a random initial condition $\boldsymbol{v}_0$, that is

$$\boldsymbol{v}(0) = \boldsymbol{v}_0 \tag{326}$$

This solution allows us to understand the transient behavior of the Langevin equation. In Fig. 24 we show a typical case. We see that the instantaneous spectrum has an overshoot effect at the beginning of the transient. Also the spread of the solution is larger for small times. Then the solution rapidly approaches the stationary spectrum, the well known Lorentzian distribution. The

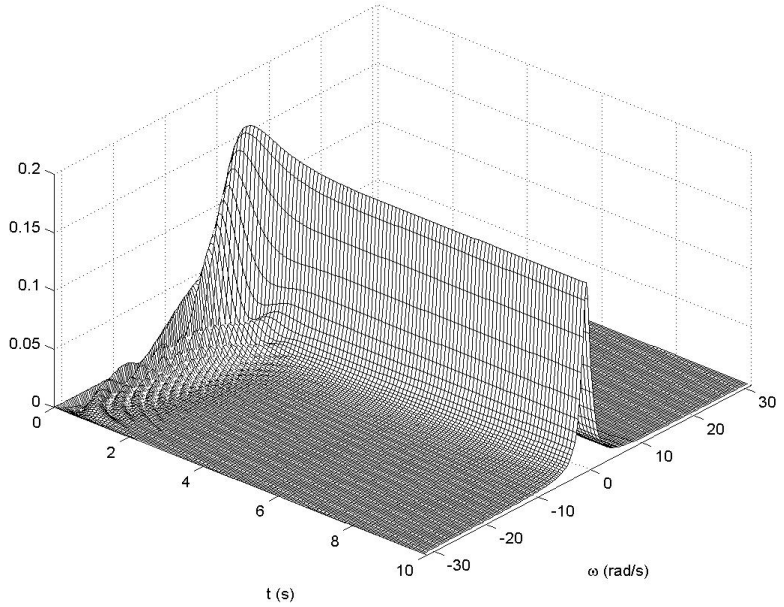

Figure 24: The complete instantaneous spectrum of Brownian motion, given in Eq. (325). Notice the overshoot at the beginning of the transient, and the increased spread of the Wigner spectrum. As $t \to \infty$ the Wigner spectrum reaches the stationary solution, that is the Lorentzian distribution of Eq. (327).

behavior of the frequencies in the transient suggests the possibility of designing systems so to have smooth transitions of the instantaneous spectrum from zero to the stationary solution. This can be a fundamental issue in minimizing the electromagnetic interference of an electronic device that is suddenly turned off, or in reducing the risk of breaking down an engine or a vibrating structure by a sudden rough start. These two physical situations are just an example of the importance of transients in designing and understanding a physical systems. We note that as time goes to infinity we have that

$$\lim_{t\to 0} \overline{W}_{\boldsymbol{v}}(t,\omega) = \frac{N_0}{\beta_0^2+\omega^2} \tag{327}$$

which is the classical Wang-Uhlenbeck result.

26 Example: Quantum Langevin Equation

The quantum Langevin equation is

$$m\frac{d^2\mathbf{x}(t)}{dt^2} + m\beta\frac{d\mathbf{x}(t)}{dt} + V'(\mathbf{x}) = \xi(t) \tag{328}$$

where $\mathbf{x}$ is the position operator, $V(\mathbf{x})$, the external potential, and $\xi(t)$ is the noise operator that satisfies

$$\left\langle [\xi(t),\xi(t')]_+ \right\rangle = \frac{\gamma\hbar}{\pi}\int_{-\infty}^{\infty} \omega e^{i\omega(t-t')}\coth\frac{\hbar\omega}{2kT}d\omega \tag{329}$$

If one considers Eq. (328) as a classical type equation then it is called the *quasi-classical* Langevin equation. In such a case one replaces the operators by ordinary variables

$$m\frac{d^2x(t)}{dt^2} + m\beta\frac{dx(t)}{dt} + V'(x) = \xi(t) \tag{330}$$

and the autocorrelation function is then

$$R(\tau) = \frac{\gamma\hbar}{2\pi}\int_{-\infty}^{\infty} \omega e^{i\omega\tau}\coth\frac{\hbar\omega}{2kT}d\omega \tag{331}$$

We consider here the case of no external potential and rewrite Eq. (328) as

$$\dot{p}(t) + \beta p(t) = \xi(t) \tag{332}$$

with

$$R_\xi(\tau) = 2DZ\int_{-\infty}^{\infty} \omega e^{i\omega\tau}\coth Z\omega d\omega \tag{333}$$

and

$$Z = \frac{\hbar}{2kT} \tag{334}$$

Using the standard Wiener-Khinchen theorem the power spectrum is given by

$$S_\xi(\omega) = 2DZ\omega\coth Z\omega \tag{335}$$

We note that as $Z \to 0$

$$\lim_{Z\to 0} R_\xi(\tau) = 2D\delta(\tau) \tag{336}$$

Using our general approach we have that the differential equation for the Wigner spectrum is

$$\left[\frac{1}{4}\frac{\partial^2}{\partial t^2} + \beta\frac{\partial}{\partial t} + \beta^2 + \omega^2\right]\overline{W}_p(t,\omega) = \frac{DZ}{\pi}\omega\coth Z\omega \tag{337}$$

The exact solution is

$$\overline{W}_p(t,\omega) = \frac{W_\xi}{\beta^2+\omega^2}\left[1 - e^{-\frac{2\gamma}{m}t}\cos 2\omega t\right] \tag{338}$$

$$= \frac{1}{\beta^2+\omega^2}\frac{DZ}{\pi}\omega\coth Z\omega\left[1 - e^{-\frac{2\gamma}{m}t}\cos 2\omega t\right] \tag{339}$$

We see that Eq. (339) can now be thought of as the generalization of the Wang and Uhlenbeck process for quantum noise.

The quantum Wiener process is obtained by taking $\gamma = 0$ and hence the differential equation is

$$\dot{p}(t) = \xi(t) \tag{340}$$

The governing equation is

$$\frac{1}{4}\frac{\partial^2\overline{W}_p(t,\omega)}{\partial t^2} + \omega^2\overline{W}_p(t,\omega) = \frac{DZ}{\pi}\omega\coth Z\omega \tag{341}$$

giving

$$W_p(t,\omega) = \frac{DZ}{\pi}\omega\coth Z\omega(1-\cos 2\omega t) \tag{342}$$

$$= \frac{2DZ}{\pi}\omega\coth Z\omega\sin^2\omega t \tag{343}$$

27 Example: Time-variant random systems

In many physical situations a random process can be seen as the output of a random system whose parameters change with time. The variation can be due to a sudden breakdown, aging, or cyclic variations of temperature, humidity, and other physical quantities that can influence the system behavior. In these cases the process is inherently nonstationary.

We now consider the case addressed by a time-dependent Brownian motion process

$$\frac{d\boldsymbol{v}(t)}{dt} + \beta(t)\boldsymbol{v}(t) = \boldsymbol{f}(t) \tag{344}$$

We rewrite it in polynomial notation

$$[D + \beta(t)]\boldsymbol{v}(t) = \boldsymbol{f}(t) \tag{345}$$

where we take $\beta(t)$ to be time-dependent with a linear law

$$\beta(t) = \beta_0 + \epsilon t \tag{346}$$

and also we take $\epsilon \ll 1$. These conditions imply a slow variation with time. We now transform the equation in time to an equation in time-frequency, using Eq. (282) to obtain

$$\left[\frac{1}{4}\frac{\partial^2}{\partial t^2} + \frac{\epsilon^2}{4}\frac{\partial^2}{\partial \omega^2} + \beta(t)\frac{\partial}{\partial t} + \epsilon\omega\frac{\partial}{\partial \omega} + \beta^2(t) + \omega^2\right]\overline{W}_{\boldsymbol{v}}(t,\omega) = \frac{N_0}{2\pi} \tag{347}$$

Taking into account that ϵ is small, we neglect the terms containing ϵ,

$$\left[\frac{1}{4}\frac{\partial^2}{\partial t^2} + \beta(t)\frac{\partial}{\partial t} + \beta^2(t) + \omega^2\right]\overline{W}_{\boldsymbol{v}}(t,\omega) = \frac{N_0}{2\pi} \tag{348}$$

Since there are no derivatives with respect to ω, we can solve this equation as an ordinary differential equation with respect to time. We have to choose the initial conditions, which we fix using the following reasoning. We assume that the system was started at $-\infty$ with $\beta = \beta_0$ and hence it has reached equilibrium. At $t = 0$ we turn on the time dependence as given by Eq. (346). Therefore the initial conditions to Eq. (348) are

$$\overline{W}_{\boldsymbol{v}}(0,\omega) = \frac{N_0}{\beta_0^2 + \omega^2} \tag{349}$$

$$\frac{\partial}{\partial t}\overline{W}_{\boldsymbol{v}}(t,\omega) = 0, \quad t = 0 \tag{350}$$

The first initial condition, Eq. (349), is the Wigner spectrum of the stationary solution. This stationary distribution has been reached because an infinite amount of time has passed since the system was turned on at $t = -\infty$. As a consequence of being in a stationary phase before $t = 0$ there must be no change in time of the instantaneous spectrum. This condition is stated by Eq. (350).

Using these initial conditions Eq. (348) can be easily solved with numerical algorithms. In Fig. 25 we plot the solution $\overline{W}_{\boldsymbol{v}}(t,\omega)$. In Fig. 26 a numerical simulation of the Wigner spectrum is shown. The agreement confirms our approach.

The behavior of the instantaneous spectrum is in accordance with intuition. The shape of the Wigner spectrum is in fact very similar to a Lorentzian distribution, for any given time. A similarity with the lowpass filter represented by the RC circuit can be used to explain the change in spread that the instantaneous spectrum exhibits. An RC circuit driven by white noise has the same equation of Brownian motion. In this case we can think of a time-varying RC circuit, where the time constant $\tau = RC$ is a function of time, $\tau = \tau(t)$. It is well known that when τ is large, the RC filter has a strong lowpass behavior, which corresponds to a small spread of the Lorentzian spectrum. On the contrary, when τ is small, the RC circuit has a weak lowpass behavior. Since the time constant is related to the β coefficient by an inverse proportionality, the increase of the β coefficient, which we assumed for our case, turns out to be a decrease of the τ constant. Therefore we expect the time-varying system under study to become a weaker lowpass filter as time goes by, which is precisely what happens in Fig. 25.

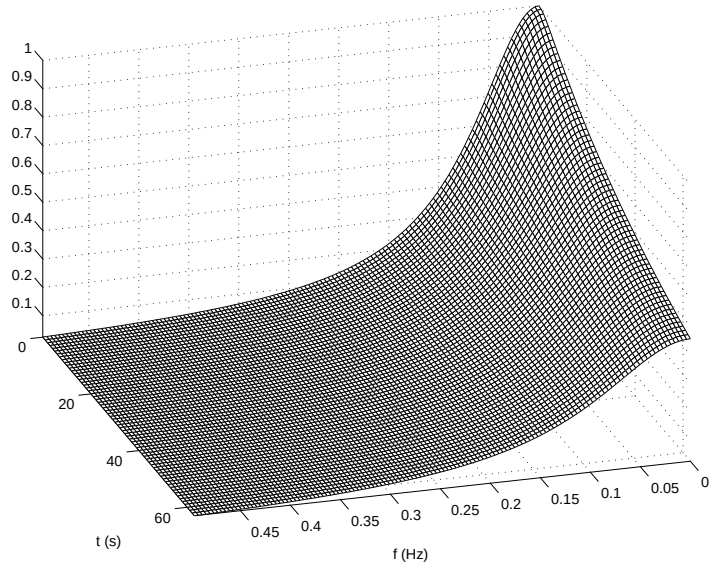

Figure 25: Approximated Wigner spectrum of a time-varying Brownian motion.

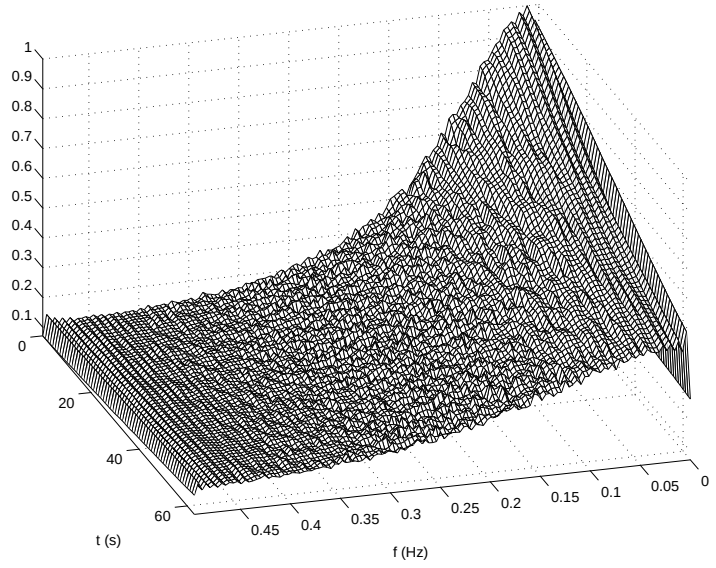

Figure 26: Simulated Wigner spectrum of a time-varying Brownian motion.

28 Example: oscillator with constant coefficients

We consider the case of a harmonic oscillator with constant coefficients and random Gaussian noise as input,

$$\frac{d^2\boldsymbol{x}}{dt^2} + 2\mu\frac{d\boldsymbol{x}}{dt} + \omega_0^2\boldsymbol{x} = \boldsymbol{f}(t) \tag{351}$$

where we choose a Gaussian noise $\boldsymbol{f}(t)$ with zero mean and autocorrelation $R_{\boldsymbol{f}}(\tau) = N_0\delta(\tau)$. Our intention is to study how the frequency in the random output $\boldsymbol{x}(t)$ of the systems are distributed in time, that is the instantaneous power spectrum as defined by the Wigner spectrum. Of course for this case we expect the spectrum to be constant in time. First we consider the problem by standard methods and then apply our method and compare. Subsequently we consider the problem where we make one of the constants time dependent, and of course the standard method can not deal with that situation.

28.1 Standard result

We recall the standard result for the classical power spectrum $G_{\boldsymbol{x}}(\omega)$ of $\boldsymbol{x}(t)$, defined as usual as the Fourier transform of the autocorrelation function $R_{\boldsymbol{x}}(\tau)$

$$G_{\boldsymbol{x}}(\omega) = |H(\omega)|^2\, G_{\boldsymbol{f}}(\omega) \tag{352}$$

where $H(\omega)$ is the transfer function of the system, simply obtained by evaluating the polynomial version of Eq. (268) in $i\omega$, that is

$$H(\omega) = P(i\omega) \tag{353}$$

(Notice that with constant coefficients the polynomial is not a function of time anymore). Since the power spectrum of the Gaussian noise is constant and equal to $G_{\boldsymbol{f}}(\omega) = N_0$, we obtain from Eqs. (352)-(353)

$$G_{\boldsymbol{x}}(\omega) = \frac{N_0}{(\omega_0^2 - \omega^2)^2 + 4\mu^2\omega^2} \tag{354}$$

This is the result obtained by Wang and Uhlenbeck [**?**]. In Fig. 27 we represent the obtained power spectrum $G_x(\omega)$ when the following set of parameters is chosen

$$\mu = 1 \tag{355}$$

$$\omega_0 = 2\pi \tag{356}$$

$$N_0 = 1 \tag{357}$$

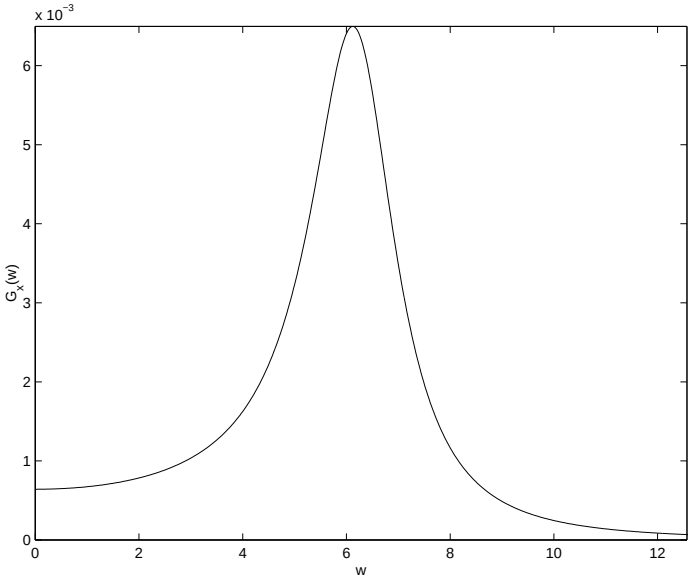

Figure 27: Power spectrum of the state variable $\boldsymbol{x}(t)$ of the harmonic oscillator of Eq. 351. Notice the bandpass behavior of the function.

We point out the bandpass behavior of the power spectrum, that selectively filters the input frequencies contained in the random noise $\boldsymbol{f}(t)$.

28.2 Wigner spectrum

We now obtain the equation for the Wigner spectrum by applying our method. We rewrite Eq. (351) in polynomial notation

$$\left[D^2 + 2\mu D + \omega_0^2\right] \boldsymbol{x}(t) = \boldsymbol{f}(t) \tag{358}$$

and we apply the transformation to the Wigner spectrum domain, having

$$\left[A^2 + 2\mu A + \omega_0^2\right] \left[B^2 + 2\mu B + \omega_0^2\right] \overline{W}_{\boldsymbol{x}}(t,\omega) = \overline{W}_{\boldsymbol{f}}(t,\omega) \tag{359}$$

This is a partial differential equation of fourth order, that can be written in the following general way

$$\left[b_4 \frac{\partial^4}{\partial t^4} + b_3 \frac{\partial^3}{\partial t^3} + b_2 \frac{\partial^2}{\partial t^2} + b_1 \frac{\partial}{\partial t} + b_0\right] \overline{W}_{\boldsymbol{x}}(t,\omega) = \overline{W}_{\boldsymbol{f}}(t,\omega) \tag{360}$$

One can show that the coefficient b_0 is inversely proportional to the square modulus of the transfer function

$$b_0 = \left(|H(\omega)|^2\right)^{-1} \tag{361}$$

This means that in general Eq. (360) can be written as

$$\left[b_4\frac{\partial^4}{\partial t^4}+b_3\frac{\partial^3}{\partial t^3}+b_2\frac{\partial^2}{\partial t^2}+b_1\frac{\partial}{\partial t}+\left(|H(\omega)|^2\right)^{-1}\right]\overline{W}_{\boldsymbol{x}}(t,\omega)=\overline{W}_{\boldsymbol{f}}(t,\omega) \tag{362}$$

As can be easily seen, the Wigner spectrum of white noise is a (two-dimensional) constant function

$$\overline{W}_{\boldsymbol{f}}(t,\omega)=N_0 \tag{363}$$

We then use this result in Eq. (362) and we solve the equation as prescribed by our method, that means we look for the solution that is the convolution of the Green's function with the input function. This solution is seen to be constant with respect to time, and in particular

$$\overline{W}_{\boldsymbol{x}}(t,\omega)=N_0\,|H(\omega)|^2 \tag{364}$$

Surprisingly, we obtain the same solution as in the case of the classical power spectrum. But there is the important difference that here we are evaluating a function of time and frequency. The result obtained means that the instantaneous power spectrum of the solution $\boldsymbol{x}(t)$ is constant in time. A simple and intuitive explanation of this conclusion can be given by considering Eq. (351) as a filtering problem. In this perspective what the system does is filter the input noise $\boldsymbol{f}(t)$ with a bandpass filter to produce an output signal $\boldsymbol{x}(t)$. But since both the input random noise and the filter/system are stationary in time, then also the output is stationary. This stationary is contained in the time-invariant property of the instantaneous power spectrum $\overline{W}_{\boldsymbol{x}}(t,\omega)$. Also it can be easily noticed that the property obtained in Eq. (364) is valid for any system defined by Eq. (268).

29 Example: Harmonic oscillator with time dependent coefficients

We now consider a time-variant harmonic oscillator described by the following differential equation

$$\frac{d^2\boldsymbol{x}}{dt^2}+2\mu\frac{d\boldsymbol{x}}{dt}+K(t)\boldsymbol{x}=\boldsymbol{f}(t) \tag{365}$$

where

$$K(t)=\omega_0^2+\epsilon t, \qquad\qquad \epsilon\ll 1 \tag{366}$$

This is a slightly perturbed version of the standard harmonic oscillator that shows though a basic time-varying behavior. Our intention is to study the system in the time interval $0\leq t\leq T$, where T is large enough to show a variation in the $K(t)$ coefficient. In particular we choose

$$K(T)=4K(0)=4\omega_0^2 \tag{367}$$

The equation for the Wigner spectrum is

$$\left[A^2 + 2\mu A + K(E)\right]\left[B^2 + 2\mu B + K(F)\right]\overline{W}_{\boldsymbol{x}}(t,\omega) = \overline{W}_{\boldsymbol{f}}(t,\omega) \tag{368}$$

This equation is a partial differential equation with varying coefficients, that cannot be solved as an ordinary differential equation (there are derivatives with respect to ω). But if we take into account the fact that $K(t)$ is slowly varying, we can approximate it by

$$\left[\frac{1}{16}\frac{\partial^4}{\partial t^4} + \frac{\mu}{2}\frac{\partial^3}{\partial t^3} + \left(\mu^2 + \frac{1}{2}\left(K(t)+\omega^2\right)\right)\frac{\partial^2}{\partial t^2} \right.$$
$$\left. +2\mu\left(K(t)+\omega^2\right)\frac{\partial}{\partial t} + \left(K(t)-\omega^2\right)^2 + 4\mu^2\omega^2\right]\overline{W}_{\boldsymbol{x}} = \overline{W}_{\boldsymbol{f}} \tag{369}$$

This is again a partial differential equation but contains no derivatives with respect to ω and can hence be solved as an ordinary differential equation. The only other issue is to set proper initial conditions at $t = 0$. Since the system is slowly time-varying, due to the fact that ϵ is very small, we suppose that its instantaneous spectrum will be slowly varying. If this is the case, then the instantaneous spectrum at $t = 0$, when $K(t = 0) = \omega_0^2$, will not be very different from the instantaneous spectrum of the stationary system that has always $K(t) = \omega_0^2$ (the one analyzed in Sect. 28). Following this approximation we choose

$$\overline{W}_{\boldsymbol{x}}(0,\omega) = \frac{N_0}{\left(\omega_0^2 - \omega^2\right)^2 + 4\mu^2\omega^2} \tag{370}$$

$$\frac{\partial\overline{W}_{\boldsymbol{x}}}{\partial t}(0,\omega) = \frac{\partial^2\overline{W}_{\boldsymbol{x}}}{\partial t^2}(0,\omega) = \frac{\partial^3\overline{W}_{\boldsymbol{x}}}{\partial t^3}(0,\omega) = 0 \tag{371}$$

The solution of Eq. (369) with the set of initial conditions given in Eqs. (370)-(371) can be obtained analytically using a power series expansion. In Fig. 28 we represent this solution, that has been instead obtained with a standard numerical integration method. This is necessary since the domain of integration is large and the power series solution should be computed for too many terms, far beyond the machine precision. (The problem can be handled with a symbolic program but here we use a numerical integration scheme because of its easy and robust implementation).

It is very important to notice that the computed Wigner spectrum $\overline{W}_{\boldsymbol{x}}(t,\omega)$ looks exactly as we expected. It is basically a bandpass spectrum as in Fig. 352 with a time-varying central frequency. Also the amplitude of the spectrum changes in time, and the reason is that this is embedded in the equation defining the time-varying harmonic oscillator, Eq. (365). The smooth transition between the initial spectrum at $t = 0$ and the final spectrum at $t = T$ is a consequence of the small value of the ϵ

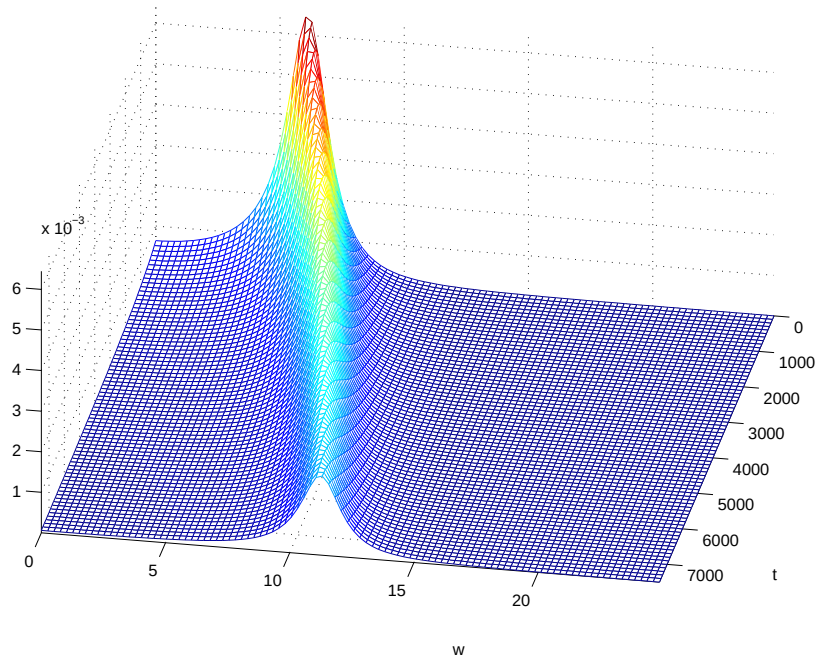

Figure 28: Wigner spectrum of the solution $x(t)$ to Eq. 365.

parameter, that makes $K(t) = \omega_0^2 + \epsilon t$ a slowly varying function. Now the crucial step is to compare this result that satisfies our intuition with the estimated Wigner spectrum obtained by simulation. This is done in Sect. 29.1.

29.1 Comparison with simulations

To check the validity of the solution shown in Fig. 28, we compare it with the estimated time-varying spectrum obtained by simulation. We first solve Eq. (365) with a scheme that is valid for a stochastic differential equation (e.g. an Euler scheme), and we thus obtain an approximation to $\boldsymbol{x}(t)$. Then we estimate the instantaneous power spectrum $P_x(t, \omega)$ with a sliding estimator method. This method consists in truncating the signal with a moving window, and then estimating the power spectrum at that time with a standard technique. Here a parametric ARMA estimator has been used, since we know that the truncated signal is coming from a second order differential equation. In Fig. 29 we show the result of such estimation. It can be noticed that our approximation, shown in Fig. 28 and the estimated spectrum are very close to each other. In particular Fig. 29 shows again the bandpass behavior that we were expecting from an intuitive point of view and that our approximation confirmed.

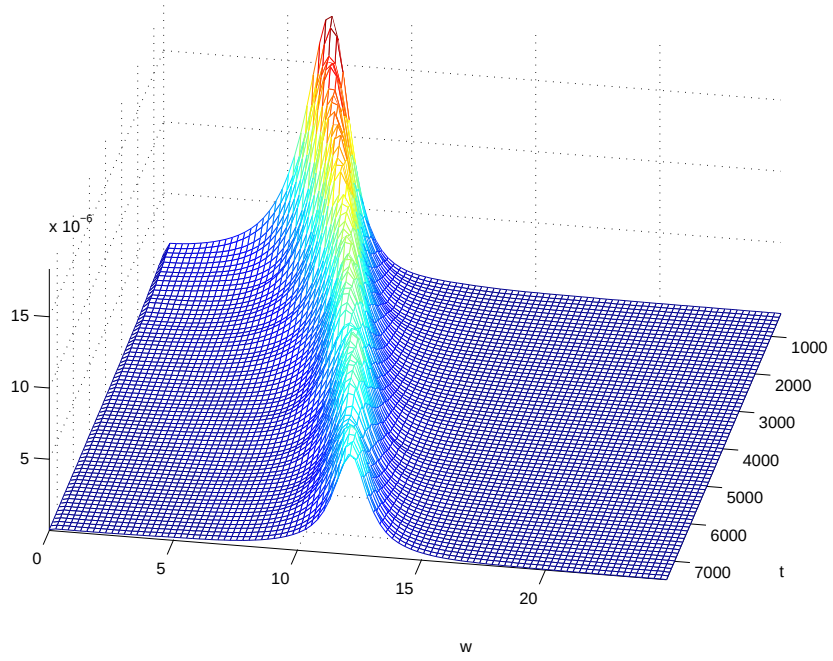

Figure 29: Numerical estimation of the Wigner spectrum of the solution to Eq. (365). Notice the quality of the approximation obtained in Fig. 28 that fits in an excellent way the estimated instantaneous spectrum.

30 Clouds

The study of cloud coverings is important for many reasons, among them is that we want to remove the clouds from images. Our aim is to understand certain aspects of clouds in regard to their statistical properties. Considering a cloud as a signal we ask where in the Fourier transform is the cloud-like information stored. In particular, is it in the spectral amplitude or spectral phase? The reason this is important is that by understanding this issue it may help in designing methods for the denoising of clouds, that is, methods that eliminate cloud coverings [**?**, **?**]. The idea of studying the relative importance of spectral amplitude and phase of a signal originated with the classical paper by Oppenheim and Lim [**?**] and subsequently many studies have been made.

We will start by studying these issues on artificially generated clouds.

30.1 Generation of clouds

For a two dimensional image, $s(x, y)$, we write its Fourier spectrum as

$$F(\omega_x, \omega_y) = \iint s(x, y) e^{-ix\omega_x - iy\omega_y} dxdy \tag{372}$$

and consequently the power spectrum is given by

$$P_s(\omega_x, \omega_y) = |F(\omega_x, \omega_y)|^2 \tag{373}$$

One way of generating cloud-like images is by using the fact that their Fourier power spectrum is of the type

$$P_s(\omega_x, \omega_y) = \frac{1}{\left(\sqrt{\omega_x^2 + \omega_y^2}\right)^{2\gamma}} \tag{374}$$

where γ is a parameter that controls the cloud-like appearance of the image. This type of power spectra is observed in natural clouds [**?**, **?**, **?**, **?**]. When one wants to generate artificial clouds it is hence reasonable to use Eq. (374) as a model for the numerical algorithm. A fast method to generate clouds is due to Perlin [**?**]. We instead use a direct implementation since we are not limited by time considerations. One generates a cloud $s(x, y)$ by filtering white noise, $N(x, y)$, with a filter whose shape in the frequency domain has the form given by Eq. (374),

$$H_\gamma(\omega_x, \omega_y) = \frac{1}{\left(\sqrt{\omega_x^2 + \omega_y^2}\right)^{\gamma}} \tag{375}$$

where $H_\gamma(\omega_x, \omega_y)$ is the transfer function of the linear filter. In particular, we start with white noise where the power spectrum is constant

$$P_N(\omega_x, \omega_y) = N_0 \tag{376}$$

and form the power spectrum of the cloud by way of

$$P_s(\omega_x, \omega_y) = |H_\gamma(\omega_x, \omega_y)|^2 \, P_N(\omega_x, \omega_y) \tag{377}$$

Then, the cloud is given by

$$s(x, y) = \iint h_\gamma(x - x', y - y') N(x', y') dx' dy' \tag{378}$$

where $h_\gamma(x, y)$ is the impulse response of the filter. In this way the output power spectrum of the cloud will be the same type as in Eq. (374).

In Fig. 1 we show several clouds generated with this method. In every of the five pictures we change the value of the spectral amplitude γ, and we obtain different "types" of clouds. In particular in Fig. 1a we have $\gamma = 0$, that is we generate white noise without any filtering. Then in Fig. 1b with $\gamma = 0.5$ we begin observing a less uniform pattern in the generated image, and in Fig. 1c and Fig. 1d obtained respectively with $\gamma = 1$ and $\gamma = 1.5$ we have the more cloud-like aspect of natural clouds. Fig. 1e with $\gamma = 2$ gives an image resembling natural clouds quite well. Fig. 1f, with $\gamma = 5$, shows that at the limit the generated images are very clustered.

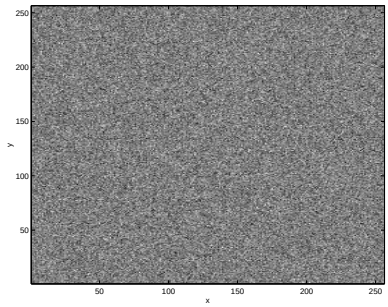

Fig. 1a. $\gamma = 0$.

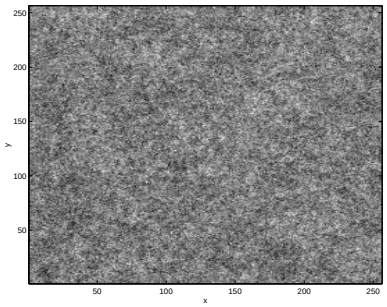

Fig. 1b. $\gamma = 0.5$.

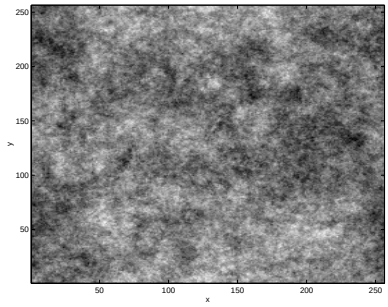

Fig. 1c. $\gamma = 1$.

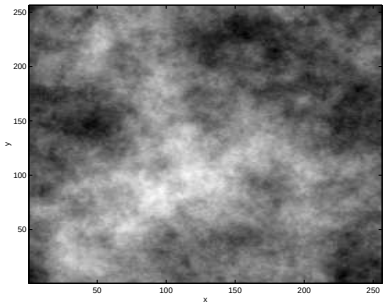

Fig. 1d. $\gamma = 1.5$.

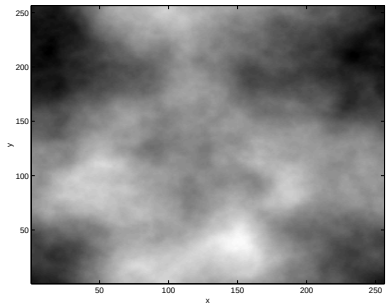

Fig. 1e. $\gamma = 2$.

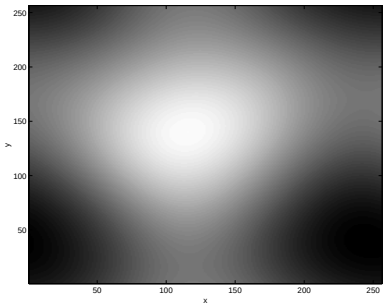

Fig. 1f. $\gamma = 5$.

30.2 Relative phase-amplitude importance

We write the Fourier transform in terms of its amplitude and phase

$$F(\omega_x, \omega_y) = A(\omega_x, \omega_y) e^{i\Phi(\omega_x, \omega_y)} \tag{379}$$

To study the relative importance of spectral amplitude and phase we use the idea of Oppenheim and Lim and reconstruct the image using phase and/or amplitude only to see the relative importance. In fact we take a somewhat more general approach. We define a modified Fourier transform by the

following

$$F_{\alpha\beta}(\omega_x, \omega_y) = A^{\alpha}(\omega_x, \omega_y) e^{\beta\Phi(\omega_x, \omega_y)} \tag{380}$$

and reconstruct the modified image by

$$s_{\alpha\beta}(x, y) = \int\int F_{\alpha\beta}(\omega_x, \omega_y) e^{ix\omega_x + iy\omega_y} d\omega_x d\omega_y \tag{381}$$

In Equation (381) α and β are parameters and by varying α and β we can ascertain the relative importance of phase and amplitude. In particular if we take $\alpha = 0$ and $\beta = 1$ then we are reconstructing phase only images, and if we take $\beta = 0$ and $\alpha = 1$ then it is amplitude only images. Our aim is to take a particular cloud and reconstruct it by the above procedure with a variety of values of α and β with the expectation that visual inspection will give us some indication where the cloud-like information resides, amplitude or phase.

In Fig. 2 we show amplitude only and phase only reconstruction of the first five clouds of Fig. 1. In particular, in the first column of the figure are the original images. Column two represents amplitude only reconstruction and column three represents phase only reconstruction. In terms of the model given in Sect. 30.1. when we reconstruct the image from the amplitude we take $\alpha = 1$ and $\beta = 0$, while the image reconstructed from the phase content has $\alpha = 0$ and $\beta = 1$. From a study of Fig. 2, it is reasonable to conclude that both amplitude and phase are important for the reproduction of the original image.

In Fig. 3 we have taken the image of the realistic cloud case, namely the one where $\gamma = 2$ in Fig. 1, and varied α and β as described in Section 3. In the first column the original phase is kept ($\beta = 1$) and the amplitude significance is varied according to $\alpha = 0,\ 0.2,\ 0.4,\ 0.6,\ 0.8,\ 0.95$. In the second column the amplitude is kept fixed ($\alpha = 1$) and the relative importance of the phase is varied by taking $\beta = 0,\ 0.2,\ 0.4,\ 0.6,\ 0.8,\ 0.95$. Also Fig. 3 proves that both amplitude and phase are important to generate realistic clouds.

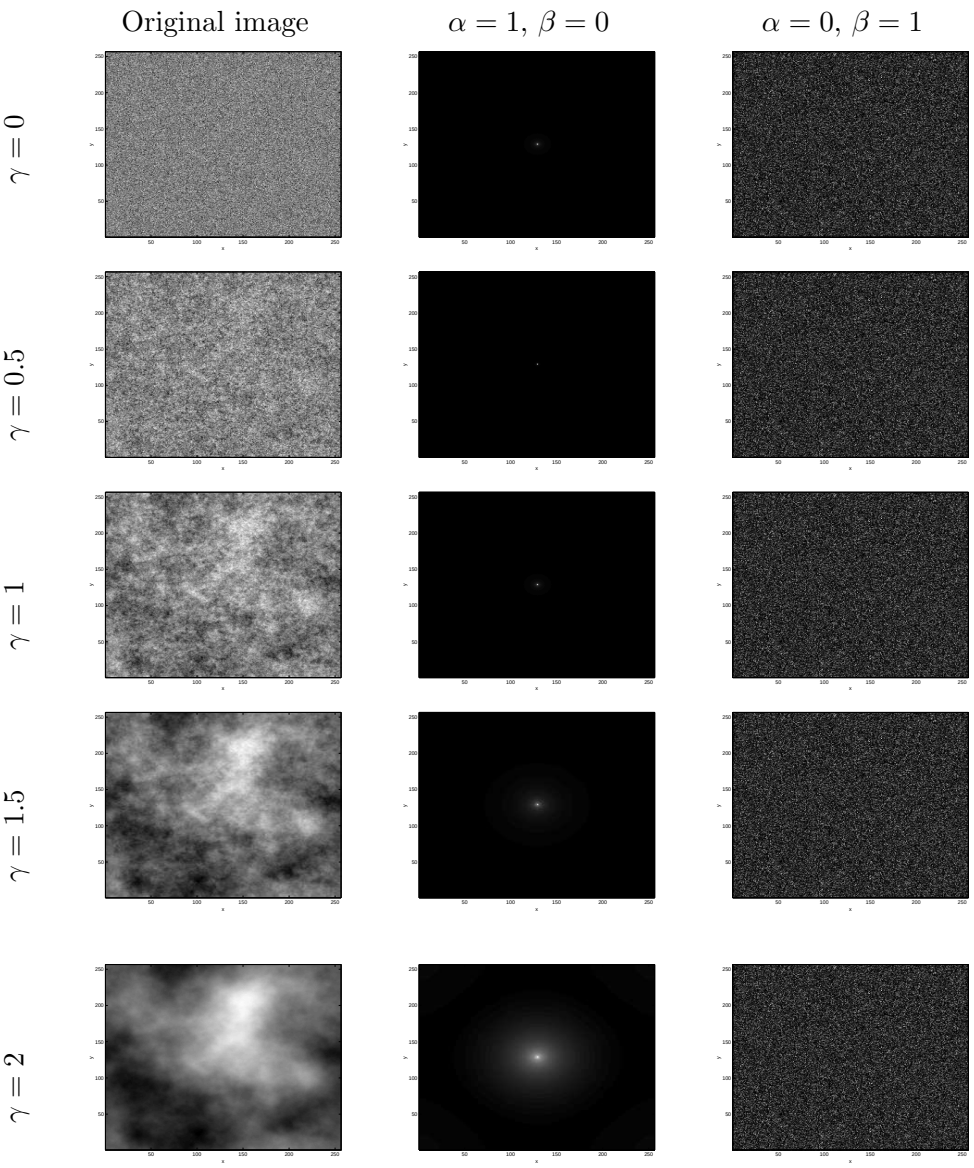
Original image
$\alpha = 1,\ \beta = 0$
$\alpha = 0,\ \beta = 1$
$\gamma = 0$
$\gamma = 0.5$
$\gamma = 1$
$\gamma = 1.5$
$\gamma = 2$

Fig. 2

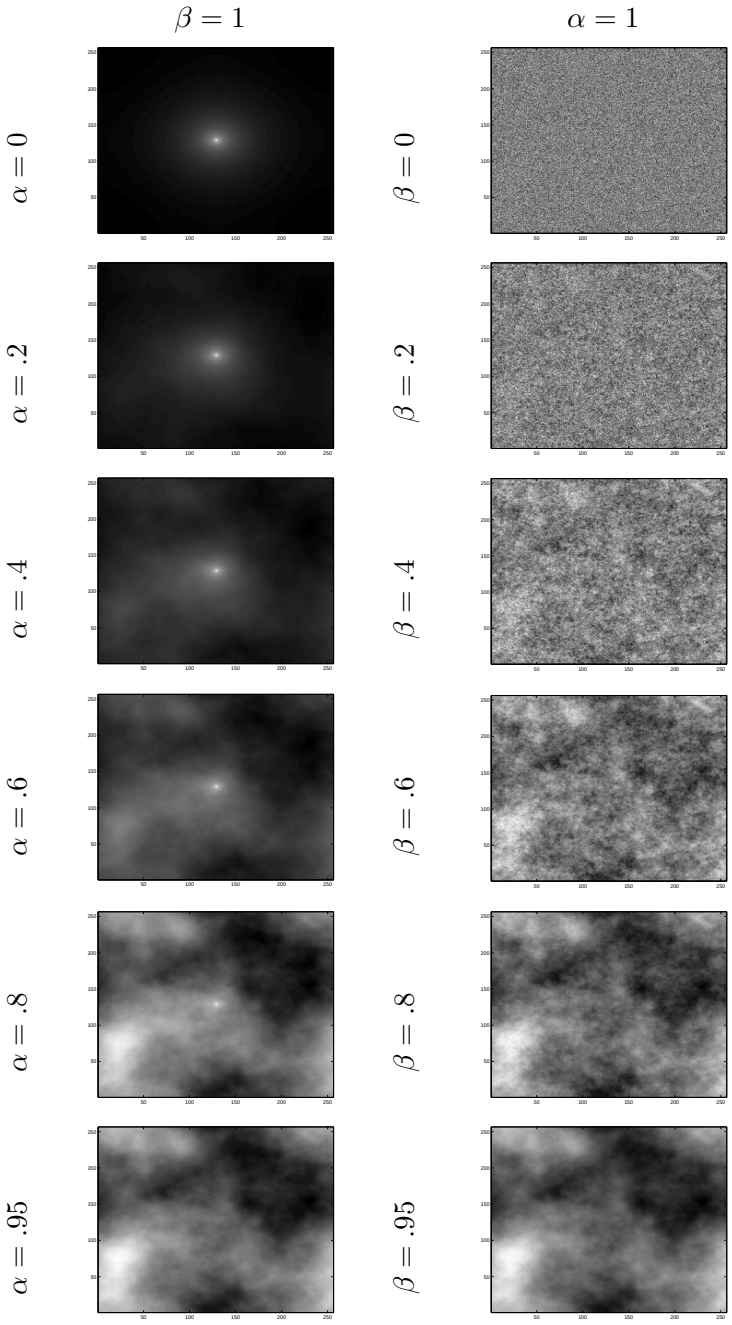

Fig. 3

30.3 The $1/f$ model for cloud generation

In the previous sections we have considered a cloud as a signal and we have investigated where in the Fourier transform is the cloud-like information stored, that is in the spectral amplitude or spectral phase. We will now study the generation of clouds from a different perspective, that is we generalize the algorithm that we have used before by using a stochastic fractional differential equation model. In particular we study these issues on artificially generated clouds.

It is generally argued that clouds have an $1/f$ spectra, and it has been well known that this can be used to generate clouds. We will investigate whether this is indeed true, in the sense that do other spectra also generate clouds, or must there be an $1/f$ behavior in the spectra?

The $1/f$ approach to generate clouds assumes that the power spectra of the generated cloud is of the form

$$P(\omega_x, \omega_y) = \frac{1}{\left(\sqrt{\omega_x^2 + \omega_y^2}\right)^{2\gamma}} \tag{382}$$

where γ is the $1/f$ parameter that controls the cloud like appearance of the image. We generated a cloud $s(x, y)$ by filtering white noise, $N(x, y)$, with a filter whose shape in the frequency domain has the form

$$H_\gamma(\omega_x, \omega_y) = \frac{1}{\left(\sqrt{\omega_x^2 + \omega_y^2}\right)^{\gamma}} \tag{383}$$

$$= \frac{1}{\omega^\gamma} \tag{384}$$

where $H_\gamma(\omega_x, \omega_y)$ is the transfer function of the linear filter and

$$\omega = \sqrt{\omega_x^2 + \omega_y^2} \tag{385}$$

In particular, we started with white noise where

$$P_N(\omega_x, \omega_y) = N_0 \tag{386}$$

and formed the power spectrum of the cloud by

$$P_s(\omega_x, \omega_y) = |H_\gamma(\omega_x, \omega_y)|^2 P_N(\omega_x, \omega_y) \tag{387}$$

$$= \frac{N_0}{\left(\sqrt{\omega_x^2 + \omega_y^2}\right)^{2\gamma}} \tag{388}$$

The cloud is then given by

$$s(x, y) = \iint h_\gamma(x - x', y - y') N(x', y') dx' dy' \tag{389}$$

where $h_\gamma(x, y)$ is the impulse response of the filter. Eq. (387) has the power spectrum given by Eq. (374).

In Fig. 4 we reproduce some clouds generated by this method with various parameters. We point out that for every picture we are using a two-dimensional transfer function that has a radial symmetry, and $H(\omega)$ given in Eq. (390) is precisely the value of that transfer function at any angle from the reference point of the image (located in the middle of the image), and at the radius value ω.

30.4 Other Power Spectra for the Generation of Clouds

Our aim is to investigate whether indeed only $1/f$ power spectra generates cloud like images. Towards that end we first consider spectra formed by the process described above but where we take the transfer function to be of the form

$$H(\omega) = \frac{1}{(i\omega)^\gamma + (i\omega)^\delta} \tag{390}$$

This produces a power spectrum given by

$$P_s(\omega_x, \omega_y) = \left| \frac{1}{(i\omega)^\gamma + (i\omega)^\delta} \right|^2 \tag{391}$$

$$= \frac{1}{\omega^{2\gamma} + \omega^{2\delta} + [(-1)^\delta + (-1)^\gamma] i^{\gamma+\delta} \omega^{\gamma+\delta}} \tag{392}$$

$$= \frac{1}{\omega^{2\gamma} + \omega^{2\delta} + 2\omega^{\gamma+\delta} \cos\left[\pi/2(\gamma - \delta)\right]} \tag{393}$$

We also consider transfer functions of the following form

$$H(\omega) = \frac{1}{\omega^\gamma + i\omega^\delta} \tag{394}$$

in which case the power spectrum is

$$P_s(\omega_x, \omega_y) = \left| \frac{1}{\omega^\gamma + i\omega^\delta} \right|^2 \tag{395}$$

$$= \frac{1}{\omega^{2\gamma} + \omega^{2\delta}} \tag{396}$$

We emphasize that this power spectrum is not the power spectrum of the sum of two $1/f$ power spectra. If γ and δ differ by multiples of π, then clearly Eq. (391) and Eq. (395) are the same power spectrum. To generate the cloud we use the procedure described in Sect. 30.5. Namely, we generate white noise and construct the cloud as before, but we use for the transfer function Eq. (390) and Eq. (394). In the next section we give the results we obtained by varying γ and δ.

30.5 Differential Equation Approach

We point out that one can formulate these types of processes and procedures as fractional differential equations. Consider the following fractional differential equation

$$D^\gamma x(t) + D^\delta x(t) = F(t) \tag{397}$$

where D^γ is called the fractional derivative when γ is not an integer. There are many possible definitions of fractional derivative. Here we use the Weil definition [**?**]

$$D^\gamma x(t) = \frac{1}{\Gamma(\gamma)} \int_{-\infty}^{t} (t - t')^{\gamma-1} x(t') dt' \tag{398}$$

When γ is an integer, say $\gamma = n$, this reduces to the n-the derivative of $x(t)$. In Eq. (397) $F(t)$ can be any function but here we take it to be white Gaussian noise.

Now consider the Fourier transform of both sides of the differential equation. We define the Fourier transform $G(\omega)$ of a function $g(t)$ by

$$G(\omega) = \mathcal{F}\left[g(t)\right] = \frac{1}{\sqrt{2\pi}} \int g(t) e^{-i\omega t} dt \tag{399}$$

Also we define $X(\omega)$ to be the Fourier transform of $x(t)$

$$X(\omega) = \mathcal{F}\left[x(t)\right] \tag{400}$$

Now one can show that

$$\mathcal{F}\left[D^{\gamma} x(t)\right] = (i\omega)^{\gamma} \mathcal{F}\left[x(t)\right] = (i\omega)^{\gamma} X(\omega) \tag{401}$$

and therefore taking the Fourier transform of both sides we have that

$$\mathcal{F}[D^{\gamma} x(t) + D^{\delta} x(t)] = \mathcal{F}[F(t)] \tag{402}$$

or

$$(i\omega)^{\gamma} X(\omega) + (i\omega)^{\delta} X(\omega) = \mathcal{F}[F(t)] \tag{403}$$

giving

$$X(\omega) = \frac{\mathcal{F}[F(t)]}{(i\omega)^{\gamma} + (i\omega)^{\delta}} \tag{404}$$

Thus we see that the transfer function is equal to

$$H(\omega) = \frac{1}{(i\omega)^{\gamma} + (i\omega)^{\delta}} \tag{405}$$

that is Eq. (390).

For the transfer function given by Eq. (394) consider the following fractional differential equations,

$$i^{-\gamma} D^{\gamma} x(t) + i^{1-\delta} D^{\delta} x(t) = F(t) \tag{406}$$

For this equation using the same procedure as above we have that

$$X(\omega) = \frac{\mathcal{F}[F(t)]}{\omega^{\gamma} + i\omega^{\delta}} \tag{407}$$

We note that for fractional derivatives, just as for ordinary derivatives, we have that

$$D^{\gamma}\left[a x(t)\right] = a D^{\gamma} x(t) \tag{408}$$

where a is an arbitrary constant.

We first discuss the results for the first transfer function, Eq. (390), which produces the power spectra given by Eq. (391). In Figs. 2a, 2b and 2c we show the pictures obtained by using all the

combinations of γ and δ ranging in the values 0.01, 0.5, 1, 1.5 and 2. The symmetric combinations like $(\gamma, \delta) = (1, 2)$ and $(\gamma, \delta) = (2, 1)$ have been avoided, since they clearly generate identical fractional equations and hence processes $x(t)$, as can be seen from Eq. (397). The rows show the values $\gamma = 2, 1.5, 1, 0.5, 0.01$ (in descending order), while the columns are associated to $\delta = 2, 1.5, 1, 0.5, 0.01$ (from left to right). Similar results have been obtained in Figs. 3a-3d, where we have used the transfer function given by Eq. (394). All the possible combinations of γ and δ used in the previous case have been considered, except $\gamma = \delta = 0.01$, which corresponds to white noise, already shown in Fig. 2c. Clearly there are many values of the parameters that generate cloud like pictures and hence we have to conclude that it is not the case that clouds must have an $1/f$ spectra.

We now address the general issue of $1/f$ spectra. It has often been said that many things in nature have $1/f$ spectra, examples being clouds, speech, natural scenes, etc. and that this is a fundamental characteristic. The definition of $1/f$ spectra often gets extended to mean $1/f^{\gamma}$. We are currently studying the issue as to what is common about the spectra that produce cloud like images. We speculate that what is going on is the following. First, we point out that if the autocorrelation function is of such a nature that there is no correlations at all we get white noise and if the autocorrelation function has infinite correlation we get a uniform gray. We believe that cloud like images are formed when the autocorrelation has a certain range and/or spectral shape and further that for such autocorrelation functions there are many types of spectra that can produce them, not only $1/f$. Of course, there is a one to one relationship between a given autocorrelation function and power spectra but what we are saying is that for a class or range of correlation functions there are many power spectra of very different functional forms that can produce such autocorrelation functions.

Insert pictures from file CloudFigures.tex here

30.6 Nonstationary clouds

Due to the different local conditions of wind, humidity, and temperature, there is an evident variation in the uniformity of the shape of clouds. Since clouds vary in nature with position, it is natural to think that also their spectral representation will be a function of position. It is hence interesting to build a realistic model of such nonstationarities.

We have seen that the power spectrum $P_s(\omega_x, \omega_y)$ of a cloud $s(x, y)$ can be modeled as

$$P_s(\omega_x, \omega_y) = \frac{1}{\left(\sqrt{\omega_x^2 + \omega_y^2}\right)^{2\gamma}} \tag{409}$$

To obtain this power spectrum we have processed white Gaussian noise $f(x, y)$ with a filter that has

a transfer function given by

$$H(\omega_x, \omega_y) = \frac{1}{\left(\sqrt{\omega_x^2 + \omega_y^2}\right)^{\gamma}} \tag{410}$$

We remind that if we start with white Gaussian noise, which has a constant power spectrum given by

$$P_f(\omega_x, \omega_y) = N_0 \tag{411}$$

the result of the filtering is [**?**]

$$P_s(\omega_x, \omega_y) = |H(\omega_x, \omega_y)|^2 P_f(\omega_x, \omega_y) \tag{412}$$

$$= \frac{N_0}{\left(\sqrt{\omega_x^2 + \omega_y^2}\right)^{2\gamma}} \tag{413}$$

This is exactly the type of spectrum we seek, namely Eq. (409). In the spatial domain the filtering is given by a two-dimensional convolution

$$s(x, y) = \iint h(x - x', y - y') f(x', y') dx' dy' \tag{414}$$

where $h(x, y)$ is the impulse response of the filter, obtained from the transfer function via Fourier inversion

$$h(x, y) = \frac{1}{(2\pi)^2} \iint H(\omega_x, \omega_y) e^{i\omega_x x + i\omega_y y} d\omega_x d\omega_y \tag{415}$$

The type of clouds generated by the described method depends on the parameter γ. In Fig. 30 we show the cloud corresponding to $\gamma = 1$, while in Fig. 31 the case $\gamma = 1.5$ is shown. One notices that as γ increases, the clouds are bigger and change slower with respect to position. This effect is due to the increased lowpass nature of the filter $H(\omega_x, \omega_y)$ used to generate the cloud.

Since the clouds vary in nature with position, it is natural to think that also their spectral representation will be a function of position. Given that we are using a $1/f^{\gamma}$ spectral model, an immediate way of modeling a nonstationary cloud is to make γ a function of position, that is to have $\gamma(x, y)$. In order to do this, we use the filter approach reviewed in the introduction where now we take the transfer function to depend on position in the following way

$$H(\omega_x, \omega_y, x, y) = \frac{1}{\left(\sqrt{\omega_x^2 + \omega_y^2}\right)^{\gamma(x,y)}} \tag{416}$$

That is, the dependence of the filter shape on position is obtained by making $\gamma(x, y)$ a function of position. Therefore the convolution operation of Eq. (414) that generates the cloud $s(x, y)$ from the white Gaussian noise $f(x, y)$ will be replaced by the general integral

$$s(x, y) = \iint h(x, x', y, y') f(x', y') dx' dy' \tag{417}$$

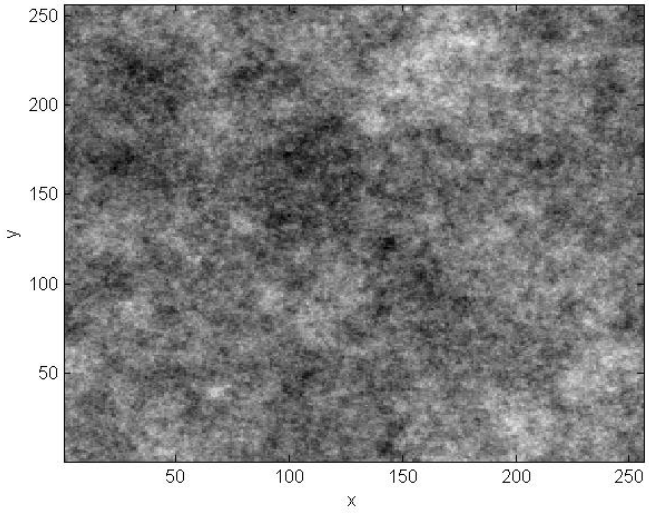

Figure 30: Stationary cloud obtained with $\gamma = 1$.

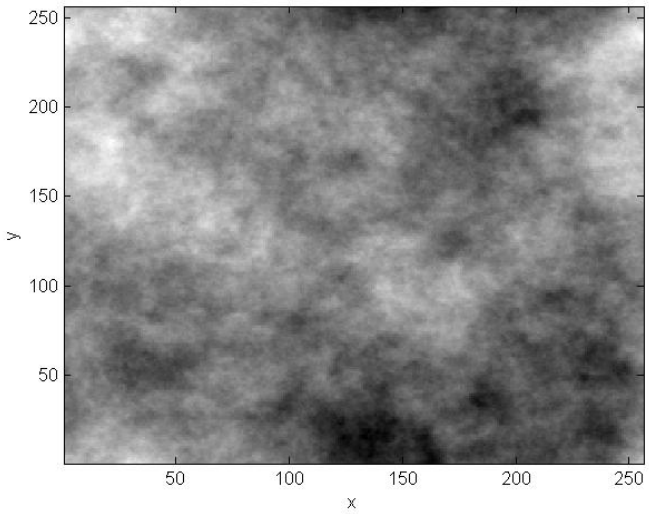

Figure 31: Stationary cloud obtained with $\gamma = 1.5$.

where now $h(x, x', y, y')$ is the Green's function given by

$$h(x, x', y, y') = \frac{1}{(2\pi)^2} \iint H(\omega_x, \omega_y, x, y) e^{i\omega_x x' + i\omega_y y'} d\omega_x d\omega_y \tag{418}$$

The corresponding algorithm is a direct implementation of the Green's integral of Eq. (417).

We now test the method by imposing different laws for the parameter $\gamma(x, y)$.

Radial case

We first impose γ to be constant for all the positions that have the same distance from a given reference point. We choose as the reference point the position $(x, y) = (0, 0)$, and we model γ with

$$\gamma(r) = \gamma_1 + \frac{\gamma_2 - \gamma_1}{R} r \tag{419}$$

where r is the radius given by

$$r = \sqrt{x^2 + y^2} \tag{420}$$

and R is the maximum distance from the reference point, that is reached in the corner (x_{MAX}, y_{MAX}) that is the farthest from the reference point

$$R = \sqrt{x_{MAX}^2 + y_{MAX}^2} \tag{421}$$

Hence Eq. (419) imposes a linear variation of γ from an initial value of γ_1 in the reference point to a final value of γ_2 in the farthest point. Fig. 32 represents the values taken by γ on the image, when $\gamma_1 = 1$ and $\gamma_2 = 1.8$. In Fig. 33 we show the result of our method. We notice that the uniformity of the clouds vary with position. In the lower bottom corner the clouds are more similar to the ones of Fig. 30, obtained for the stationary case with $\gamma = 1$. While we reach the upper top corner we see that the clouds become similar to the one of Fig. 31, that represents the stationary case with $\gamma = 1.5$. We have hence obtained our goal to generate nonstationary clouds by changing the local shape of the filter $H(\omega_x, \omega_y, x, y)$.

Lateral case

We now impose γ to be a function of x only, that is

$$\gamma(x) = \gamma_1 + \frac{\gamma_2 - \gamma_1}{x_{MAX}} x \tag{422}$$

Hence we have chosen γ to increase linearly from γ_1 to γ_2 with the x position, and to be constant with respect to y. Fig. 34 shows the values taken by γ, when $\gamma_1 = 1$ and $\gamma_2 = 1.8$. In Fig. 35 the clouds obtained in this case are shown. We notice that the clouds located towards the left side of the picture are similar to the ones obtained in the stationary case with $\gamma = 1$, shown in Fig. 30. While we move towards the right side of the picture we see that the clouds become more similar to the ones obtained in the stationary case with $\gamma = 1.5$ and represented in Fig. 31.

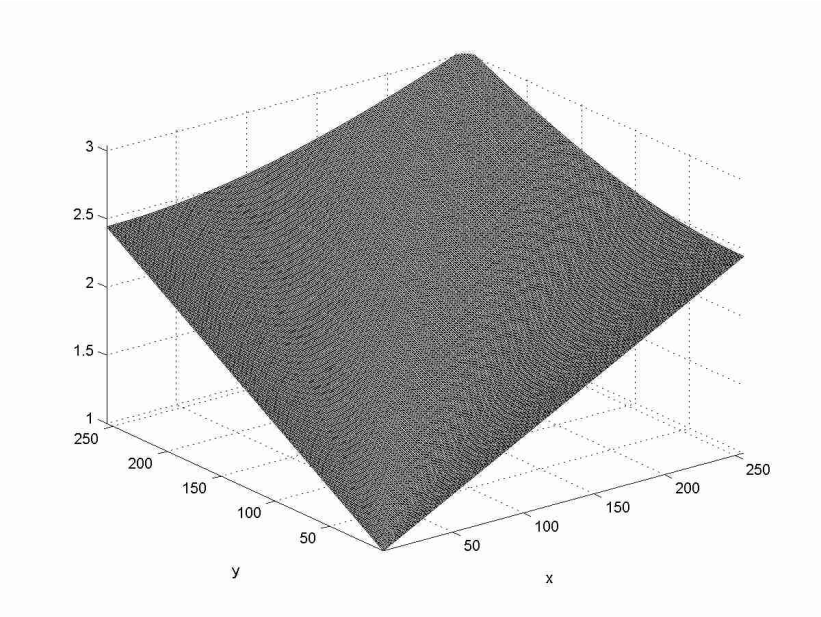

Figure 32: These are the values taken by the γ parameter in the model of Eq. (418). The parameter γ follows Eq. (419), with $\gamma_1 = 1$ and $\gamma_2 = 1.8$.

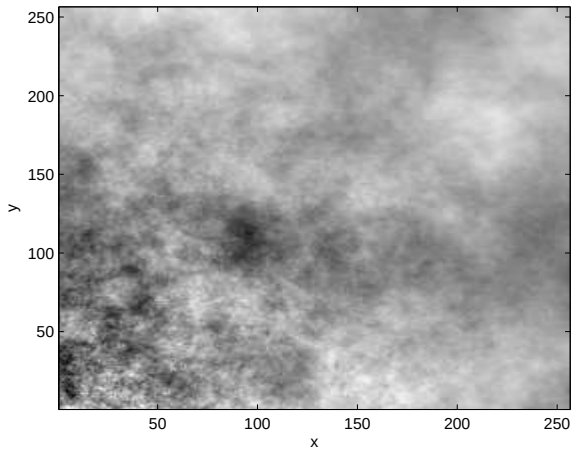

Figure 33: This picture shows nonstationary clouds that have been obtained by imposing the parameter γ to change as per Eq. (419). The clouds in the region around the bottom left corner are similar to the ones of Fig. 30, while the clouds around the upper right corner are better represented by the ones in Fig. 31.

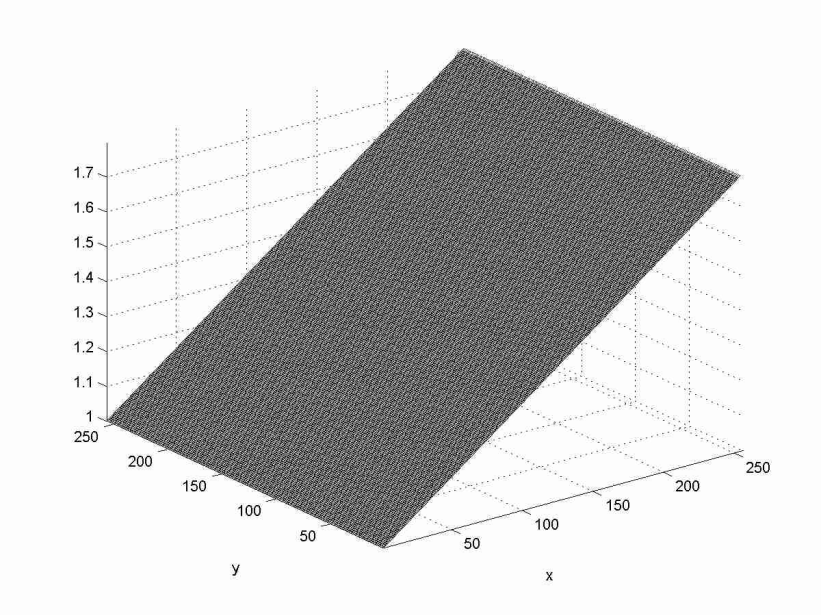

Figure 34: These are the values taken by the γ parameter in the model of Eq. (418). The parameter γ follows Eq. (422), with $\gamma_1 = 1$ and $\gamma_2 = 1.8$.

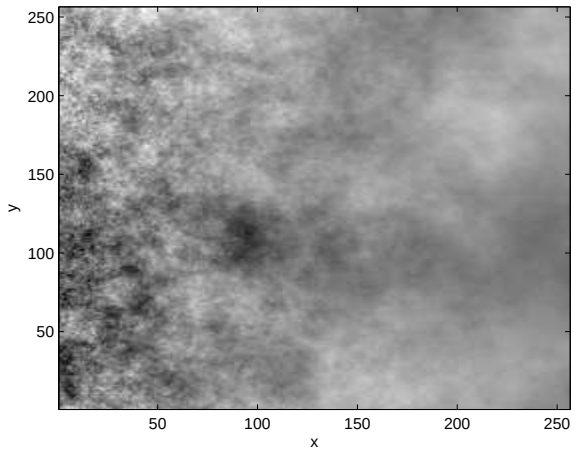

Figure 35: This picture shows nonstationary clouds that have been obtained by imposing the parameter γ to change as per Eq. (422). The clouds in the region around the left side of the image are similar to the ones of Fig. 30, while the clouds in the region around the right side of the image are better represented by the ones in Fig. 31.

31 Adjustable bandwidth concept

The adjustable bandwidth concept (ABC) is a method that enhances the performances of detection and estimation algorithms [**?**, **?**, **?**]. The aim is to enhance nonstationary signals in noise, that is, to bring out the main features of signals that may be buried in noise. This is essential for detection and classification and the method may be thought of as a "preprocessing algorithm" for classification applications and in particular for automatic target recognition methods. In this article we show that the ABC approach is a time-frequency method in that its basic idea is to treat time and frequency jointly. In particular we show that the algorithm transforms a time-frequency distribution by means of individual time-frequency transformations into a set of final time-frequency distributions. Each step of the procedure can be understood and formulated in terms of the kernel method, a technique that is standard in time-frequency analysis [**?**, **?**]. Once the procedure is formulated in terms of kernels, the ABC properties can be better studied and can suggest further enhancement and effectiveness of the method. We develop an exactly solvable example that illustrates some of the main issues and also shows the behavior of the method.

31.1 Time-frequency and the kernel method

A fundamental idea of time-frequency distributions is the concept of a kernel. The kernel characterizes the distribution and its properties and typically by examining the kernel one can ascertain the properties of the distribution. There have been many methods and distributions proposed over the years, among them the Wigner distribution, the spectrogram, the Choi-Williams, Margenau-Hill or Rihaczek and the Zam distributions and several others. Among the many areas to which they have been applied are biomedical signal analysis (e.g., heart sounds, heart rate, the electroencephalogram (EEG), the electromyogram (EMG) and others), machine fault monitoring, radar and sonar signals, acoustic scattering, wave propagation, speech processing, analysis of marine mammal sounds, musical instruments, linear and nonlinear dynamical systems, among many others. The primary reason for the applicability of these methods to such a variety of fields is that in all the cases cited, the spectra of the signals of interest change with time and these changes are fundamental to understand as they reflect the source and/or propagation medium [**?**].

All time-frequency distributions may be generated from the general class that is given by [**?**]

$$C(t,\omega) \;=\; \frac{1}{4\pi^2}\iiint s^*(u-\frac{1}{2}\tau)\,s(u+\frac{1}{2}\tau)\,\phi(\theta,\tau)\,e^{-j\theta t-j\tau\omega+j\theta u}d\,u d\,\tau d\,\theta \tag{423}$$

where $\phi(\theta,\tau)$ is a two dimensional function, the kernel. An alternative and useful formulation is to write

$$C(t,\omega) \;=\; \frac{1}{4\pi^2}\iint M(\theta,\tau)\,e^{-j\theta t-j\tau\omega}d\,\theta d\,\tau \tag{424}$$

where

$$M(\theta,\tau) = \phi(\theta,\tau)\int s^*(u-\frac{1}{2}\tau)\,s(u+\frac{1}{2}\tau)\,e^{j\theta u}d\,u \tag{425}$$

$$= \phi(\theta,\tau)\,A(\theta,\tau) \tag{426}$$

and where $A(\theta,\tau)$ is the standard ambiguity function commonly used in radar for the design of signals. The function $M(\theta,\tau)$ is called the characteristic function of the distribution.

We now briefly mention some kernels and their respective distributions. If the kernel is taken to be one then the Wigner distribution is obtained [**?**]. To avoid the cross term problems of the Wigner distribution a kernel methodology has been developed for kernel design and these ideas were initiated by Choi and Williams and Zhao, Atlas and Marks [**?**]. The Choi-Williams kernel is given by $\phi(\theta,\tau) = \exp(-\theta^2\tau^2/\sigma)$ and the Zam kernel by $\phi(\theta,\tau) = g(\tau)\,|\tau|\,\frac{\sin a\theta\tau}{a\theta\tau}$. Williams and co-workers devised and crystallized the idea of kernel design [**?**, **?**]. They developed a methodology for the construction of distributions with desirable properties. Of particular interest is the spectrogram, given by

$$C_S(t,\omega) = \left|\frac{1}{\sqrt{2\pi}}\int w(t-t')s(t')e^{-i\omega t'}dt'\right|^2 \tag{427}$$

where $w(t)$ is the window. The kernel for the spectrogram is given by

$$\phi(\theta,\tau) = \int w^*(u-\frac{1}{2}\tau)\,w(u+\frac{1}{2}\tau)\,e^{j\theta u}d\,u \tag{428}$$

That is, the kernel of the spectrogram is the ambiguity function of the window. We point out that the squared magnitude of the wavelet transform can be used as a time frequency distribution and formulated in the above terms [**?**, **?**]. Also, a number of fundamental results on the relation between the distribution and kernel have been developed, over the last ten years, the paper by Loughlin et. all being fundamental [**?**]

While the kernel method has generally been used to study, obtain, and characterize distributions, we discuss here the fact that it can also be used as a way of transforming distributions. The reason we emphasize this is that the ABC method is a sequence of time-frequency distribution transformations. Here we give some general properties of transformation. Suppose we have two distributions, C_1 and C_2, with corresponding kernels, ϕ_1 and ϕ_2. Their respective characteristic functions are related by

$$M_1(\theta,\tau) = \frac{\phi_1(\theta,\tau)}{\phi_2(\theta,\tau)}\,M_2(\theta,\tau) \tag{429}$$

This relationship connects the characteristic functions of any two distributions. To obtain the relationship between the distributions one uses Eq. (424) to obtain

$$C_1(t,\omega) = \iint g_{12}(t'-t,\omega'-\omega)\,C_2(t',\omega')d\,t'd\,\omega' \tag{430}$$

with

$$g_{12}(t,\omega) \;=\; \frac{1}{4\pi^2}\iint \frac{\phi_1(\theta,\tau)}{\phi_2(\theta,\tau)}\, e^{j\theta t + j\tau\omega} d\,\theta d\,\tau \tag{431}$$

What this shows is that one distribution can be transformed into another by way of a two-dimensional convolution where the convolution function is given in terms of the kernels of each distribution.

31.2 ABC Method

The ABC approach is a multi-stage procedure that operates on a starting time-frequency distribution, $C_S(t,\omega)$, and generates N output distributions, $C_1(t,\omega)$, $C_2(t,\omega)$, ... , $C_N(t,\omega)$. In this paper we show that the procedure at each stage is a time-frequency distribution transformation and that the end distribution can be characterized by a kernel which is a functional of the kernels at each stage.

We first give an overall view of the basic algorithm and indeed we present two but equivalent views. The first formulates everything in the time-frequency plane and the second formulates some of the steps in the kernel or ambiguity function domain as discussed above. Each formulation has certain advantages, the first formulation allows a clearer mathematical view of the issues but the second formulation lends itself to more detailed discussion of the implementation issues. We present both formulations but in this paper we discuss in detail the second one. The first view is presented in detail in [**?**] where also an analytic example is given. The equivalence of the two formulations is given in [**?**].

In the first formation the basic idea is to take a time-frequency distribution and from it obtain N new distributions. The new distributions have progressively different perspectives or resolutions of the original distribution. For the starting distribution we use $C_S(t,\omega)$, and the N resulting distributions are $C_1(t,\omega)$, $C_2(t,\omega)$, ... $C_N(t,\omega)$. However the actual iterative process is done on N intermediate distributions that we call $A_1(t,\omega)$, $A_2(t,\omega)$,..., $A_N(t,\omega)$. The iterative process is

$$A_m(t,\omega) = A_{m-1}(t,\omega) - \int h_{m-1}(t-t',\omega-\omega')\, A_{m-1}(t',\omega')dt'd\omega' \tag{432}$$

and to start one takes $A_1(t,\omega) = C_S(t,\omega)$. The $h_m(t,\omega)$ are fixed functions. We note that at each stage one removes from the distribution the effect that the second term of Eq. (432) produces. The iterative scheme, Eq. (432), is self contained and produces distributions with certain properties that are achieved by the judicious choice of the $h_m(t,\omega)$ so chosen to achieve required results, such as frequency smoothing. Now, to further manipulate and enhance the result we obtain $C_m(t,\omega)$ from $A_m(t,\omega)$ by

$$C_m(t,\omega) \;=\; \int g_m(t-t',\omega-\omega')A_m(t',\omega')dt'd\omega' \tag{433}$$

where again $g_1(t,\omega), g_2(t,\omega), ..., g_N(t,\omega)$ are fixed filter functions prechosen to achieve desired characteristics. Of course one can just stick with the A's and from a mathematical point of view

that can be achieved by taking delta functions for the g's, in which case the result would be that $C_m(t,\omega) = A_m(t,\omega)$. Also, one can combine Eq. (433) and Eq. (432) but we have found it clearer to write the procedure in the above form. We note that both transformations in Eq. (433) and Eq. (432) are of the form as given by Eq. (430).

In the second formulation, at each stage of the algorithm there is an input distribution $A_m(t,\omega)$, an intermediate distribution $B_m(t,\omega)$, and an output distribution $C_m(t,\omega)$. The input distribution at the stage 1 is $A_1(t,\omega) \equiv C_S(t,\omega)$. The distributions $A_m(t,\omega)$ and $B_m(t,\omega)$ are needed to calculate the output *and* to go on to the next stage. In particular we tabulate here the overall steps:

$$A_m(t,\omega) = A_{m-1}(t,\omega) - B_{m-1}(t,\omega) \tag{434}$$

$$B_m(t,\omega) = \text{is calculated from } A_m(t,\omega) \text{ through a frequency average} \tag{435}$$

$$C_m(t,\omega) = \text{is calculated from } B_m(t,\omega) \text{ through a time average} \tag{436}$$

In addition, we will need the characteristic functions for each distribution and we use the following notation $a_m(\theta,\tau)$, $b_m(\theta,\tau)$ and $c_m(\theta,\tau)$. That is

$$a_m(\theta,\tau) = \iint A_m(t,\omega)\ e^{j\theta t + j\tau\omega} d\,t d\omega\tau \tag{437}$$

and similarly for $b_m(\theta,\tau)$, and $c_m(\theta,\tau)$. We now describe the two steps indicated above. For both of them we will use the characteristic function formulation, because it makes the derivation much easier.

31.3 First sub step: Calculation of $B_m(t,\omega)$ from $A_m(t,\omega)$ through a frequency average

The distribution $B_m(t,\omega)$ is obtained from $A_m(t,\omega)$ through a lowpass filtering, with the aim of smoothing out noise along the frequency axis of the input distribution of the stage. The amount of filtering is in general a function of the stage. In the characteristic function domain we have that, at stage $m = 1, 2, \ldots N$

$$b_m(\theta,\tau) = \sqrt{2\pi} H_m(\tau) a_m(\theta,\tau) \tag{438}$$

where $H_m(\tau)$ is the transfer function of the lowpass filter at the m-th stage. We have defined

$$H_N(\tau) \equiv 1 \tag{439}$$

Also, because of Eq. (434) we see that for $m = 2, 3, \ldots N$

$$a_m(\theta,\tau) = [1 - \sqrt{2\pi} H_{m-1}(\tau)] a_{m-1}(\theta,\tau) \tag{440}$$

$$= \prod_{l=1}^{m-1} [1 - \sqrt{2\pi} H_{m-l}(\tau)] M_S(\theta,\tau) \tag{441}$$

Putting together Eq. (438) and Eq. (440) we obtain

$$b_m(\theta,\tau) = \phi_{\omega_m}(\tau) M_S(\theta,\tau) \tag{442}$$

$$= \left[\sqrt{2\pi} H_m(\tau) \prod_{l=1}^{m-1} [1 - \sqrt{2\pi} H_{m-l}(\tau)]\right] M_S(\theta,\tau) \tag{443}$$

where we have defined the frequency averaging kernel as

$$\phi_{\omega_m}(\tau) = \sqrt{2\pi} H_m(\tau) \prod_{l=1}^{m-1} [1 - \sqrt{2\pi} H_{m-l}(\tau)] \tag{444}$$

31.4 Second sub step: Calculation of $C_m(t,\omega)$ from $B_m(t,\omega)$ through a time average

The distribution $C_m(t,\omega)$ is obtained from $B_m(t,\omega)$ through a moving average in time, with the aim of reducing noise along the time direction of the input distribution of the stage. If we consider the m-th stage of the algorithm, $m = 1, 2, \ldots, N$, the time averaging can be written in the time-frequency domain as

$$C_m(t,\omega) = \frac{1}{T_m} \int_{t-T_m/2}^{t+T_m/2} B_m(t',\omega) dt' \tag{445}$$

$$= \frac{1}{T_m} \int P_{T_m}(t-t') B_m(t',\omega) dt' \tag{446}$$

$$= \frac{1}{T_m} P_{T_m}(t) * B_m(t,\omega) \tag{447}$$

where the star sign indicates convolution and $P_{T_m}(t)$ is the rectangular window defined as

$$P_{T_m}(t) = \begin{array}{ll} 1 & -T_m/2 < t < T_m/2 \\ 0 & \text{elsewhere} \end{array} \tag{448}$$

and also $b_N(\theta,\tau) \equiv a_N(\theta,\tau)$. In the characteristic function domain we have that

$$c_m(\theta,\tau) = \phi_{t_m}(\theta) b_m(\theta,\tau) \tag{449}$$

$$= \sqrt{2\pi} \frac{1}{T_m} \bar{P}_{T_m}(\theta) b_m(\theta,\tau) \tag{450}$$

where $\bar{P}_{T_m}(\theta)$ is the inverse Fourier transform of $P_{T_m}(t)$ and we have defined the time averaging kernel as

$$\phi_{t_m}(\theta) = \sqrt{2\pi} \frac{1}{T_m} \bar{P}_{T_m}(\theta) \tag{451}$$

31.5 Time-Frequency averaging in the ABC algorithm

We will now derive the exact expression for the output distributions generated by the algorithm. We see by considering Eq. (449) and Eq. (442) that the output of stage m is

$$c_m(\theta,\tau) = \phi_{t_m}(\theta) b_m(\theta,\tau) \tag{452}$$

$$= \phi_{t_m}(\theta)\phi_{\omega_m}(\tau) M_S(\theta,\tau) \tag{453}$$

$$= \left[2\pi \frac{1}{T_m} \bar{P}_{T_m}(\theta) H_m(\tau) \prod_{l=1}^{m-1} [1 - \sqrt{2\pi} H_{m-l}(\tau)] \right] M_S(\theta,\tau) \tag{454}$$

$$= \phi_m(\theta,\tau) M_S(\theta,\tau) \tag{455}$$

where

$$\phi_m(\theta,\tau) = \phi_{t_m}(\theta)\phi_{\omega_m}(\tau) \tag{456}$$

$$= 2\pi \frac{1}{T_m} \bar{P}_{T_m}(\theta) H_m(\tau) \prod_{l=1}^{m-1} [1 - \sqrt{2\pi} H_{m-l}(\tau)] \tag{457}$$

is the kernel of the distribution at stage m, that is hence independent from the input distribution. We note that at stage $m = 1$ the multiplication operation $\prod$ has to be set equal to 1.

Convergence and weighted averages.[6] We now address the issue of the convergence of the algorithm. We have found from experience that the algorithm always converges and we believe that some insight into this issue can be gained by the following considerations. In [**?**] it is shown for the discrete-time case that the ABC frequency averaging of the input is equivalent to a filter-bank decomposition. Therefore, just as the output components of a filter bank can be recombined to "converge" to the input, the outputs identified by Eq. (433) can be recombined to "converge" to the input. Also, in [**?**] a simple analytic example is presented and at least for that example one can see the that indeed at each step one gets the appropriate convergence. One of the advantages of formulating the algorithm by way of Eqs. (433) and (432) is that it crystallized the procedures and allows for the possibility of a mathematical study of the convergence. This issue is currently being studied.

In the above some parameters are estimated and averaged simply but of course one could use weighted average. Weighted average is always an option and any specific choice of filter parameters will always be "optimal" for some signal scenarios and "sub-optimal" for others. This paper focuses on formulating the ABC process in continuous-time and continuous-frequency, from the original discrete-time, discrete-frequency formulation. This new formulation then lends itself to study this issue. Similar issues regarding weighted averages are considered in [**?**].

[6] We thank the referees for bringing some of these points to our attention.

Relation between direct time-frequency formulation and the ambiguity function domain. We repeat here the two formulations of the ABC algorithm for convenience. In time-frequency we have the two equations

$$A_m(t,\omega) = A_{m-1}(t,\omega) \tag{458}$$
$$- \int h_{m-1}(t-t',\omega-\omega')\, A_{m-1}(t',\omega') d\, t' d\, \omega'$$
$$C_m(t,\omega) = \int g_m(t-t',\omega-\omega') A_m(t',\omega') d\, t' d\, \omega' \tag{459}$$

with $A_1(t,\omega) \equiv C_S(t,\omega)$. In the characteristic function domain it is

$$c_m(\theta,\tau) = \phi_m(\theta,\tau) M_S(\theta,\tau) \tag{460}$$
$$= \phi_{t_m}(\theta)\phi_{\omega_m}(\tau) M_S(\theta,\tau) \tag{461}$$
$$= \left[2\pi \frac{1}{T_m} \bar{P}_{T_m}(\theta) H_m(\tau) \right] \times \tag{462}$$
$$\left[\prod_{l=1}^{m-1} [1 - \sqrt{2\pi} H_{m-l}(\tau)] \right] M_S(\theta,\tau) \tag{463}$$

To point out the connection we write Eq. (458) and Eq. (459) in the characteristic function domain

$$a_m(\theta,\tau) = \left[1 - \bar{h}_m(\theta,\tau)\right] a_{m-1}(\theta,\tau) \tag{464}$$
$$= \textstyle\prod_{k=1}^{m} \left[1 - \bar{h}_k(\theta,\tau)\right] a_1(\theta,\tau) \tag{465}$$

and

$$c_m(\theta,\tau) = \bar{g}_m(\theta,\tau) a_m \tag{466}$$
$$= \bar{g}_m(\theta,\tau) \textstyle\prod_{k=1}^{m} \left[1 - \bar{h}_k(\theta,\tau)\right] a_1(\theta,\tau) \tag{467}$$

where $\bar{h}_m(\theta,\tau)$ and $\bar{g}_m(\theta,\tau)$ are the filters $h_m(t,\omega)$ and $g_m(t,\omega)$ in the characteristic function domain. Since

$$a_1(\theta,\tau) \equiv M_S(\theta,\tau) \tag{468}$$

we see that if we choose

$$\phi_m(\theta,\tau) = \bar{g}_m(\theta,\tau) \textstyle\prod_{k=1}^{m} \left[1 - \bar{h}_k(\theta,\tau)\right] \tag{469}$$

we have the equivalent formulation of the characteristic function domain. By further relaxing the constraint of the time kernel $\phi_{t_m}(\theta)$ to be a function of θ only and the frequency kernel $\phi_{\omega_m}(\tau)$ to be a function of τ only we establish the connection

$$\phi_{t_m}(\theta,\tau) = \bar{g}_m(\theta,\tau) \tag{470}$$
$$\phi_{\omega_m}(\tau) = \textstyle\prod_{k=1}^{m} \left[1 - \bar{h}_k(\theta,\tau)\right] \tag{471}$$

thus showing the one to one relationship among the two formulations.

31.6 Examples

To demonstrate the application of the ABC process we present a number of cases. The first is a signal composed of the sum of a sinusoid, a chirp (swept frequency), an impulse, and additive white Gaussian noise. The term "white" refers to the fact that the noise power is uniform across frequency. For this case, the noise power is low, with the signal-to-noise power ratio (SNR) set to 70 dB for the sinusoid as measured in a frequency bin. The spectrogram generated is based on a 1024 sample FFT, with a rectangular data window, no data overlap between time segments and logarithmic scaling. The amplitudes of the chirp and impulse signal components are set to achieve similar power levels per FFT bin as the sinusoid component. The intent is to demonstrate separation of these unique signal components into the various output stages by the ABC process.

The second example is essentially the same as the first, with the exception that the additive noise component is increased substantially such that the sinusoidal SNR is now 10 dB per FFT bin. Thus the sinusoid, chirp and impulse are the same as in the first signal. For each case, the signal is quantized to 16 bits for storage to file prior to the ABC processing.

For both signals, the ABC parameters are set to the same values. In particular, 3 processing stages are used. The first stage lowpass filter is a finite impulse response (FIR) filter of 129 coefficients, each coefficient equal to 1/129. Likewise, the stage 2 lowpass filter is a 7 coefficient FIR filter, each coefficient equal to 1/7. Thus both filters are implemented as simple moving averages. Note that filter design will affect the ABC processing performance. While the parameters chosen are appropriate for the signal scenarios presented, these parameters have not been optimized. (The effect of this choice of parameters will be apparent.) In addition to frequency averaging, time averaging is accomplished in the second and third stages of the implemented ABC process. An average of 2 time segments is accomplished in the second stage, and an average of 10 time segments is accomplished in the third stage.

Results are shown in Figs. 1-4 for the 70 dB SNR case, and Figs. 5-8 for the 10 dB SNR case. As seen in Fig. 1, the sinusoid is at bin 240 for all segments. The chirp component sweeps up in frequency from bin 0 to 511, then back down to 0. The impulse occurs at time segment 256. Note that in progressing from stage to stage, the desired components are much more distinguishable from each other, and from the background additive noise. However, note also that the energy of the chirp signal is present in both stage 1 and stage 3, in addition to the dominant chirp output in stage 2. Likewise, the sinusoidal component is dominant in stage 3, but also noticeable in stage 2. This observation relates to the need for optimization of the filter parameters of the ABC process, when there exists a-priori information regarding the input.

In Fig. 5, note the adverse affects of increasing the additive noise component. The sinusoid, chirp

Figure 36: Input distribution $C_S(t, \omega)$ when $SNR = 70$dB.

Figure 37: Output distribution $C_1(t, \omega)$ at stage 1 ($SNR = 70$dB).

Figure 38: Output distribution $C_2(t, \omega)$ at stage 2 ($SNR = 70$dB).

Figure 39: Output distribution $C_3(t, \omega)$ at stage 3 ($SNR = 70$dB).

Figure 40: Input spectrogram $C_S(t, \omega)$ when $SNR = 10$dB.

Figure 41: Output distribution $C_1(t, \omega)$ at stage 1 ($SNR = 10$dB).

Figure 42: Output distribution $C_2(t, \omega)$ at stage 2 ($SNR = 10$dB).

Figure 43: Output distribution $C_3(t, \omega)$ at stage 3 ($SNR = 10$dB).

and impulse are difficult to discern. Even so, the benefits of the ABC process are easily observed. The desired signal components are separated in preparation for post-processing, such as threshold-based detection.

Example 2

We consider a specific example to see the effect of the procedure. For the signal we take a chirp with no amplitude modulation

$$s(t) \;=\; e^{jkt^2/2} \tag{472}$$

For the starting distribution we take

$$C_S(t,\omega) \;= \delta(\omega - kt) \tag{473}$$

which is the Wigner distribution of the signal[**?**, **?**]. The instantaneous frequency is $\omega_i \;=\; kt$ and therefore the distribution is totally concentrated along the instantaneous frequency. For this example we calculate $C_1(t,\omega),\ A_2(t,\omega)$ and $C_2(t,\omega)$.

For the filters we take

$$g_1(t,\omega) = \frac{\sqrt{\alpha_1\beta_1}}{\pi}\exp(-\alpha_1 t^2 - \beta_1\omega^2) \tag{474}$$

$$g_2(t,\omega) = \sqrt{\alpha_2/\pi}\exp(-\alpha_2 t^2)\delta(\omega) \tag{475}$$

$$h_1(t,\omega) = \sqrt{\beta_1/\pi}\delta(t)\exp(-\beta_1\omega^2) \tag{476}$$

We have taken these filters because they are directly connected in a simple way to Noga's original formulation of the algorithm. In particular, the filter $g_1(t,\omega)$ is the combination of the lowpass filtering and the time averaging performed by the algorithm at the first stage. The lowpass filter has impulse response $h_1(t,\omega)$ and the first time average is $\exp(-\alpha_1 t^2)\delta(\omega)$. The time average for the second stage is given by $g_2(t,\omega)$. All these filters are defined in the time-frequency plane, while in the original formulation they are defined on time and frequency separately.

A straightforward calculation gives the following results

$$C_1(t,\omega) = \sqrt{\frac{\alpha_1\beta_1}{\pi(\alpha_1+\beta_1 k^2)}} \tag{477}$$

$$\exp\left[-\alpha_1 t^2 - \beta_1\omega^2 + \frac{(\alpha_1 t + \beta_1 k\omega)^2}{\alpha_1+\beta_1 k^2}\right]$$

$$= \sqrt{\frac{\alpha_1\beta_1}{\pi(\alpha_1+\beta_1 k^2)}}\exp\left[-\alpha_1\beta_1\frac{(\omega-kt)^2}{\alpha_1+\beta_1 k^2}\right] \tag{478}$$

$$A_2 = \delta(\omega - kt) - \sqrt{\beta_1/\pi}\exp\left[-\beta_1(\omega-kt)^2\right] \tag{479}$$

$$C_2(t,\omega) = \frac{1}{|k|}\sqrt{\alpha_2/\pi}\exp(-\alpha_2(\omega-kt)^2/k^2) \tag{480}$$
$$-\sqrt{\frac{\alpha_2\beta_1}{\pi(\alpha_2+\beta_1k^2)}}\exp\left[-\alpha_2t^2-\beta_1\omega^2+\frac{(\alpha_2t+\beta_1k\omega)^2}{\alpha_2+\beta_1k^2}\right]$$
$$= \frac{1}{|k|}\sqrt{\alpha_2/\pi}\exp(-\alpha_2(\omega-kt)^2/k^2) \tag{481}$$
$$-\sqrt{\frac{\alpha_2\beta_1}{\pi(\alpha_2+\beta_1k^2)}}\exp\left[-\alpha_2\beta_1\frac{(\omega-kt)^2}{\alpha_2+\beta_1k^2}\right]$$

We choose the following parameters: $\alpha_1 = 1000$, $\alpha_2 = 100$, $\beta_1 = 0.01$ and $k = 2\pi$ and we show the quantities $C_S(t,\omega)$, $C_1(t,\omega)$ and $C_2(t,\omega)$. In Fig. 44 we plot the input distribution $C_S(t,\omega)$, that is a chirp concentrated along the instantaneous frequency $\omega_i = \beta t$. In Fig. 45 we have $C_1(t,\omega)$, the output of the first stage of the algorithm. We notice that the chirp has been spread in both time and frequency. This effect is generated by the filter $g_1(t,\omega)$ that performed a time and frequency smoothing on the input distribution. The importance of the smoothing is related to noise suppression, but here we investigated a noise free deterministic case in order to understand the basic operation performed by the method. Finally in Fig. 46 we show the second output of the algorithm, $C_2(t,\omega)$. With judicial choices of filter parameters, we can adjust the amount of frequency and time averaging in each stage. In the same fashion as evaluating time filters with an input impulse and observing the output response, here we have chosen a swept impulse in the time-frequency plane to evaluate and observe the output results. We observe that the first stage output responds only slightly to the chosen input signal, while the second stage responds substantially. This is due to the fact that the input signal is narrow in (instantaneous) bandwidth. We point out that the output distributions can be locally negative, as a consequence of having chosen the Wigner distribution. This fact has little interest since one could have chosen a modified Wigner distribution that guarantees positivity and still have very similar results. These results demonstrate the two key points of the ABC method:

1. Every output distribution $C_k(t,\omega)$ is smoothed in time and frequency with respect to the initial distribution $C_S(t,\omega)$.

2. Every stage of the algorithm emphasizes a different region of the characteristic function domain of the input distribution.

We mention two subsidiary issues. First is the issue of the starting distribution. Noga, in his original work used the log-spectrogram, but other starting distributions are possible, and perhaps may be more effective. How the final distribution depends on the initial distribution can now be

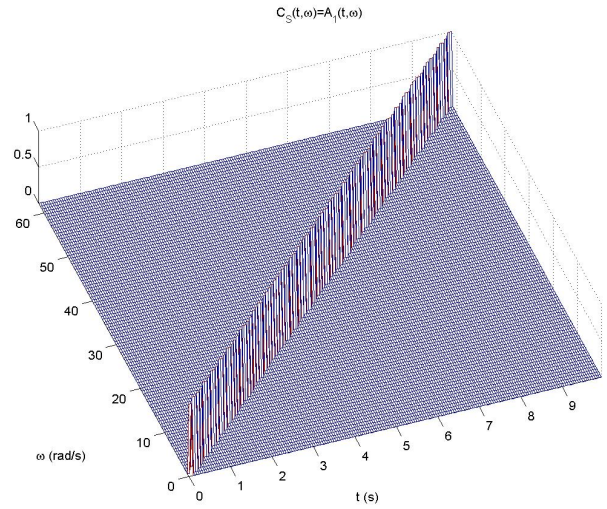

Figure 44: Input distribution $C_S(t\,,\omega)$. The Dirac function is represented by its numerical version.

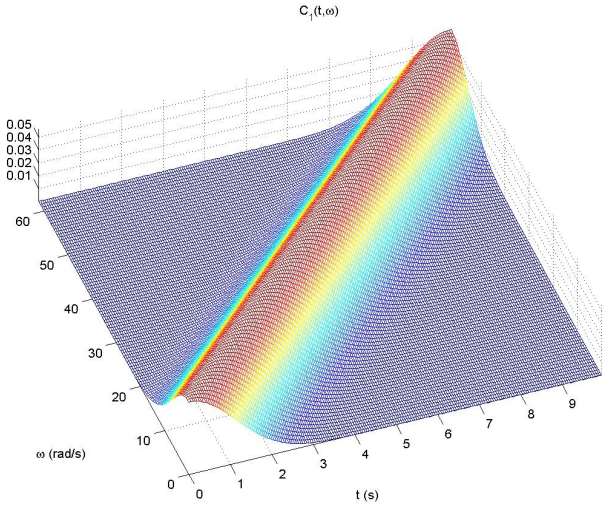

Figure 45: Output distribution $C_1(t,\omega)$ at the first stage.

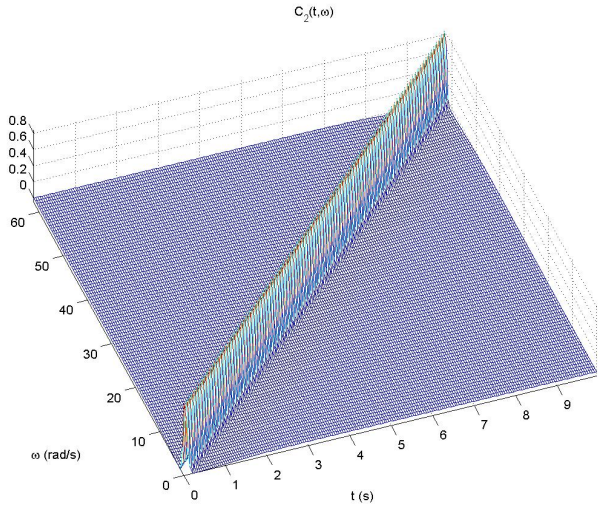

Figure 46: Output distribution $C_2(t, \omega)$ at the second stage.

studied theoretically because one can explicitly express the steps in the determination of the kernels. This should be explored. Secondly, in the original formulation the log-spectrogram was used and this has a number of advantages. We have not done so in the current formulation because we wanted to understand the time and frequency averaging operation done by the algorithm and keep that issue separate from the benefits of using the log-spectrum.